

# NEW TECHNIQUES FOR NEW HYDROCARBON DISCOVERIES—SURFACE GEOCHEMICAL SURVEYS IN THE LISBON AND LIGHTNING DRAW SOUTHEAST FIELD AREAS, SAN JUAN COUNTY, UTAH

BY DAVID M. SENESHEN, THOMAS C. CHIDSEY, JR., CRAIG D. MORGAN,  
AND MICHAEL D. VANDEN BERG



Miscellaneous Publication 10-2  
Utah Geological Survey  
*a division of*  
Utah Department of Natural Resources  
**2010**

# **NEW TECHNIQUES FOR NEW HYDROCARBON DISCOVERIES— SURFACE GEOCHEMICAL SURVEYS IN THE LISBON AND LIGHTNING DRAW SOUTHEAST FIELD AREAS, SAN JUAN COUNTY, UTAH**

*by David M. Seneshen, Direct Geochemical/Vista Geoscience*

*and*

*Thomas C. Chidsey, Jr., Craig D. Morgan, and Michael D. Vanden Berg,  
Utah Geological Survey*

ISBN: 978-1-55791-826-0

*Cover photo: Lisbon and Lightning Draw Southeast field area, San Juan County, Utah. Lisbon gas plant in foreground, and the Abajo Mountains in the distance; view to the southwest.*



**Miscellaneous Publication 10-2  
UTAH GEOLOGICAL SURVEY**

*a division of*

**UTAH DEPARTMENT OF NATURAL RESOURCES**

**2010**

**STATE OF UTAH**

Gary R. Herbert, Governor

**DEPARTMENT OF NATURAL RESOURCES**

Michael Styler, Executive Director

**UTAH GEOLOGICAL SURVEY**

Richard G. Allis, Director

**PUBLICATIONS**

contact

Natural Resources Map & Bookstore

1594 W. North Temple

Salt Lake City, UT 84114

telephone: 801-537-3320

toll-free: 1-888-UTAH MAP

Web site: [mapstore.utah.gov](http://mapstore.utah.gov)

email: [geostore@utah.gov](mailto:geostore@utah.gov)

**UTAH GEOLOGICAL SURVEY**

contact

1594 W. North Temple, Suite 3110

Salt Lake City, UT 84114

telephone: 801-537-3300

Web site: [geology.utah.gov](http://geology.utah.gov)

*The Miscellaneous Publication series provides non-UGS authors with a high-quality format for documents concerning Utah geology. Although review comments have been incorporated, this document does not necessarily conform to UGS technical, editorial, or policy standards. The Utah Department of Natural Resources, Utah Geological Survey, makes no warranty, expressed or implied, regarding the suitability of this product for a particular use. The Utah Department of Natural Resources, Utah Geological Survey, shall not be liable under any circumstances for any direct, indirect, special, incidental, or consequential damages with respect to claims by users of this product.*

## FORWARD

In 2003, the Utah Geological Survey (UGS) began a five-year study of the Mississippian Leadville Limestone in the northern Paradox Basin, referred to as the Paradox fold and fault belt, of Utah and Colorado. The UGS was the lead agency over a multidisciplinary team funded in part through the U.S. Department of Energy (DOE), National Energy Technology Laboratory's Advanced and Key Oilfield Technologies for Independents (Area 2 – Exploration) Program. The Leadville has produced over 53 million barrels (bbls) of oil/condensate (8.4 million m<sup>3</sup>) and 854 billion cubic feet of gas (24 billion m<sup>3</sup>) from seven fields in the Paradox fold and fault belt. All of these fields are currently operated by independent producers. Only independent producers continue to explore for Leadville targets in the region, 85% of which is under the stewardship of the federal government.

A key objective of the study was to conduct low-cost demonstrations of new exploration technologies to identify surface geochemical anomalies that represent potential hydrocarbon-prone areas especially in the environmentally sensitive Paradox Basin. This objective is designed to assist the independent producers and explorers who have limited financial and personnel resources. The overall goals of this study were to (1) develop and demonstrate techniques and exploration methods never tried on the Leadville Limestone, (2) target areas for exploration, (3) reduce exploration costs and risk especially in environmentally sensitive areas, and (4) add new discoveries and reserves.

Exploring the Leadville Limestone is high risk, with less than a 10% chance of success based on the drilling history of the region. Prospect definition often requires expensive, three-dimensional (3D) seismic acquisition, at times in environmentally sensitive areas. These facts make exploring difficult for independents that have limited funds available to try new, unproven techniques that might increase the chance of successfully discovering hydrocarbons. We believe that one or more of the study results will reduce the risk taken by an independent producer in looking for Leadville oil and gas, not only in exploring but also in using a new technique. For example, an independent would not likely attempt surface geochemical surveys without first knowing they have been proven successful in the region. Our study demonstrates geochemical surveys are an effective technique in environmentally sensitive areas, thus saving independents both time and money exploring for Leadville hydrocarbons.



## CONTENTS

|                                                                                   |     |
|-----------------------------------------------------------------------------------|-----|
| FORWARD .....                                                                     | iii |
| ABSTRACT .....                                                                    | 1   |
| INTRODUCTION .....                                                                | 2   |
| GENERAL GEOLOGY AND HYDROCARBON PRODUCTION .....                                  | 7   |
| Lisbon Field Synopsis .....                                                       | 8   |
| Lightning Draw Southeast Field Synopsis .....                                     | 8   |
| SURFACE JOINTING .....                                                            | 12  |
| METHODS USED IN THE GEOCHEMICAL SURVEY .....                                      | 14  |
| Sample Collection .....                                                           | 14  |
| Collection of Surface Soils .....                                                 | 16  |
| Collection of Fracture-Fill Lichen, Bryophyte, and Soil .....                     | 19  |
| Collection of 6-Foot-Deep Free-Gas Samples .....                                  | 19  |
| Laboratory Analysis .....                                                         | 19  |
| Interpretation and Mapping .....                                                  | 19  |
| RESULTS OF THE GEOCHEMICAL SURVEY .....                                           | 23  |
| Thermally Desorbed Hydrocarbons: Surface Soils .....                              | 23  |
| Absolute Hydrocarbon Concentrations .....                                         | 23  |
| Discriminant Analysis Results .....                                               | 26  |
| Three-Component Discriminant Analysis .....                                       | 26  |
| Two-Component Discriminant Analysis .....                                         | 26  |
| Thermally Desorbed Hydrocarbons: Fracture-Fill Bryophyte, Lichen, and Soils ..... | 31  |
| Fracture-Fill Bryophyte and Lichen .....                                          | 31  |
| Fracture-Fill Soils .....                                                         | 37  |
| Fluorescence of Solvent-Extractable Aromatic Hydrocarbons (Surface Soils) .....   | 37  |
| Hydrocarbons and Fixed Gases (Free-Gas Samples) .....                             | 43  |
| Acid-Extractable Metals (Soils and Fracture-Fillings) .....                       | 45  |
| DISCUSSION .....                                                                  | 53  |
| Hydrocarbon Anomalies .....                                                       | 53  |
| Discriminant Analysis Models .....                                                | 53  |
| Free Gas Results .....                                                            | 56  |
| Trace Metal and Anion Results .....                                               | 56  |
| SUMMARY AND RECOMMENDATIONS .....                                                 | 56  |
| ACKNOWLEDGMENTS .....                                                             | 59  |
| REFERENCES .....                                                                  | 59  |
| APPENDIX A - SURFACE SOILS - C <sub>1</sub> -C <sub>12</sub> DATA .....           | 62  |
| APPENDIX B - SURFACE SOILS - SSF DATA .....                                       | 62  |
| APPENDIX C - SURFACE SOILS - ELEMENTAL DATA .....                                 | 62  |
| APPENDIX D - FRACTURE-FILL BRYOPHYTE AND LICHEN DATA .....                        | 62  |
| APPENDIX E - FRACTURE-FILL SOIL DATA .....                                        | 62  |
| APPENDIX F - FREE-GAS SAMPLE DATA .....                                           | 62  |

## FIGURES

|                                                                                                                                                   |    |
|---------------------------------------------------------------------------------------------------------------------------------------------------|----|
| Figure 1. Regional setting and oil and gas fields .....                                                                                           | 3  |
| Figure 2. Location of oil and gas fields that produce from the Mississippian Leadville Limestone, Utah and Colorado .....                         | 4  |
| Figure 3. General surface geology of the Lisbon field area .....                                                                                  | 5  |
| Figure 4. Detailed cross section through the Lisbon and Lightning Draw Southeast fields .....                                                     | 6  |
| Figure 5. Cross-sectional model of hydrocarbon microseepage-related alteration over petroleum deposits .....                                      | 7  |
| Figure 6. Paleozoic stratigraphic section for the central Paradox Basin near Monticello .....                                                     | 8  |
| Figure 7a. Top of structure of the Leadville Limestone, Lisbon field .....                                                                        | 9  |
| Figure 7b. Top of structure of the Leadville Limestone superimposed over the topographic base and Lisbon field outline .....                      | 10 |
| Figure 8a. Structure contour map of the Leadville Limestone, Lightning Draw Southeast field .....                                                 | 11 |
| Figure 8b. Top of structure of the Leadville Limestone superimposed over the topographic base and Lightning Draw<br>Southeast field outline ..... | 12 |
| Figure 9. Subvertical joints in the Triassic-Jurassic Wingate Sandstone from Lisbon field .....                                                   | 13 |
| Figure 10. Examples of joints in the Lisbon field area .....                                                                                      | 13 |

|                                                                                                                                                                                                                                          |    |
|------------------------------------------------------------------------------------------------------------------------------------------------------------------------------------------------------------------------------------------|----|
| Figure 11. Bryophyte (moss) and lichen that commonly grow along thin, moisture-rich joints in sandstone, Lisbon area .....                                                                                                               | 14 |
| Figure 12. Joint orientations at sample localities over the gas cap, oil leg, and water leg of Lisbon field.....                                                                                                                         | 15 |
| Figure 13. Joint orientations at sample localities near the Lightning Draw Southeast field.....                                                                                                                                          | 15 |
| Figure 14. Distribution of grid, line, and training set soil samples collected over and around the Lisbon and Lightning Draw<br>Southeast fields .....                                                                                   | 17 |
| Figure 15. Sampling methods used in the Lisbon/Lightning Draw Southeast area.....                                                                                                                                                        | 18 |
| Figure 16. The Lisbon No. C-910 gas well and sample site .....                                                                                                                                                                           | 19 |
| Figure 17. Fracture-fill bryophyte, lichen, and soil sample locations over the Lisbon gas cap, oil leg, and water leg, and over<br>the Lightning Draw Southeast field .....                                                              | 20 |
| Figure 18. Location of 6-foot-deep free-gas samples over and off Lightning Draw Southeast field .....                                                                                                                                    | 21 |
| Figure 19. Schematic of synchronous scanned fluorescence spectra depicting the aromatic hydrocarbons and corresponding<br>emission wavelengths .....                                                                                     | 22 |
| Figure 20. Distribution of toluene Z-scores in surface soils over the Lisbon and Lightning Draw Southeast fields .....                                                                                                                   | 25 |
| Figure 21. Surface soil training set samples used for three-component Lisbon gas cap versus oil leg versus water leg<br>discriminant analysis model .....                                                                                | 27 |
| Figure 22. Distribution of Lisbon gas-oil probabilities derived from three-component discriminant analysis of thermally<br>desorbed C <sub>1</sub> to C <sub>12</sub> hydrocarbons from surface soils .....                              | 28 |
| Figure 23. Distribution of Lisbon oil probabilities derived from three-component discriminant analysis of thermally desorbed<br>C <sub>1</sub> to C <sub>12</sub> hydrocarbon from surface soils .....                                   | 29 |
| Figure 24. Surface soil training set samples used for two component Lisbon gas cap/oil leg versus water leg and Lightning<br>Draw Southeast gas versus Lisbon water leg discriminant analysis models .....                               | 30 |
| Figure 25. Distribution of Lisbon gas-oil probabilities derived from two-component discriminant analysis of thermally desorbed<br>C <sub>1</sub> to C <sub>12</sub> hydrocarbon from surface soils.....                                  | 32 |
| Figure 26. Distribution of Lightning Draw Southeast gas probabilities derived from two-component discriminant analysis of<br>thermally desorbed C <sub>1</sub> to C <sub>12</sub> hydrocarbon from surface soils.....                    | 33 |
| Figure 27. Bryophyte and lichen training set samples used for three-component Lisbon gas cap versus oil leg versus water leg<br>and two-component Lightning Draw Southeast gas versus Lisbon water leg discriminant analysis models..... | 34 |
| Figure 28. Distribution of Lisbon gas probability derived from three-component discriminant analysis of thermally desorbed<br>C <sub>1</sub> to C <sub>12</sub> hydrocarbon from bryophyte and lichen samples .....                      | 35 |
| Figure 29. Distribution of Lisbon oil probability derived from three-component discriminant analysis of thermally desorbed<br>C <sub>1</sub> to C <sub>12</sub> hydrocarbon from bryophyte and lichen samples.....                       | 36 |
| Figure 30. Distribution of Lightning Draw Southeast gas probabilities derived from two-component discriminant analysis of<br>thermally desorbed C <sub>1</sub> to C <sub>12</sub> hydrocarbon from bryophyte and lichen samples.....     | 38 |
| Figure 31. Fracture-fill soil training set samples used for three-component Lisbon gas cap versus oil leg versus water leg and<br>two-component Lightning Draw Southeast gas versus Lisbon water leg discriminant analysis models.....   | 39 |
| Figure 32. Distribution of Lisbon gas probability derived from three-component discriminant analysis of thermally desorbed<br>C <sub>1</sub> to C <sub>12</sub> hydrocarbon from fracture-fill soil samples.....                         | 40 |
| Figure 33. Distribution of Lisbon oil probability derived from three-component discriminant analysis of thermally desorbed<br>C <sub>1</sub> to C <sub>12</sub> hydrocarbon from fracture-fill soil samples .....                        | 41 |
| Figure 34. Distribution of Lightning Draw Southeast gas probabilities derived from two-component discriminant analysis of<br>thermally desorbed C <sub>1</sub> to C <sub>12</sub> hydrocarbon from fracture-fill soil samples.....       | 42 |
| Figure 35. Synchronous scanned fluorescence spectra of high, medium, and low gravity oil .....                                                                                                                                           | 43 |
| Figure 36. Distribution of 395 to 470 nm factor scores in surface soils over Lisbon and Lightning Draw Southeast fields .....                                                                                                            | 44 |
| Figure 37. Distribution of propane concentrations in 6-foot-deep free gas over Lightning Draw Southeast field and<br>background areas.....                                                                                               | 46 |
| Figure 38. Distribution of isohexane concentrations in 6-foot-deep free gas over Lightning Draw Southeast field and<br>background areas.....                                                                                             | 47 |
| Figure 39. Distribution of hydrogen concentrations in 6-foot-deep free gas over Lightning Draw Southeast field and<br>background areas .....                                                                                             | 48 |
| Figure 40. Distribution of carbon dioxide concentrations in 6-foot-deep free gas over Lightning Draw Southeast field and<br>background areas.....                                                                                        | 49 |
| Figure 41. Distribution of helium concentrations in 6-foot-deep free gas over Lightning Draw Southeast field and background areas .....                                                                                                  | 50 |
| Figure 42. Distribution of cadmium-uranium-molybdenum-vanadium-manganese-lead factor scores in surface soils over<br>Lisbon and Lightning Draw Southeast fields .....                                                                    | 51 |
| Figure 43. Distribution of mercury-organic carbon-lead factor scores in surface soils over Lisbon and Lightning Draw<br>Southeast fields.....                                                                                            | 52 |
| Figure 44. Distribution of fluoride Z-scores in surface soils over Lisbon and Lightning Draw Southeast fields .....                                                                                                                      | 54 |
| Figure 45. Distribution of arsenic Z-scores in surface soils over Lisbon and Lightning Draw Southeast fields .....                                                                                                                       | 55 |

|                                                                                                                                                                                                     |    |
|-----------------------------------------------------------------------------------------------------------------------------------------------------------------------------------------------------|----|
| Figure 46. Distribution of hydrocarbon and fixed-gas anomalies in free gas over Lightning Draw Southeast field .....                                                                                | 57 |
| Figure 47. Distribution of cadmium-uranium-molybdenum-vanadium-manganese-lead factor scores in surface soils over<br>Lisbon and Lightning Draw Southeast fields and location of uranium mines ..... | 58 |

TABLES

|                                                                                                                                         |    |
|-----------------------------------------------------------------------------------------------------------------------------------------|----|
| Table 1. Produced gas compositions from Lisbon and Lightning Draw Southeast fields .....                                                | 10 |
| Table 2. Components reported by four analytical methods .....                                                                           | 22 |
| Table 3. Organic and inorganic anomaly types identified in different sample media over Lisbon and Lightning Draw Southeast fields ..... | 24 |
| Table 4. Correct and incorrect classifications for discriminant models (surface soils).....                                             | 26 |
| Table 5. Correct and incorrect classifications for discriminant models (fracture-fill bryophyte and lichen) .....                       | 31 |
| Table 6. Correct and incorrect classifications for discriminant models (fracture-fill soils).....                                       | 37 |
| Table 7. Percent of anomalous free-gas samples over and off Lightning Draw Southeast field .....                                        | 45 |
| Table 8. Percent of anomalous soil samples over and off Lisbon and Lightning Draw Southeast fields .....                                | 45 |

# NEW TECHNIQUES FOR NEW HYDROCARBON DISCOVERIES— SURFACE GEOCHEMICAL SURVEYS IN THE LISBON AND LIGHTNING DRAW SOUTHEAST FIELD AREAS, SAN JUAN COUNTY, UTAH

by

*David M. Seneshen, Thomas C. Chidsey, Jr., Craig D. Morgan, and Michael D. Vanden Berg*

## ABSTRACT

Exploration for Mississippian Leadville Limestone-hosted hydrocarbon reservoirs in the Paradox Basin is high risk in terms of cost and low documented success rates (~10% based on drilling history). Only 100 wells have penetrated the Leadville over an area of 7500 mi<sup>2</sup> (19,400 km<sup>2</sup>), which equates to about one well per township. The potential for more hydrocarbon reserves is thus enormous, but the high cost of three-dimensional (3D) seismic exploration methods in environmentally sensitive areas deters small independents from exploring for Leadville hydrocarbon reservoirs.

Surface geochemical surveys have helped identify areas of poorly drained or by-passed oil in other basins. This study was therefore initiated to evaluate the effectiveness of low-cost, innovative, non-invasive, surface geochemical methods for predicting the presence of underlying Leadville hydrocarbon reservoirs. Lisbon field, San Juan County, Utah, was chosen for testing because it is the largest Leadville oil and gas producer in the Paradox Basin, sample sites are relatively easily accessible, and the surface geology is similar to the structure of the field. Also selected was a nearby Leadville field (Lightning Draw Southeast, also in San Juan County, Utah), which has similar geology to Lisbon field in terms of Leadville reservoir lithology and structure but with nearly virgin reservoir pressure. In comparison with Lisbon, Lightning Draw Southeast is smaller, has more nitrogen and helium, and contains productive intervals in the overlying Ismay zone of the Pennsylvanian Paradox Formation.

The geochemical survey consisted of collecting shallow soil samples over and around the fields covering the gas cap, oil leg (present only at Lisbon field), and background "barren" areas to map the spatial distribution of potential surface hydrocarbon anomalies. In addition, samples were collected near oil, gas, and dry wells for analogue matching purposes and to refine the discriminant model for the fields. Free-gas samples were also collected over Lightning Draw Southeast field and known non-productive areas off the structure. Finally, joints in the Jurassic Navajo and Entrada Sandstones may provide pathways for hydrocarbon microseepage to the surface. Therefore, soil, sand, bryophyte (moss), and lichen samples were collected along joints for geochemical analyses. Samples were analyzed for 39 hydrocarbon compounds in the C<sub>1</sub> to C<sub>12</sub> range, 53 major and trace elements, seven anion species, and synchronous scanned fluorescence intensities. Free-gas samples were analyzed for fixed gases and hydrocarbons.

The main conclusion of the study is that certain surface geochemical methods can discriminate between productive and non-productive Leadville reservoirs. Variables in surface soils and fracture-fill bryophyte, lichen, and soils that best distinguish productive and non-productive areas are light (C<sub>1</sub> to C<sub>6</sub>) alkane and heavy (C<sub>24</sub> to C<sub>36</sub>) aromatic hydrocarbons. The volatile and liquid hydrocarbons presumably ascend to the surface along faults within and at the margins of the fields. Mercury and lead are indirect indicators of hydrocarbon microseepage and they could be derived from the oil itself. Helium and carbon dioxide anomalies in free-soil gas at the margins of Leadville reservoirs could be the most diagnostic indicators of underlying Leadville

reservoirs. These gases are enriched in Leadville reservoirs as compared with overlying productive intervals in the Ismay zone of the Pennsylvanian Paradox Formation. Anomalous hydrocarbons, carbon dioxide, and hydrogen in free gas over Lightning Draw Southeast field may be derived from productive intervals within the Paradox, Leadville, or a combination of reservoirs in both formations.

Cost-effective regional exploration for Leadville reservoirs would first involve the collection and analysis of surface soils and/or fracture-fill soil, bryophyte, and lichen for thermally desorbed and solvent-extractable hydrocarbons. Anomalous areas could then be followed up with the collection of deep free-gas samples at short (<300 feet [100 m]) intervals and analysis of the gas for diagnostic indicators of Leadville reservoirs (that is, helium and carbon dioxide). Areas with anomalous helium and carbon dioxide in free gas could then be further explored with 3D seismic to define drillable structures.

## INTRODUCTION

The Mississippian (late Kinderhookian to early Meramecian) Leadville Limestone has produced over 53 million barrels (bbls) of oil/condensate (8.4 million m<sup>3</sup>) and 584 billion cubic feet (BCF) of gas (24 billion m<sup>3</sup>) as of November 1, 2009, from seven fields in the northern Paradox Basin region (Colorado Oil and Gas Conservation Commission, 2009; Utah Division of Oil, Gas, and Mining, 2009), referred to as the Paradox fold and fault belt, of southeast Utah and southwest Colorado (figure 1). Exploration for Leadville-hosted hydrocarbon reservoirs in the Paradox Basin is high risk in terms of cost and low documented success rates (~10% based on drilling history). Only 100 wells have penetrated the Leadville over an area of 7500 mi<sup>2</sup> (19,400 km<sup>2</sup>), which equates to about one well per township. The potential for more hydrocarbon reserves is thus enormous, but the high cost of three-dimensional (3D) seismic exploration methods in environmentally sensitive areas, with extensive outcrops, deters small independents from exploring for Leadville hydrocarbon reservoirs.

Surface exploration methods, such as geochemical, magnetic, and remote sensing, have increasingly proven to significantly reduce petroleum exploration risks and finding costs. These methods, and numerous case histories, are summarized by Schumacher and LeSchack (2002). Surface geochemical surveys in the Michigan and Williston Basins helped identify areas of poorly drained or by-passed oil in pinnacle reef fields (Wood and others, 2001, 2002), whose depositional environments are comparable in many aspects to those of the Leadville Limestone in the Paradox Basin. Surface geochemical methods detected hydrocarbon microseepage over Grant Canyon field, Nevada, and these methods are also being used to define potential faulted, carbonate reservoirs in western Utah (Seneshen and others, 2006). Anomalies are relatively easy to identify and are conclusive about the presence of subsurface hydrocarbon deposits.

Lisbon field, San Juan County, Utah, (figure 2) is ideal for a surface geochemical survey. Besides active hydrocarbon production from beneath the easily accessible area, the surface geology is similar to the subsurface structure of the field (figures 3 and 4). In addition, nearby Lightning Draw Southeast field, San Juan County, Utah (figures 3 and 4), is also accessible and is at or near original reservoir pressure making it an excellent test site to evaluate hydrocarbon seepage in comparison with that at Lisbon.

Remote sensing studies over Lisbon field have documented the presence of seep induced alteration to near surface soils and sediments (Merin and Segal, 1989; Segal and Merin, 1989). Other work has shown the potential of remote-sensing techniques for identifying kaolinite-enriched, bleached redbed Triassic-Jurassic Wingate sandstones over productive parts of Lisbon field (Connel and Alley, 1985; Segal and others, 1986). These studies used Landsat Thematic Mapper (TM) data to recognize the presence of kaolinite as well as reduced iron (that is, bleached redbed sandstones). A ratio of TM bands 2/3 was used to define variations in ferric iron content, while a band 5/7 ratio was used to highlight variations in clay content. Because vegetation also exhibits high band 2/3 ratio values, it can be confused with bleached rocks. Vegetation also shows high band 5/7 ratio values that can be confused with clay-rich rocks. Other than this work, there are no published surface geochemical studies in the Lisbon field area. The Utah Geological Survey (UGS) therefore initiated this study to test the effectiveness of several conventional and unconventional surface geochemical methods in the Lisbon area. The main objective for testing these techniques was to find effective, low-cost, non-invasive geochemical exploration methods to prescreen large areas of the Paradox Basin for subsequent geophysical surveys and lease acquisition, and also act as a follow-up to classify geophysical anomalies as "productive or barren," specifically for the Leadville Limestone or other subsurface reservoir exploration programs.

The premise behind surface geochemical exploration for petroleum is that light volatile hydrocarbons (that is, C<sub>1</sub> to C<sub>5</sub>) ascend rapidly to the surface from a pressured reservoir as buoyant colloidal-size "microbubbles" along water-filled fractures, joints, and bedding planes (Price, 1986; Klusman, 1993; Saunders and others, 1999). Studies over gas-storage reservoirs support the rapid development of soil-gas hydrocarbon anomalies over a charged reservoir, and the rapid depletion of such anomalies once the reservoir has been depleted (Coleman and others, 1977). Partial aerobic and anaerobic bacterial consumption of the ascending hydrocarbons produces carbon dioxide and hydrogen sulfide that can significantly alter the chemical and mineralogical composition of overlying sediments (Schumacher, 1996). Changes to overlying soils and sediments can include (1) precipitation of isotopically light calcite, pyrite, pyrrhotite, and uranium, sulfur, and iron (magnetic) oxides, (2) bleaching of redbeds through the removal of Fe<sup>3+</sup> by reduced fluids, (3) conversion of illitic clays and feldspars to kaolinite and removal of potassium by acidic, reduced fluids, and (4) variations in the major and trace element chemistry of soil and vegetation (Saunders and others, 1999). Chemical reactions that produce the various minerals found in "reduced chimneys" above petroleum reservoirs are shown in figure 5.



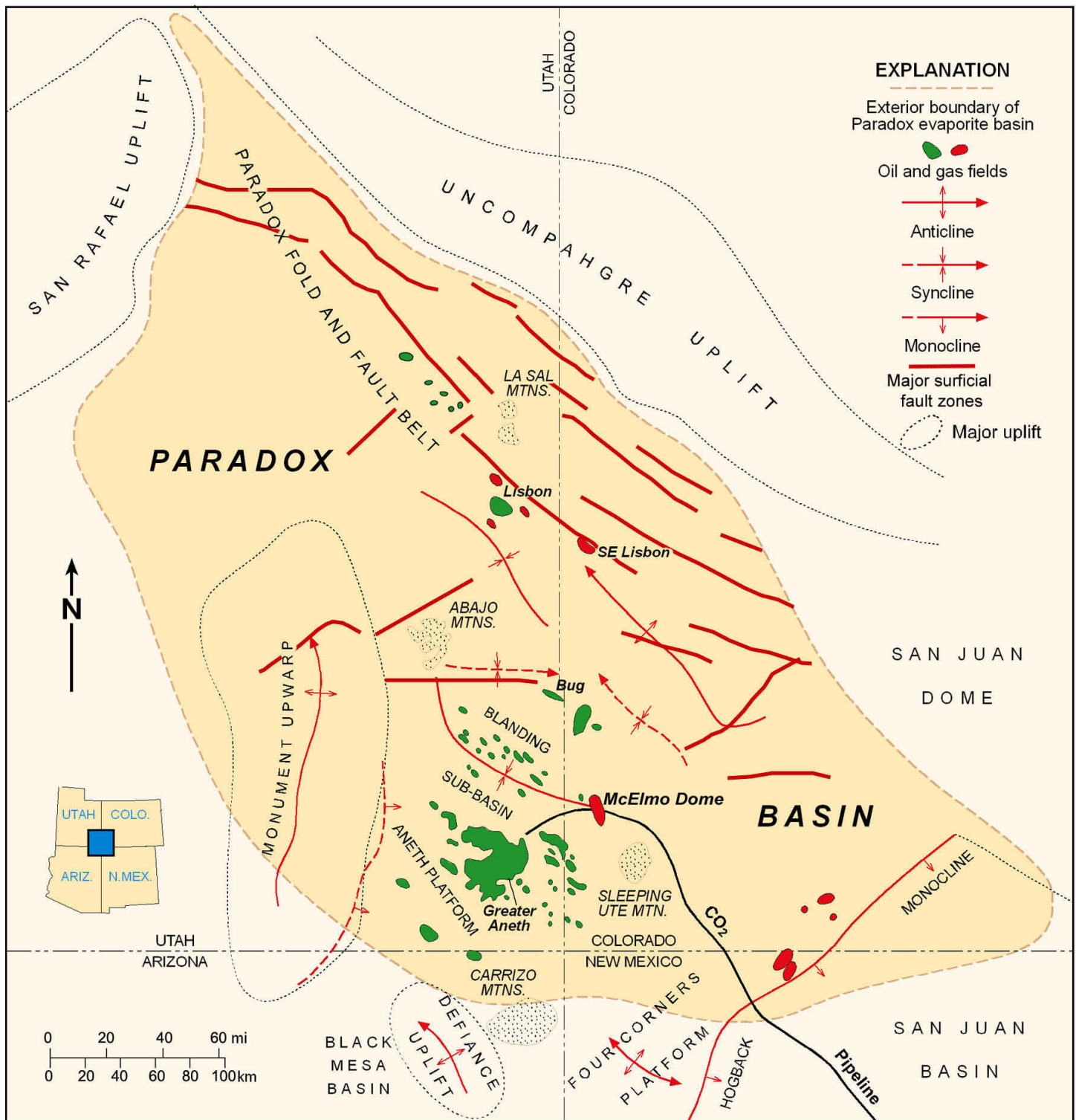


**Figure 1.** Regional setting and oil (green) and gas (red) fields in the Paradox Basin of Utah, Colorado, Arizona, and New Mexico (modified from Kitcho, 1981; Harr, 1996).

Various techniques have been tested over oil and gas reservoirs to search for direct and indirect indications of hydrocarbon micro-seepage. These techniques include analysis of (1) soil hydrocarbon fluorescence (Herbert, 1984), (2) hydrocarbons adsorbed to and occluded in soils (Horvitz, 1985), (3) delta C and soil salts (Duchscherer, 1986), (4) major and trace elements of soils (Duchscherer,

1984), (5) hydrocarbon-consuming bacteria in soils (Price, 1993), (6) gas concentrations (for example, hydrocarbons, helium) and stable isotopic composition of hydrocarbons in pore-space soil air (Roberts and others, 1976; Bammel and others, 1994), (7) passive gas collections (Potter and others, 1996), and (8) vegetation for trace elements (Klusman and others, 1992).

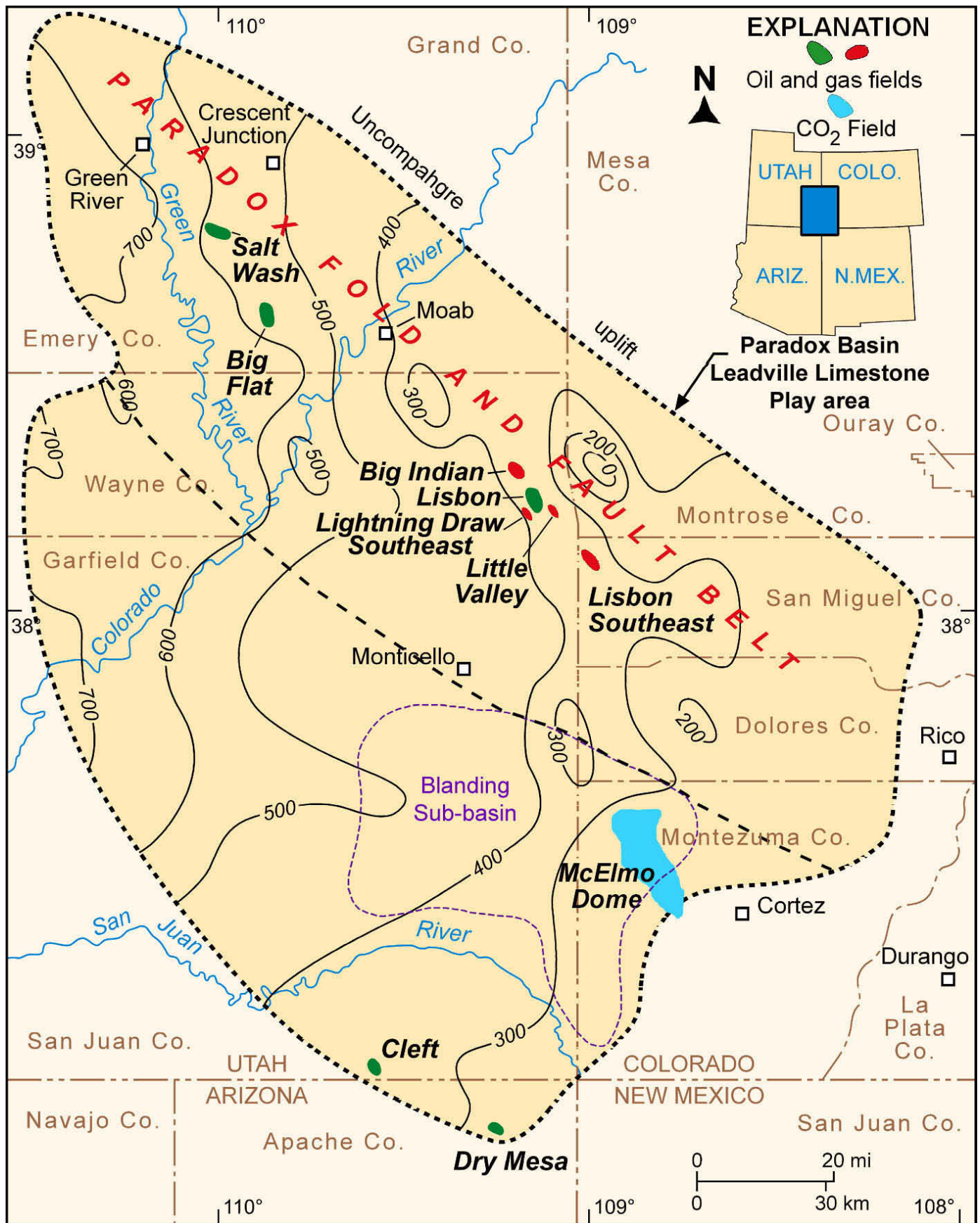


**Figure 2.** Location of oil and gas fields that produce from the Mississippian Leadville Limestone, Utah and Colorado. Thickness of the Leadville is shown; contour interval is 100 feet (modified from Parker and Roberts, 1963).



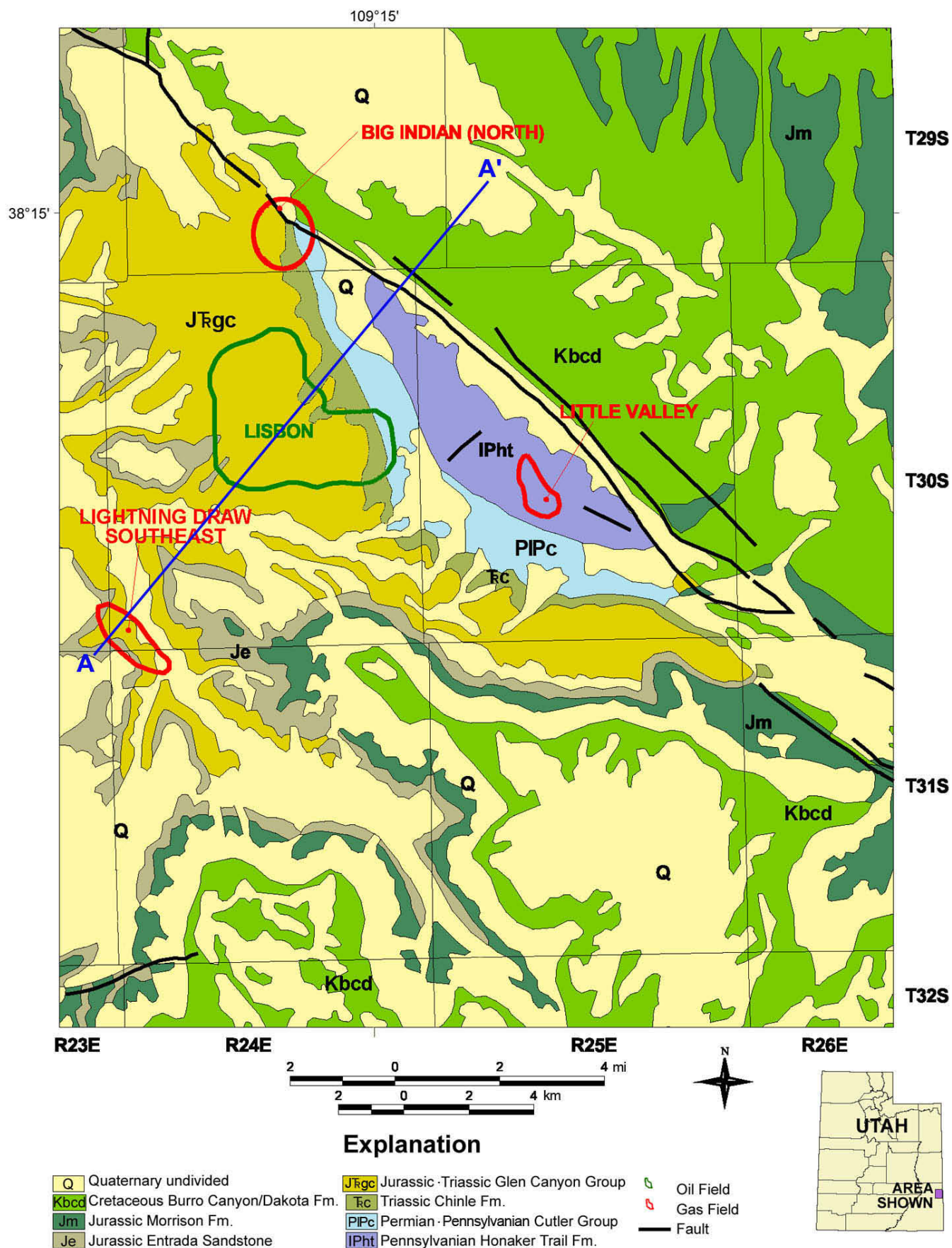
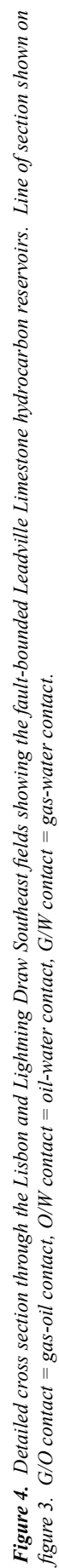
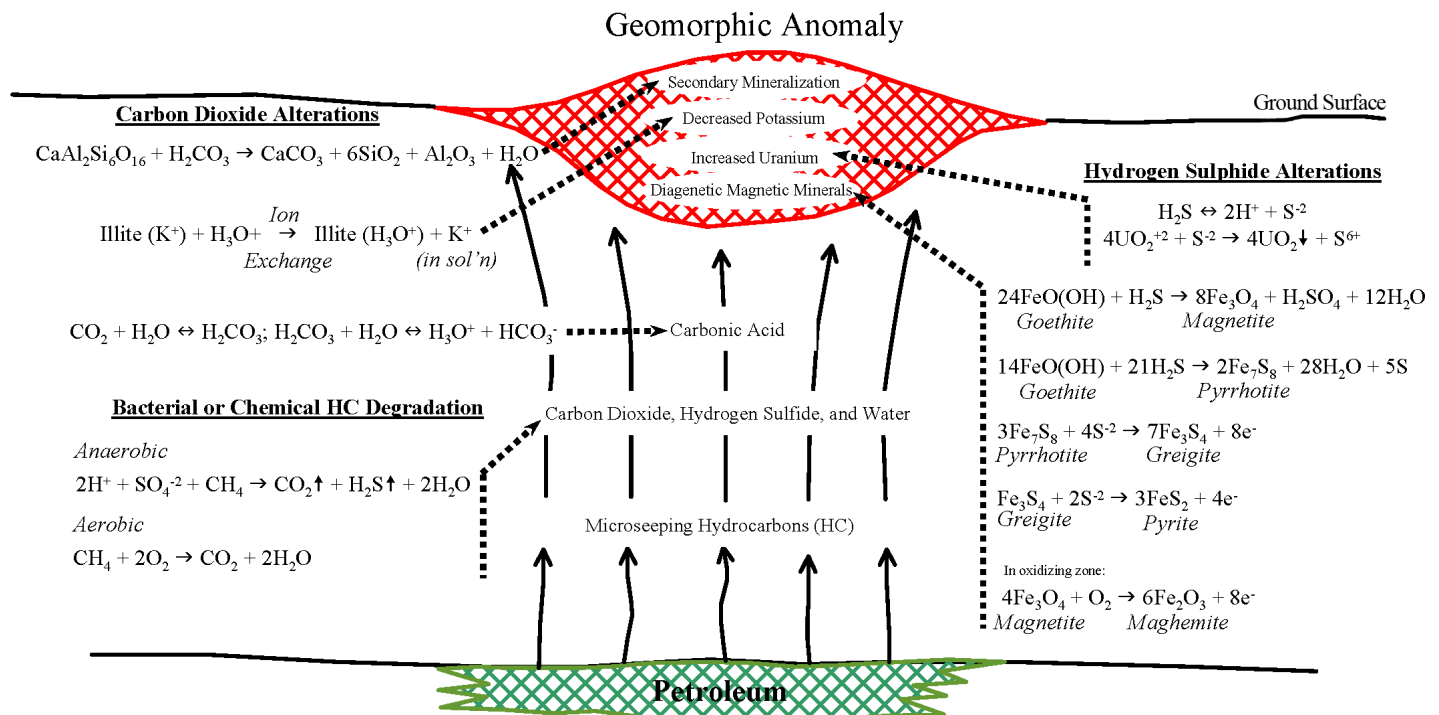


Figure 3. General surface geology of the Lisbon field area (modified from Hintze and others, 2000). Cross section A-A' shown on figure 4.



**Figure 4.** Detailed cross section through the Lisbon and Lightning Draw Southeast fields showing the fault-bounded Leadville Limestone hydrocarbon reservoirs. Line of section shown on figure 3. G/O contact = gas-oil contact, O/W contact = oil-water contact, G/W contact = gas-water contact.



**Figure 5.** Cross-sectional model of hydrocarbon microseepage-related alteration over petroleum deposits (after Saunders and others, 1999), by permission of the American Association of Petroleum Geologists.

Time and budget constraints did not allow for testing of all of the above-mentioned techniques. The direct and indirect geochemical methods chosen for testing over the Lisbon area were based on the available sample media, composition of produced gas, and analytical methods offered by Direct Geochemical at the time. For example, the produced Leadville gas is rich in carbon dioxide and helium compared with overlying formations. It was therefore decided to analyze free-gas samples over Lightning Draw Southeast field for carbon dioxide and helium in addition to hydrocarbons. Direct methods included the assessment of hydrocarbon compositional signatures in surface soils, fracture-fill soils, bryophyte (moss), and lichen, and 6-foot (2-m) deep free-gas samples. Indirect methods are those not related to hydrocarbons, such as the evaluation of major/trace element and anion chemistry of surface soils and fracture-fill soils, bryophyte, and lichen to look for alteration effects resulting from hydrocarbon microseepage.

This surface geochemical study over Leadville hydrocarbon reservoirs focused on testing both "direct and indirect" methods over known "productive and non-productive areas." The techniques tested in this study are termed "new" mainly because they have not been tested previously in the Lisbon area. Some of the sampling and analytical techniques are in fact methods that have not been previously employed for hydrocarbon exploration. One truly new technique tested is Direct Geochemical's proprietary thermal desorption hydrocarbon analysis of soil samples and the unique interpretation of the data. Also, organic and inorganic

analyses of fracture-fill vegetation is introduced here as a new technique for geochemical exploration for oil and gas reservoirs.

## GENERAL GEOLOGY AND HYDROCARBON PRODUCTION

The Paradox Basin is located mainly in southeastern Utah and southwestern Colorado, with a small portion in northeastern Arizona and northwestern New Mexico (figure 1). The basin is an elongate, northwest-southeast-trending, evaporitic basin that predominately developed during the Pennsylvanian. The Mississippian Leadville Limestone is one of two major oil and gas reservoirs in the Paradox Basin, the other being the Pennsylvanian Paradox Formation (figure 6); minor amounts of oil are produced from the Devonian McCracken Sandstone at Lisbon field.

Lisbon, Big Indian, Little Valley, and Lightning Draw Southeast fields (figures 3 and 4) are anticlines that close against the Lisbon or other fault zones. The Leadville reservoirs in Lisbon and Lightning Draw Southeast fields are separated from upper Paleozoic and Mesozoic strata by cyclic evaporites in the Pennsylvanian Paradox Formation (figure 6). These conditions are typical of what might be expected when exploring for similar drilling targets in the basin. Three factors create reservoir heterogeneity within productive zones: (1) variations in carbonate fabrics and facies, (2) diagenesis (including karstification and late-stage bitumen plugging), and (3) fracturing. The extent of these factors and how they are combined



| Age  | Stratigraphic Unit  |                    | Thickness | Lithology | Products          |
|------|---------------------|--------------------|-----------|-----------|-------------------|
| PENN | Hermosa Group       | Paradox Fm         | 0-14,000' |           | potash & salt<br> |
|      |                     | Pinkerton Trail Fm | 0-150'    |           |                   |
|      | Molas Formation     |                    | 0-100'    |           |                   |
| M    | Leadville Limestone |                    | 300-600'  |           |                   |
| DEV  | Ouray Limestone     |                    | 0-150'    |           |                   |
|      | Elbert Formation    |                    | 100-200'  |           |                   |
|      | McCracken Ss M      |                    | 25-100'   |           |                   |
| Є    | "Lynch" Dolomite    |                    | 800-1000' |           |                   |

Oil and gas production; Condensate and oil production

**Figure 6.** Paleozoic stratigraphic section for the central Paradox Basin near Monticello, Utah (after Hintze and Kowallis, 2009).

affect the degree to which they create barriers to fluid flow laterally and vertically—possibly to the surface.

### Lisbon Field Synopsis

Lisbon field (figure 2) accounts for most of the Leadville oil and gas production in the Paradox Basin. The reservoir characteristics, particularly its diagenetic overprinting and history, and Leadville lithofacies can be applied regionally to other fields and exploration trends in the Paradox Basin. A major northwest-southeast-trending anticline (tens of miles in length) along the Lisbon fault displaces the Pennsylvanian Honaker Trail Formation against Cretaceous strata (figures 3 and 4). The Lisbon trap is an elongate, asymmetric, northwest-trending anticline, with nearly 2000 feet (600 m) of structural closure and bounded on the northeast flank by a major, basement-involved normal fault with over 2500 feet (760 m) of displacement (Smith and Prather, 1981) (figures 4, 7A, and 7B). Several minor, northeast-trending normal faults divide the Lisbon Leadville reservoir into compartments.

Producing units in Lisbon field contain dolomitized crinoidal/skeletal grainstone, packstone, and wackestone fabrics. Diagenesis includes fracturing, autobrecciation, karst development, hydrothermal dolomite, and bitumen plugging. The net reservoir thickness is 225 feet (69 m) over a 5120-acre (2100 ha) area (Clark, 1978; Smouse, 1993). Reservoir quality is greatly improved by natural fracture systems associated with the Paradox fold and fault belt. Porosity averages 6% in intercrystalline and moldic networks enhanced by fractures; permeability averages 22 millidarcies (mD). The drive mechanism is an expanding gas cap and gravity drainage; original water saturation was 39% (Clark, 1978; Smouse, 1993). The bottom-hole temperature ranges from 133 to 189°F (56–87°C).

Lisbon field was discovered in 1960 with the completion of the Pure Oil Company No. 1 NW Lisbon USA well, NE1/4NW1/4 section 10, T. 30 S., R. 24 E., Salt Lake Base Line and Meridian (SLBL&M) (figure 7), with an initial flowing potential (IFP) of 179 bbls of oil per day (BOPD) (28 m<sup>3</sup>) and 4376 thousand cubic feet of gas per day (124 MCMPD). The original reservoir field pressure was 2982 pounds per square inch (psi [20,560 kPa]) (Clark, 1978). Currently, 20 producing (or shut-in) wells, 11 abandoned producers, five injection wells (four gas injection wells and one water/gas injection well), and four dry holes are in the field. Cumulative production as of November 1, 2009, was 51,175,570 bbls of oil (8,136,916 m<sup>3</sup>), 800.1 BCF of gas (22.7 BCMG) (cycled gas), and 50,532,717 bbls of water (BW) (8,034,702 m<sup>3</sup>) (Utah Division of Oil, Gas, and Mining, 2009). Hydrocarbon gas that was re-injected into the crest of the structure to control pressure decline is now being produced; acid gas is still re-injected. The overlying Pennsylvanian Paradox Formation is not productive over any part of the Lisbon field. The cumulative production and composition of produced gas from the Lisbon gas cap and oil leg are given in table 1.

### Lightning Draw Southeast Field Synopsis

Four miles (6.4 km) to the southwest of Lisbon field, Lightning Draw Southeast field (figure 2) is similar to Lisbon in terms of Leadville reservoir lithology and structure but with nearly virgin reservoir pressure. Lightning Draw Southeast (LDSE) field consists of two Leadville wells producing, primarily gas and condensate, along with barren dry wells off structure (figures 8A and 8B). Like the Lisbon trap, the LDSE trap is also an elongate, but relatively small, asymmetric, northwest-trending anticline (no surface expression), with nearly 250 feet (75 m) of structural closure. The structure is bounded on the southwest flank by a high-angle, basement-influenced reverse fault (figures 4, 8A, and

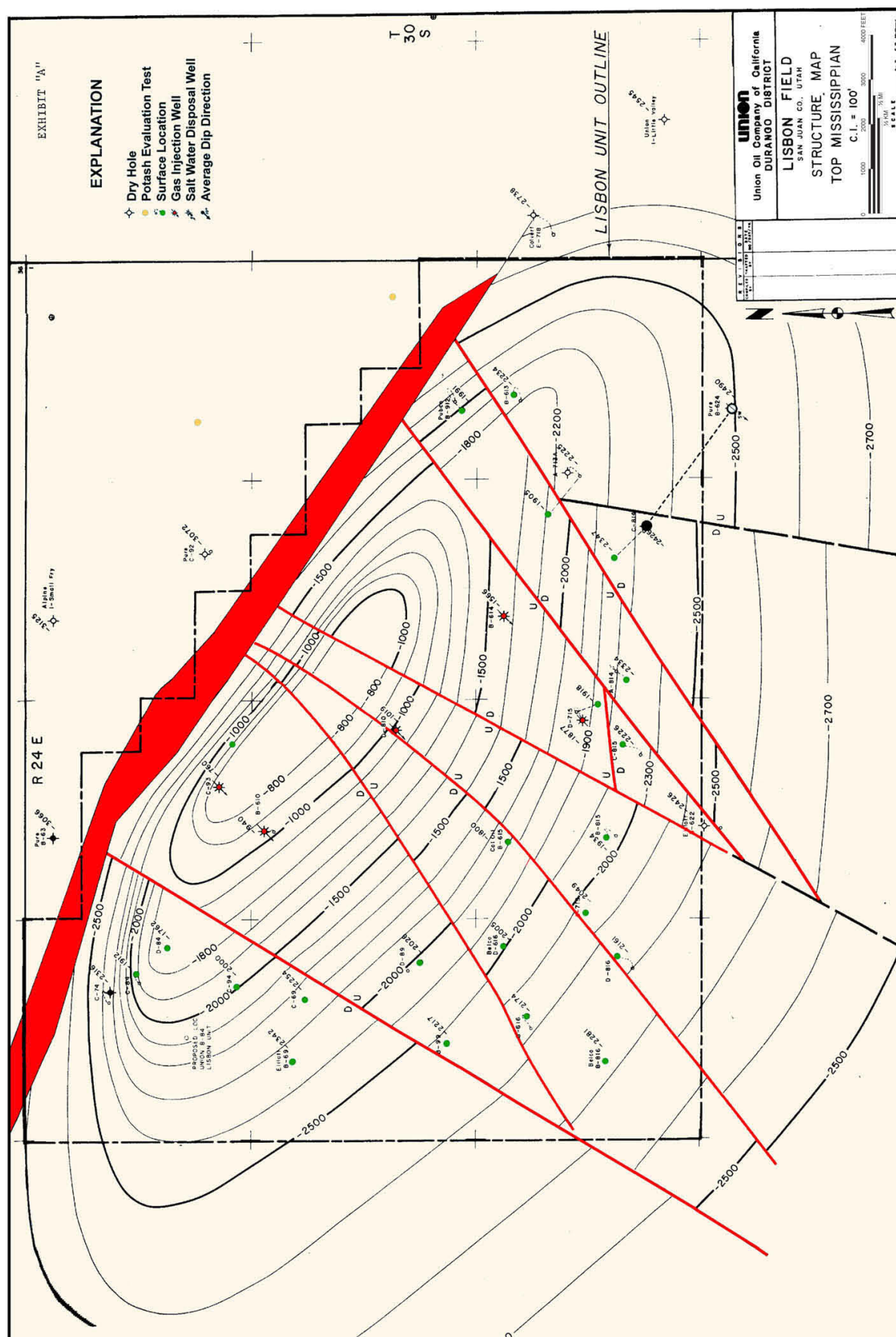
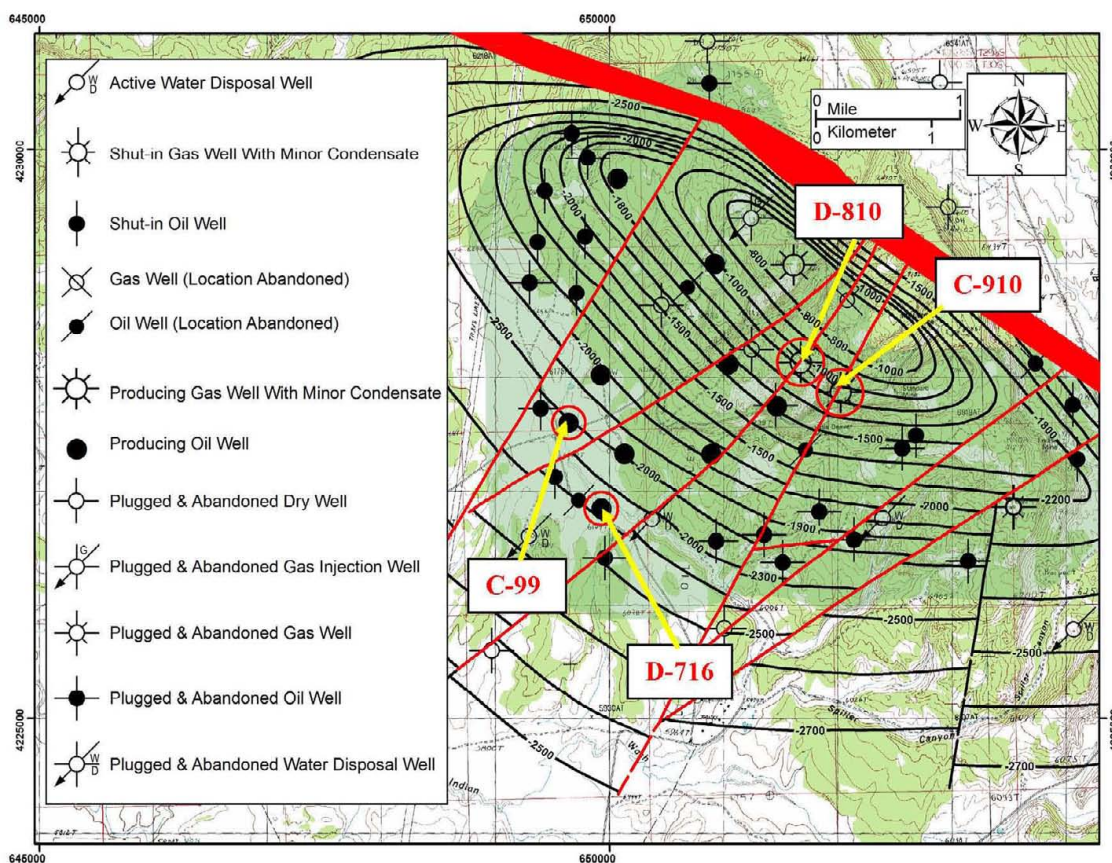


Figure 7A. Top of structure of the Leadville Limestone, Lisbon field, San Juan County, Utah (modified from C.F. Johnson, Union Oil Company of California files, 1970; courtesy of Tom Brown, Inc.).





**Figure 7B.** Top of structure of the Leadville Limestone superimposed over the topographic base, well locations (well sites identified where detailed sampling was conducted), and Lisbon oil field outline (shaded bluish green). Base map: La Sal 30' X 60' topographic quadrangle map, U.S. Geological Survey. See figure 2 for location of Lisbon field in the Paradox Basin.

**Table 1.** Cumulative production and produced gas compositions (weight percent) from Lisbon and Lightning Draw Southeast fields. Gas compositions courtesy of EnCana Oil & Gas (USA) Inc., and ST Oil Company.

| Well No.                                     | Lisbon Gas Cap         |                        | Lisbon Oil Leg          |                         | Lightning Draw Southeast Gas |                        |
|----------------------------------------------|------------------------|------------------------|-------------------------|-------------------------|------------------------------|------------------------|
|                                              | D-810                  | C-910                  | C-99                    | D-716                   | Federal 1-31                 | Evelyn Chambers Gov. 1 |
| Cumulative Production*<br>(November 1, 2009) | 23.9 BCFG<br>22,062 BO | 26.4 BCFG<br>23,952 BO | 12.9 BCFG<br>503,915 BO | 10.2 BCFG<br>557,043 BO | 0.08 BCFG<br>495 BO          | 0.34 BCFG<br>3808 BO   |
| Methane                                      | 36.16                  | 38.28                  | 37.83                   | 40.27                   | 27.01                        | 23.97                  |
| Ethane                                       | 7.44                   | 8.39                   | 8.87                    | 8.63                    | 4.85                         | 3.90                   |
| Propane                                      | 2.76                   | 2.45                   | 4.88                    | 4.40                    | 3.26                         | 2.59                   |
| Isobutane                                    | 0.48                   | 0.40                   | 0.93                    | 0.83                    | 0.71                         | 0.60                   |
| Normal Butane                                | 0.26                   | 0.21                   | 0.48                    | 0.45                    | 0.40                         | 0.34                   |
| Isopentane                                   | 0.29                   | 0.22                   | 0.55                    | 0.51                    | 0.50                         | 0.41                   |
| Normal Pentane                               | 0.35                   | 0.27                   | 0.67                    | 0.62                    | 0.58                         | 0.46                   |
| Carbon Dioxide                               | 23.58                  | 28.78                  | 30.89                   | 27.69                   | 27.02                        | 36.64                  |
| Hydrogen Sulfide                             | 1.37                   | 1.00                   | 0.20                    | 0.28                    | 0.00                         | 0.00                   |
| Nitrogen                                     | 25.97                  | 18.85                  | 13.18                   | 14.66                   | 33.48                        | 29.20                  |
| Helium                                       | 0.70                   | 0.66                   | 0.53                    | 0.66                    | 1.42                         | 1.40                   |
| Hexanes+                                     | 0.62                   | 0.50                   | 0.99                    | 1.00                    | 0.77                         | 0.48                   |
| Total                                        | 99.97                  | 100.00                 | 100.00                  | 100.00                  | 100.00                       | 100.00                 |

Division of Oil, Gas, and Mining (2009).

8B). A northwest-trending syncline separates the LDSE and Lisbon anticlines in the subsurface.

Producing units at LDSE are similar to Lisbon field in terms of depositional environments, carbonate fabrics, and diagenesis. There are two principal Leadville zones at LDSE field: an upper zone primarily of fossiliferous limestone with crinoids, brachiopods, and coated grains forming skeletal wackestone to packstone and some grainstone fabrics; and a lower zone of dolomitized mudstone with large rhombic to sucrosic dolomite crystals (David E. Eby, Eby Petrography & Consulting, Inc, verbal communication, 2007). Diagenesis consists of hydrothermal dolomitization, bitumen coating, and fracturing. The producing interval is confined to the upper zone although both have some units over 6% porosity. The net reservoir thickness is about 40 feet (12 m) over an approximate 320-acre (130 ha) area. Porosity over the perforated interval averages 17%, and permeability averages 13 mD. The drive mechanism is an expanding gas cap; water saturation is 21%. The bottom-hole temperature is 136°F (58°C).

The Leadville Limestone reservoir at LDSE field was first discovered by Texaco in 1980 in the 8826-foot-deep (2690 m) Evelyn Chambers Government No. 1 well, NE1/4NE1/4 section 6, T. 31 S., R. 24 E., SLBL&M (figure 8). The Mississippian interval tested 1.72 MMCFGPD (0.05 MCMGPD) and the upper and low-

er Ismay zones of the Paradox Formation tested 12 BOPD (condensate) (1.9 m<sup>3</sup>), 4.5 MCFGPD (0.1 MCMGPD), and 60 bbls of water per day (BWPD) (9.5 m<sup>3</sup>). ST Oil Company re-perforated the Leadville interval in Evelyn Chambers Government No. 1 well in May 2004, but production statistics are unavailable.

Subsequently, ST Oil Company completed the Federal No. 1-31 well, NW1/4SW1/4 section 31, T. 30 S., R. 24 E., SLBL&M (figures 4 and 8), in December 2004 with an IFP of 18 BOPD (condensate) (3 m<sup>3</sup>), 1543 MCFGPD (44 MCMPD), and 5 BWPD (0.8 m<sup>3</sup>). The API gravity of the condensate is 50°. The original reservoir field pressure was 1100 psi (7585 kPa). The well also intersected 34 feet and 29 feet (10 m and 8.8 m) of pay in the upper and lower Ismay zones, respectively. There is currently one producing well (Evelyn Chambers Government No. 1) and one shut-in gas/condensate well (Federal No. 1-31) from the Leadville Limestone in the field. Cumulative Leadville production as of November 1, 2009, was 4303 bbls of condensate (684 m<sup>3</sup>), 0.42 BCF of gas (0.01 BCMG), and 6053 BW (962 m<sup>3</sup>) (Utah Division of Oil, Gas, and Mining, 2009).

In comparison with the Lisbon field, the LDSE field contains a lower concentration of hydrocarbons and more nitrogen and helium (table 1), and it has productive intervals in the overlying Ismay zone of the Paradox Formation. The crosscutting, normal faults at Lisbon are not evident at LDSE from the limited drilling to date.

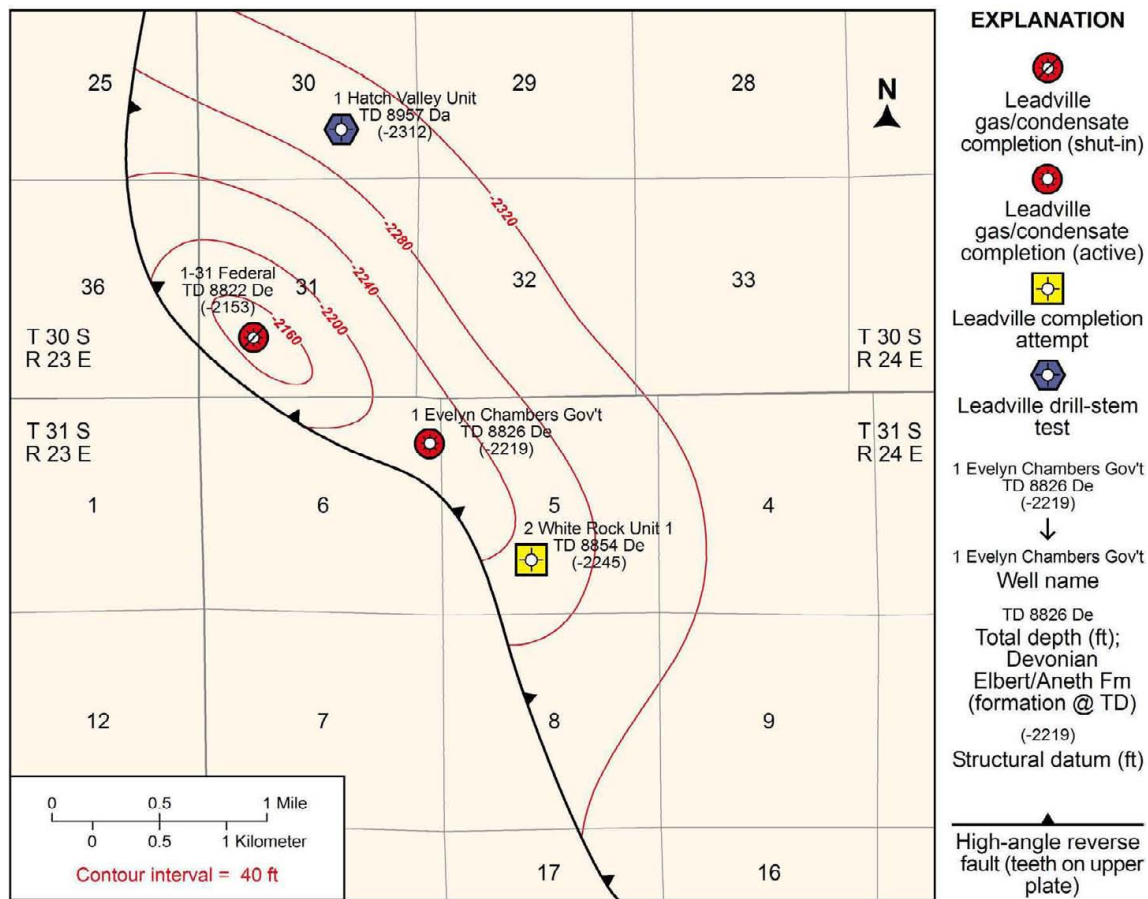


**Figure 8A.** Structure contour map of the Leadville Limestone, Lightning Draw Southeast field, San Juan County, Utah (modified from a fault map provided courtesy of ST Oil Company).



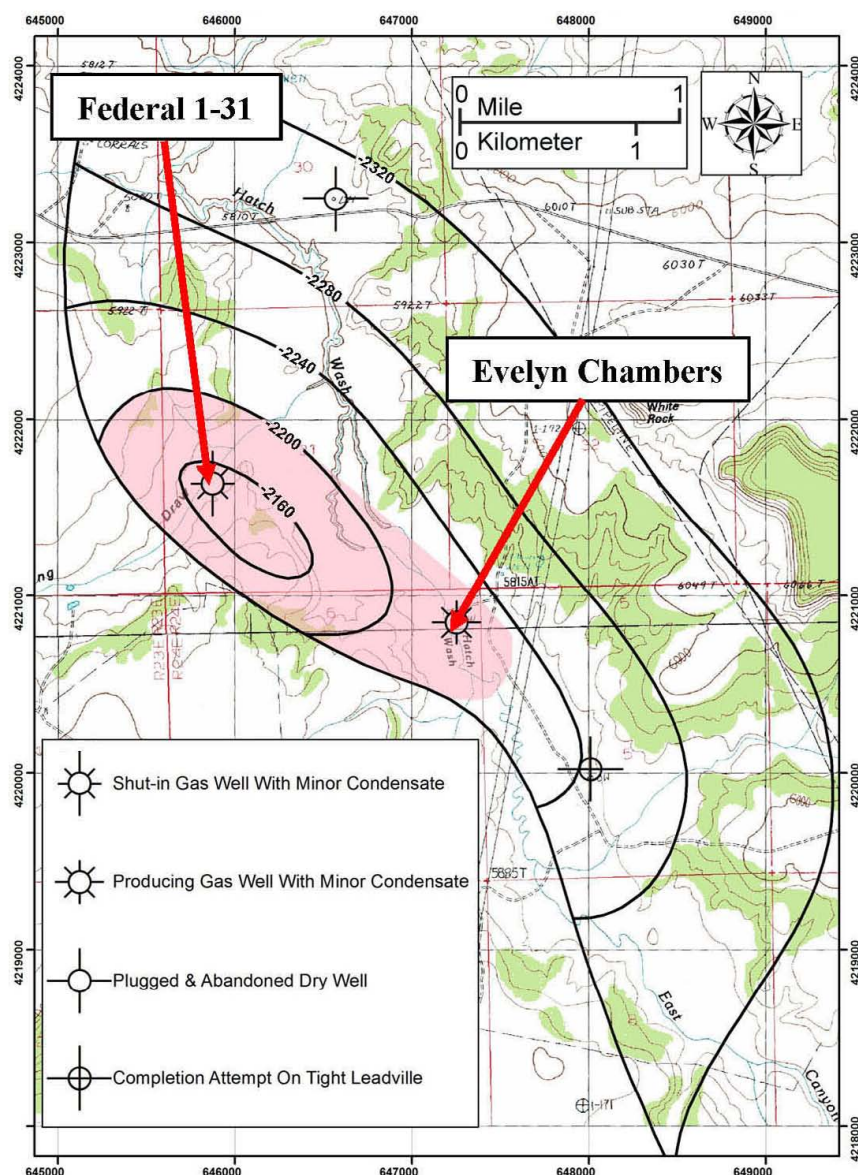


**Figure 8B.** Top of structure of the Leadville Limestone superimposed over the topographic base, well locations (well sites identified where detailed sampling was conducted), and Lightning Draw Southeast field outline (shaded pink). Base map: La Sal 30' X 60' topographic quadrangle map, U.S. Geological Survey. See figure 2 for location of Lightning Draw Southeast field in the Paradox Basin.

## SURFACE JOINTING

Surface jointing is best developed in the Triassic-Jurassic Wingate and Jurassic Navajo Sandstones (figure 9), and is also present in the intervening Jurassic Kayenta Formation although not as pronounced. Joints may be thin (less than one inch) or several feet in width (figure 10) and tens of feet or miles in length. They may also occur as (1) parallel (figure 9), (2) blocky or rectilinear joint sets (figures 10B, 11A, and 11B), and (3) curvilinear polygonal, often with several orders of size or generation (figure 11C). Joint sets in the area generally are vertical to near vertical. Many small joints contain very little soil, although enough to support bryophyte and lichen growth where there is sufficient moisture (figure 11). Some small joints are filled with thin (<0.02 inch)

silica or calcite veins (figure 10C); those joints observed over the gas cap area near the Lisbon No. C-910 well (SW1/4SE1/4 section 10, T. 30 S., R. 24 E., SLBL&M) have halos of possible iron/manganese-bearing minerals around calcite (figure 10D). Large joint sets commonly contain brecciated sandstone and fault gouge-like material.

In the Lisbon field area, joint orientation in the Wingate and Kayenta Formations on the southwest-dipping flank of the Lisbon surface anticline and over the gas cap is dominantly northwest-southeast (figure 12A), parallel to the regional structural trends. In the relatively flat-lying Navajo Sandstone farther southwest of the surface structure and over the oil leg, the dominant joint trend is nearly perpendicular, east-northeast–west-southwest, to the orientation over the gas cap (figure



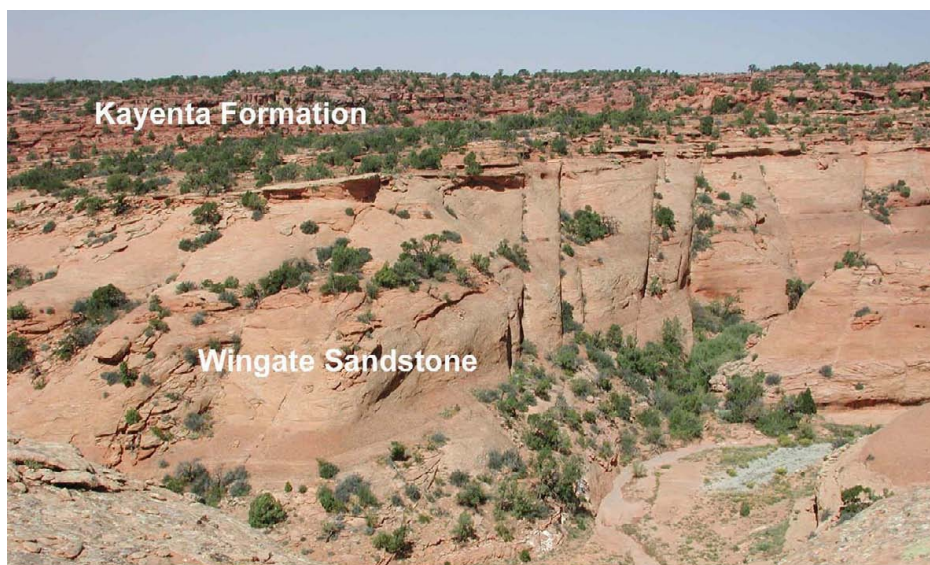


**Figure 9.** Subvertical joints in the Triassic-Jurassic Wingate Sandstone from Lisbon field; view to the northwest. The contact with the overlying Jurassic Kayenta Formation is sharp. Note that the continuation of these joints into the Kayenta is not as obvious.

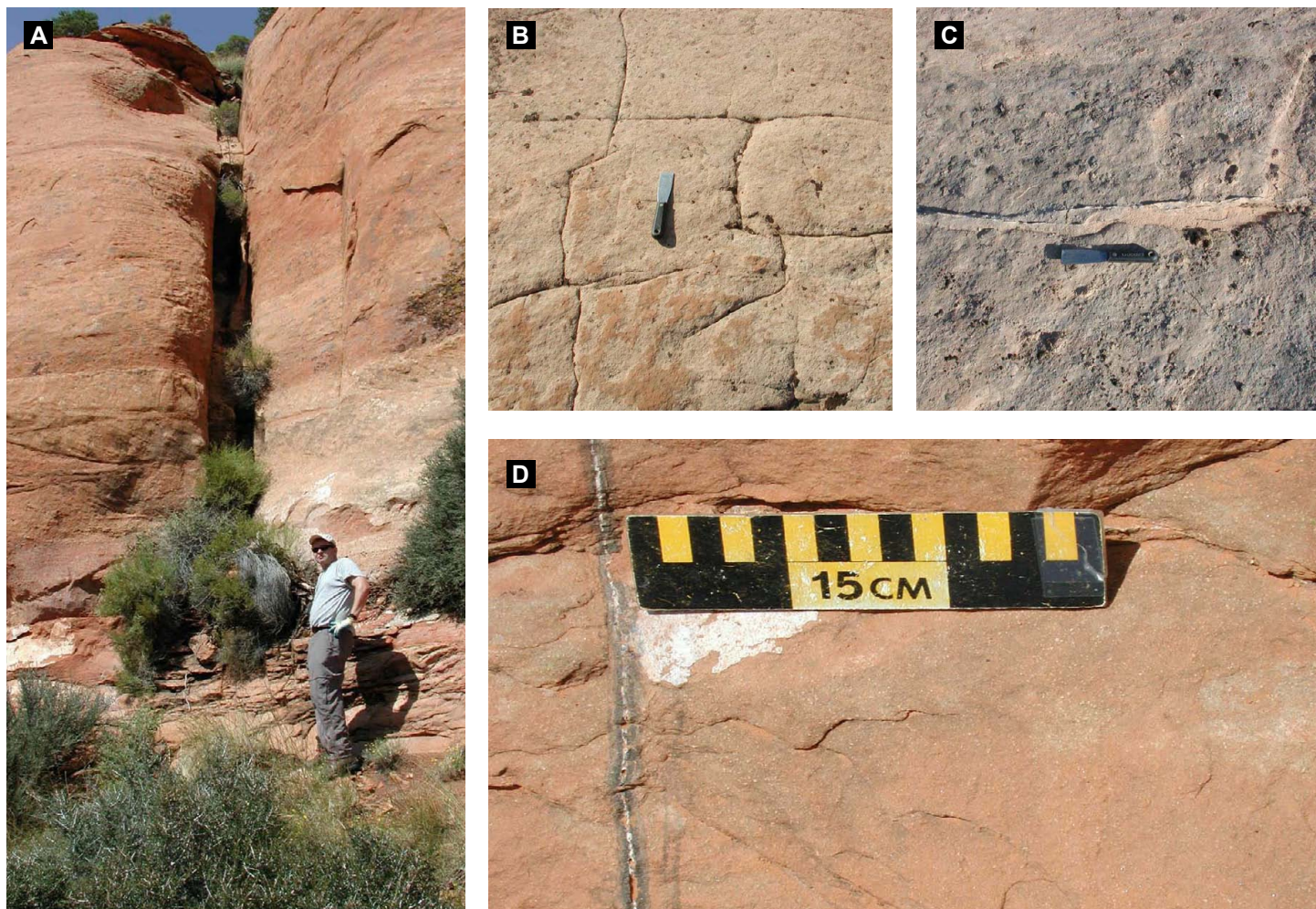


**Figure 10.** Examples of joints in the Lisbon field area. A – Large, probably regional-scale joint in the Wingate Sandstone over the gas cap. B – Blocky or rectilinear joint sets in the Navajo Sandstone over the water leg. C – Thin silica vein in a joint over the water leg. D – Very thin calcite vein with a halo of possible iron/manganese-bearing minerals over the gas cap. Figures 10A and 10D are near the Lisbon No. C-910 well (SW1/4SE1/4 section 10, T. 30 S., R. 24 E., SLBL&M); figures 10B and 10C are near the No. 21-4 Federal well (NW1/4NW1/4 section 21, T. 30 S., R. 24 E., SLBL&M).



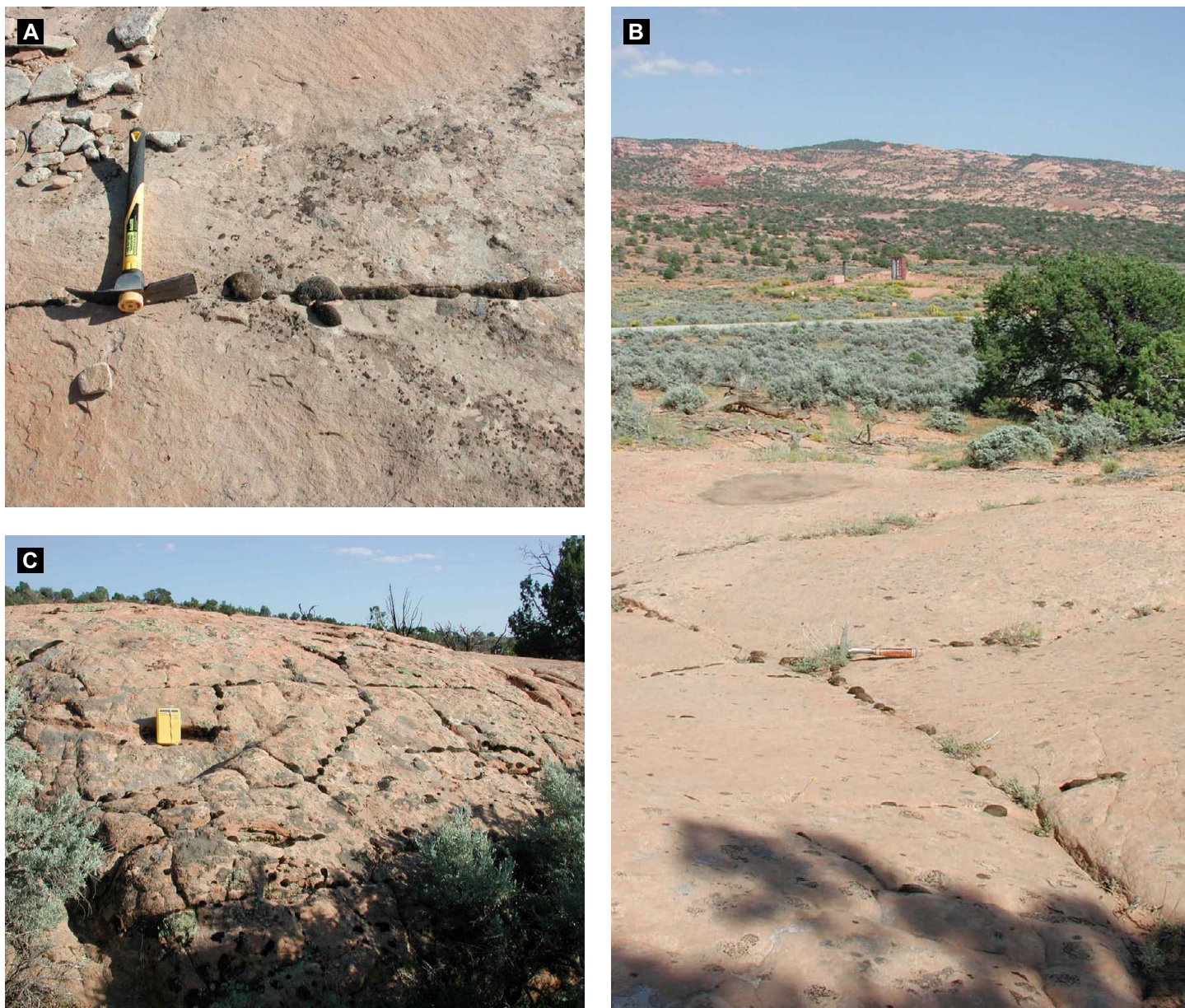


**Figure 11.** Bryophyte (moss) and lichen that commonly grow along thin, moisture-rich joints in sandstone outcrops in the Lisbon area. *A* – Close-up of bryophyte (*Grimmia* [possibly *Grimmia wrightii*] and *Bryum*) and lichen (*Collema tenax*) along a joint in the Wingate Sandstone near the Lisbon No. D-810 (NW Lisbon USA No. A-2) well (NE1/4SE1/4 section 10, T. 30 S., R. 24 E., SLBL&M) over the gas cap of Lisbon field. *B* – Bryophyte and lichen along a thin joint in the Jurassic Navajo Sandstone over the oil leg of Lisbon field. The Lisbon No. D-716 well (SE1/4NE1/4 section 16, T. 30 S., R. 24 E., SLBL&M) and southwest-dipping flank of the Lisbon anticline (Kayenta Formation) are in the background. *C* – Bryophyte and lichen along curvilinear, polygonal joints in the Navajo Sandstone near the No. 21-4 Federal well (NW1/4NW1/4 section 21, T. 30 S., R. 24 E., SLBL&M) over the water leg of Lisbon field.

12B). Joint sets in flat-lying Navajo over the water leg southwest of the field display a dominant east-west orientation (figure 12C).

In the LDSE field area, the Navajo Sandstone is also relatively flat lying. Two sets of joints are found near the Federal No. 1-31 well. Their orientations are generally north-south and northwest-southeast (figure 13A). Two joint sets are also found in the Navajo to the southeast near the Evelyn Chambers Government No. 1 well with orientations trending northwest-southeast and northeast-southwest (figure 13B).

## METHODS USED IN THE GEOCHEMICAL SURVEY

### Sample Collection

Surface soils are easily accessible by truck or on foot in the Lisbon and LDSE field areas. Permission was obtained from the field operator, EnCana Oil & Gas (USA) Inc., and the U.S. Bureau of Land Management to conduct the surface geochemical sampling program in the Lisbon field area. A safety orientation



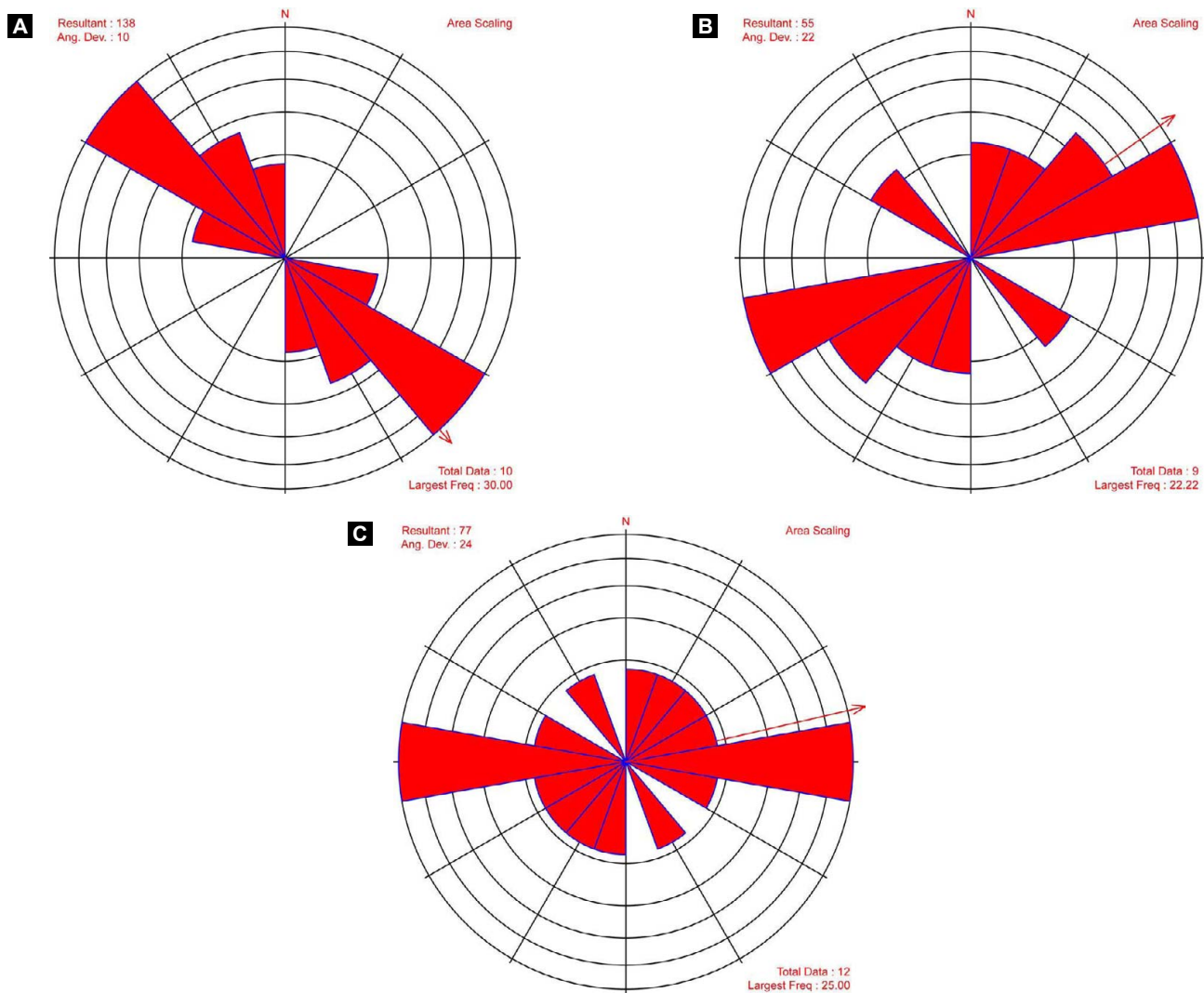


**Figure 12.** Joint orientations at sample localities over the (A) gas cap (Wingate and Kayenta Formations), (B) oil leg (Navajo Sandstone), and (C) water leg (Navajo Sandstone) of Lisbon field.

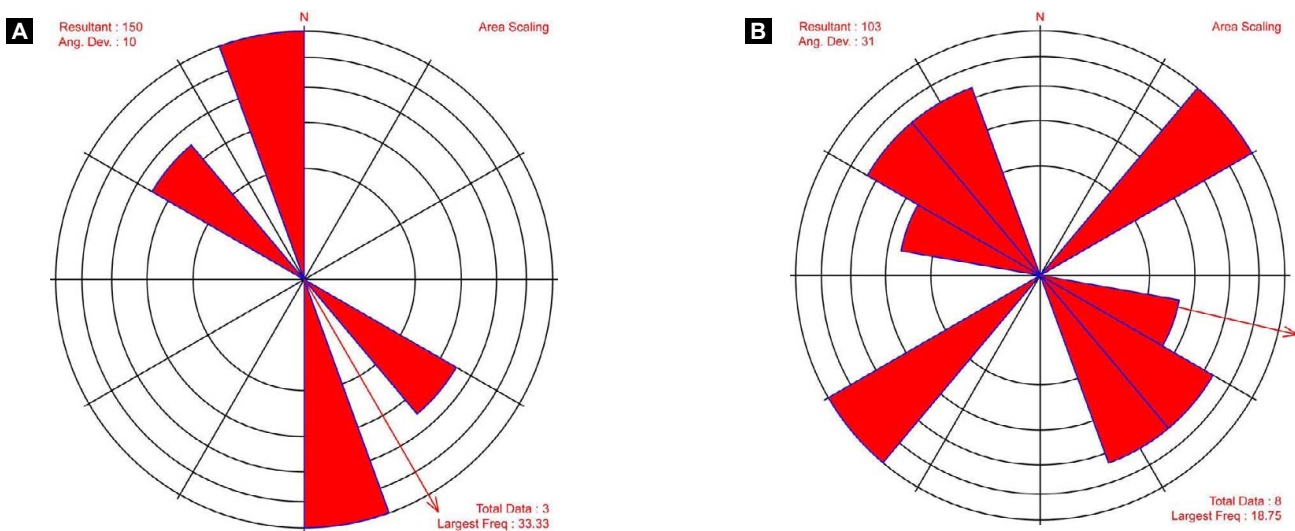


**Figure 13.** Joint orientations at sample localities near the (A) Federal No. 1-31 well (NW1/4SW1/4 section 31, T. 30 S., R. 24 E., SLBL&M), and (B) Evelyn Chambers Government No. 1 well (NE1/4NE1/4 section 6, T. 31 S., R. 24 E., SLBL&M) at Lightning Draw Southeast field.

was provided by EnCana at the Lisbon Gas Plant, and a hydrogen sulfide ( $\text{H}_2\text{S}$ ) monitor was lent to the sampling crew. Some sampling sites were relocated and the grid adjusted farther to the west to avoid an  $\text{H}_2\text{S}$  pipeline in Lisbon field.

The sample site locations were planned weeks in advance of the survey. The sample points were digitized off a topographical base using Surfer™ and a table of Universal Transverse Mercator (UTM), North America Datum 1927 (NAD27) coordinates was created and imported into Excel®. The coordinates and topographical maps were generated in Garmin™-compatible format and uploaded to Global Positioning System (GPS) units for use in the field. The field sampler would then walk to the designated sample site displayed on the GPS. At each sample site the UTM coordinates were recorded in the memory of the GPS and written in a field notebook. Field notes recorded included sample depth, soil color and texture, and signs of possible contamination from nearby wells, gas condensers, paved roads, and so forth.

### Collection of Surface Soils

Two surface soil types are evident in the study area. In outcrop-rich areas (shown as Mesozoic and Paleozoic geological units on figure 14), the thin soils that sporadically cover bedrock are classified as Rizozo-Rock Outcrop-Ildefonso types (Lammers, 1991). The dominant vegetation on these thin soils is piñon, Utah juniper, big sagebrush, Mormon tea, and galleta. Shallow Rizozo soils, formed from residual and eolian deposits, are a yellowish-red gravelly, fine-grained, sandy loam. Samples collected from depths of 8 to 12 inches (20–31 cm) are reddish-brown, sandy loam, clay loam, and fine-grained sandy loam (figure 15A). In broader valleys (eolian and alluvial deposits on figure 14), there is a mixture of Begay-Windwhistle-Ildefonso soil types (Lammers, 1991). Vegetation is primarily big sagebrush, spiny hopsage, snakeweed, and blue grama. These soils form on alluvial and eolian deposits derived mainly from sandstones, and at surface consist of reddish-brown fine sandy loam. Subsoils collected from 8 to 12 inches (20–31 cm) depth are yellowish-red, loamy, fine-grained sand.

Surface soil samples were collected at 1500-foot (500-m) intervals on a 16-square-mile (42 km<sup>2</sup>) rectangular grid over and around Lisbon field (figure 14). A total of 307 samples were collected over the field and 101 samples off the field. The survey was then expanded to include the collection of soils at 656-foot (200-m) intervals on a grid of northwest-southeast and northeast-southwest lines over LDSE (figure 14). A total of 53 samples were collected over LDSE and 66 samples off the field. All sample location coordinates, geological units under the soil, and sample identification information are included in the appendices A, B, and C.

The sample intervals chosen were based on the size of the fields themselves. The sampling grid and lines extend well beyond the proven limits of Lisbon and LDSE fields to ensure adequate background data. The areas chosen, therefore, sufficiently covered

the gas caps, oil leg (present only at Lisbon), and background “barren” areas including the footwalls of the northeast-bounding normal fault and the southwest-bounding reverse fault of Lisbon and LDSE fields, respectively (figures 4 and 14).

Along the grid and lines, shallow (generally 8- to 12-inch [20–30 cm] deep) soil samples were collected with a spade or tree-planting shovel over a 6-square-foot area (0.6 m<sup>2</sup>) at each site (figure 15A). Care was taken to avoid sampling material sluffed off the surface. The soils were placed and stored in airtight, Teflon-sealed, glass soil jars to prevent hydrocarbon contamination during transport to the laboratory. In addition to the jar samples, soils were also collected in plastic Zip-loc bags for major/trace element and anion analyses. Some sample sites had to be offset because of lack of soil in outcrop areas. Evidence of surface alteration (for example, stressed vegetation) that could be attributed to hydrocarbon seepage and fracturing was also noted. Backup samples were also collected from each site and stored in plastic bags. Sample sites around wells were located topographically high relative to the well pad to reduce the possibility of contamination (figure 16).

At Lisbon field, 90 samples were collected around two gas wells in the gas cap, two productive oil wells in the oil leg, and two barren dry wells (figures 7 and 14), with 15 samples at each well site. The two gas wells are the Lisbon No. C-910 well (SW1/4SE1/4 section 10, T. 30 S., R. 24 E., SLBL&M), which has produced 23,952 bbls of oil (3808 m<sup>3</sup>) and 26.4 BCF of gas (0.75 BCMG), and the Lisbon No. D-810 (NW Lisbon USA No. A-2) well (NE1/4SE1/4 section 10, T. 30 S., R. 24 E., SLBL&M), which has produced 22,062 bbls of oil (3508 m<sup>3</sup>) and 23.9 BCF of gas (0.68 BCMG) (Utah Division of Oil, Gas, and Mining, 2009). The two oil wells are the Lisbon No. C-99 well (SW1/4SE1/4 section 9, T. 30 S., R. 24 E., SLBL&M), which has produced 503,915 bbls of oil (80,122 m<sup>3</sup>) and 12.9 BCF of gas (0.37 BCMG), and the Lisbon No. D-716 well (SE1/4NE1/4 section 16, T. 30 S., R. 24 E., SLBL&M), which has produced 557,043 bbls of oil (88,570 m<sup>3</sup>) and 10.2 BCF of gas (0.29 BCMG) (Utah Division of Oil, Gas, and Mining, 2009). The barren dry wells include one to the west of the field in the water leg (the No. 21-4 Federal, NW1/4NW1/4 section 21, T. 30 S., R. 24 E., SLBL&M) and one northeast of the field on the low side of the fault that parallels the structure (the No. 1 State-Small Fry, NE1/4NW1/4 section 2, T. 30 S., R. 24 E., SLBL&M).

At LDSE field, 45 samples were collected around two gas wells over the gas cap and two barren dry wells (figures 8 and 14), with 10 to 15 samples at each well site. The two gas wells are the Federal No. 1-31 well, which has produced 495 bbls of condensate (79 m<sup>3</sup>) and 0.08 BCFG (0.002 BCMG) (currently shut-in), and the Evelyn Chambers Government No. 1 well, which has produced 3808 bbls of condensate (605 m<sup>3</sup>) and 0.34 BCF of gas (0.01 BCMG) (Utah Division of Oil, Gas, and Mining, 2009) (table 1). The barren dry wells are the No. 2 White Rock Unit 1 and the No. 1 Hatch Wash Unit (NW1/4SE1/4 section 30, T. 30 S., R. 24 E., SLBL&M) north of the field in the water leg.



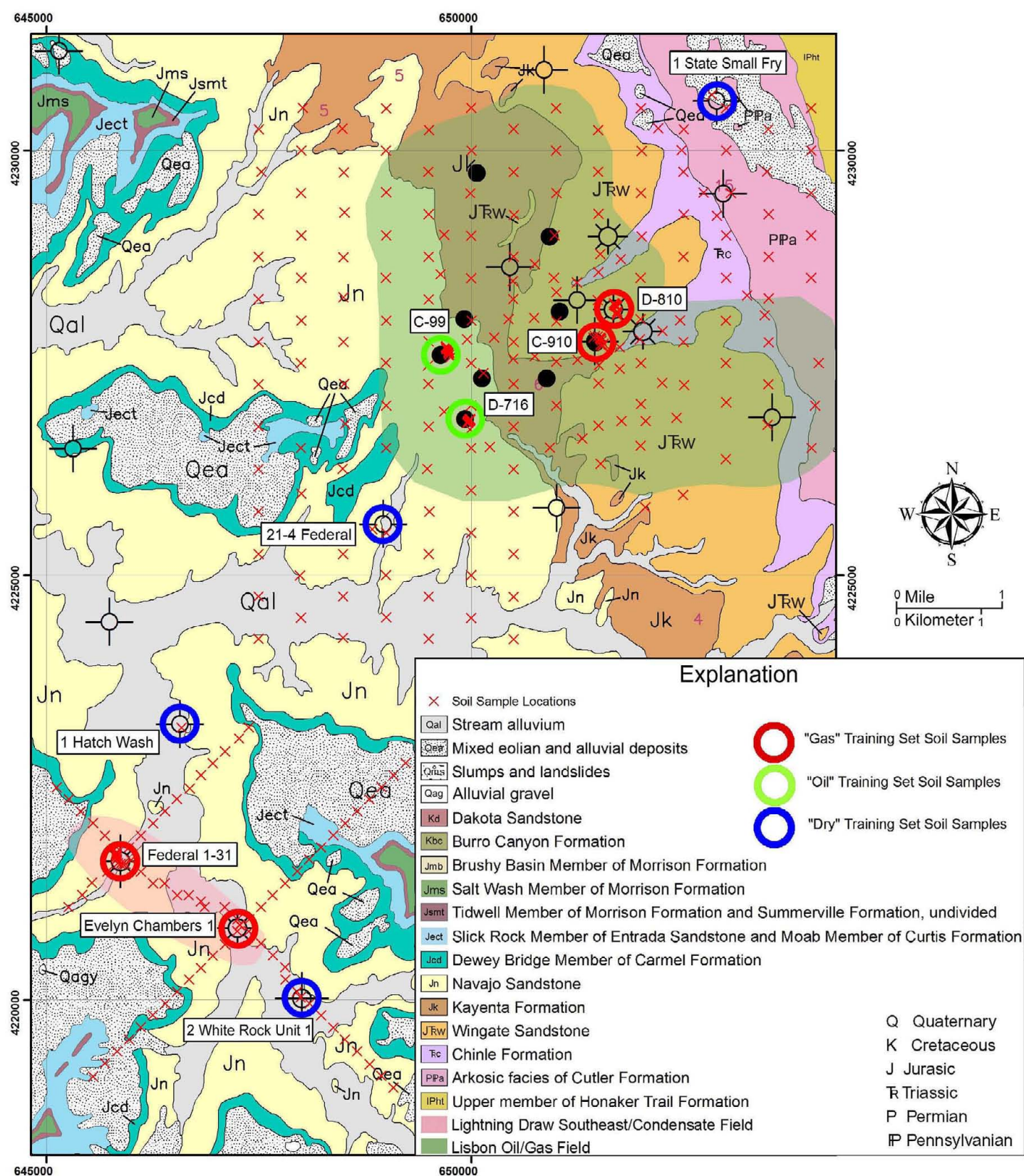


**Figure 14.** Distribution of grid, line, and training set soil samples collected over and around the Lisbon and Lightning Draw Southeast fields, superimposed over geologic map modified from Doelling (2005); see figure 7 for explanation of well symbols.





**Figure 15.** Sampling methods used in the Lisbon/Lightning Draw Southeast area. *A* – Collection of shallow, reddish-brown, fine-grained, sandy loam from 8- to 12-inch (20–30 cm) depth on Wingate Sandstone outcrop. These samples are referred to as “surface soils” throughout this report. *B* – Along joints, soil, sand, bryophyte, and lichen were sampled using a flathead screwdriver, knife, or stainless steel spoon.

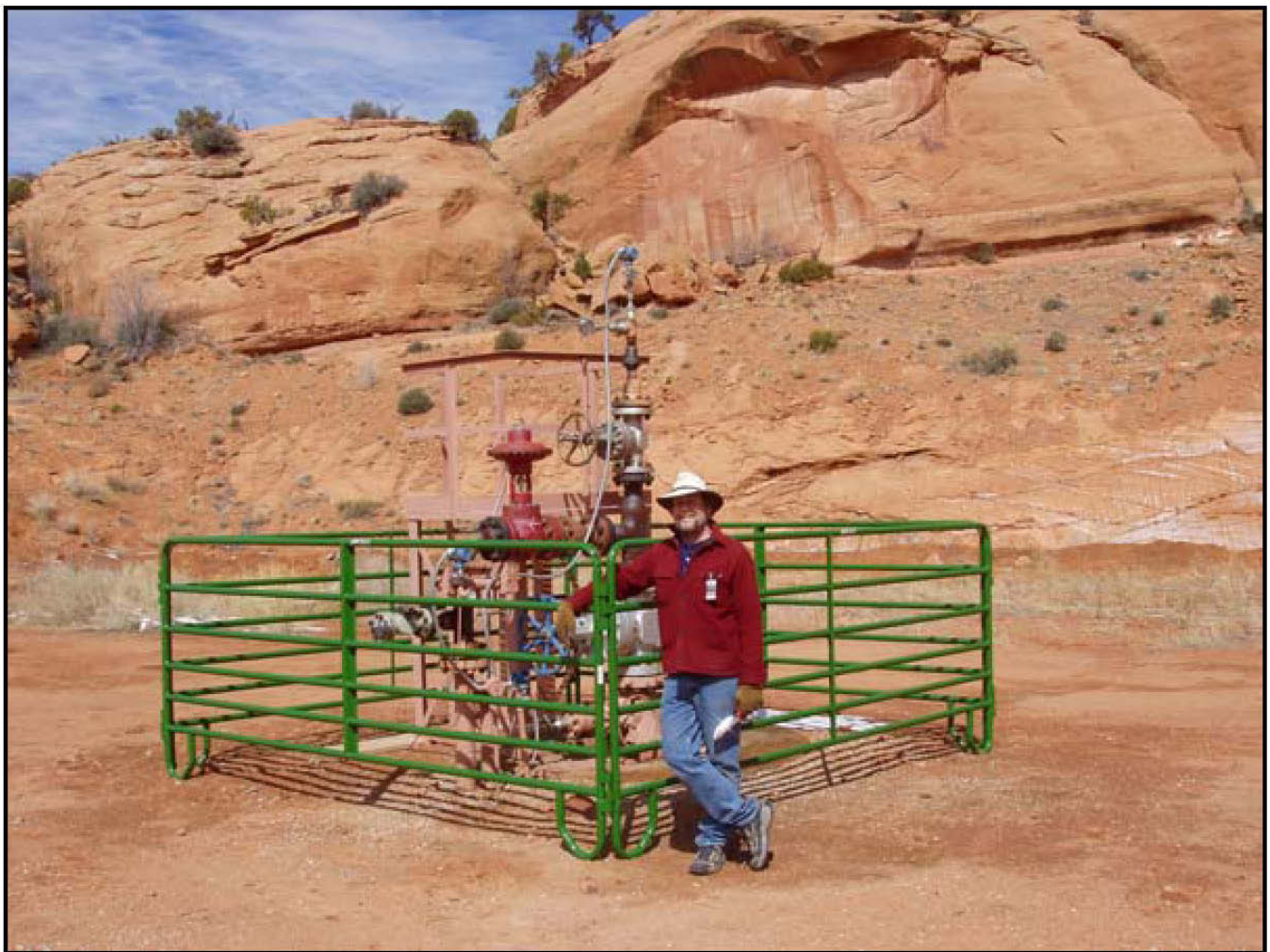


**Figure 16.** The Lisbon No. C-910 well, which produces 7 MMCF/D of low-Btu ( $\approx 670$ ) sour gas with considerable amounts of  $N_2$  and  $CO_2$  (see table 1). Soils samples were collected from the ledge above the well pad to avoid contamination.

## Collection of Fracture-Fill Lichen, Bryophyte, and Soil

Joints in outcrops may provide pathways for hydrocarbon microseepage to the surface, which may be evident in the soils and vegetation that fill the joints (figures 9, 10, and 11). Thus, the sampling program was expanded to collect soil and vegetative tissue samples from the joints for additional hydrocarbon and elemental analysis over barren and productive parts of both Lisbon and LDSE fields (figure 17, see appendices D and E for details).

Soil samples (33 samples) from joints required the same amount (that is, 4 ounces [110 g]) of sample material as was taken along the grid, but they were harder to acquire. Representative samples were often only obtained by scraping sandy soil out of the joints with a stainless steel spoon, knife, or flathead screwdriver (figure 15B). Where the joints were narrow with sparse soils or the soil zone especially shallow, this process frequently required sampling along tens of feet in order to acquire enough material. Joints with established vegetation generally have deeper soils and better sampling opportunities.

Bryophyte and lichen commonly grow along thin joints in the area where there are higher than ambient amounts of moisture (figure 11). These plants may also show a geochemical signature in their tissues indicative of underlying hydrocarbons or subsurface mineralization, so they were also sampled (30 samples) to compare with the analyses of the soils that support them (figure 15B). Two species of bryophyte and one species of lichen grow along joints in the area. The bryophytes fit into the genera *Grimmia* (possibly *Grimmia wrightii*) and *Bryum*. Both are common soil crust mosses. The lichen is *Collema tenax*—an abundant and common soil crust lichen in the intermountain western United States (Larry St. Clair, Monte L. Bean Life Science Museum, Brigham Young University, written communication, October 28, 2006).

## Collection of 6-Foot-Deep Free-Gas Samples

Free-gas samples (see appendix F for location and other details) were collected at 15- to 300-foot intervals (5–100 m) over LDSE field and in off-structure areas using the following protocol (figure 18):

1. Drill to at least a 6-foot (2-m) depth (10 feet [3 m] preferably) in unconsolidated overburden using the Geoprobe® percussion (hammer) drill with 1-inch (2.54 cm) diameter pipe (figure 18).
2. Insert polyethylene tubing into rod and secure it to a retractable point at the bottom of the rod.
3. Purge the soil air at least three times with a plastic 40 cc syringe to clear the tubing of ambient air (figure 18).
4. Draw soil air (free gas) up using the syringe and force it into a 1-liter Tedlar® bag (for hydrocarbon and fixed-gas analyses) and/or lead-lined CO<sub>2</sub> cartridge (for helium analysis).

Samples were collected from 6-foot (2-m) depth using the Geoprobe method to capture the in-situ soil air with minimal influence from dilution by atmospheric gases.

## Laboratory Analysis

The surface soils, bryophyte, and lichen were dried at 122°F (50°C) and sieved to <63 microns. Equal splits of the sieved samples were then weighed out into air-tight, 20 cc glass vials for thermal desorption at constant temperature for a constant time. Equal aliquots of headspace gas were injected into a Hewlett-Packard® 5890 gas chromatograph with flame ionization and photo ionization detectors (GC-FID/PID) for analysis of 39 hydrocarbon compounds in the C<sub>1</sub> to C<sub>12</sub> range (table 2; appendices A–E). The organic carbon content of the samples was estimated using a gravimetric technique (loss on ignition [LOI]).

In addition, a solvent extract of sieved soil splits was analyzed by synchronous scanned fluorescence (SSF), which measures relative amounts of heavy (C<sub>6</sub> to C<sub>40</sub>) aromatic hydrocarbons (appendix B). Synchronous scanning fluorescence technique is a very cost-effective way to analyze soils for traces of the much heavier liquid hydrocarbons without the high cost of elaborate extraction techniques and high-resolution gas chromatography. Solvent extracts of the soils are scanned from wavelengths of 250 nm to 500 nm. Hydrocarbons that fluoresce in oils are the ringed aromatic compounds and can be grouped by the number of (benzene type) rings chained together. These groups have fluorescence spectra maxima that increase in wavelength approximately with increasing ring numbers as shown in figure 19. Splits of the dried and sieved soil samples were also dissolved in aqua regia acid and the supernatant was analyzed for 53 major and trace elements (table 2) by inductively coupled-plasma mass spectrometry and emission spectroscopy (ICP/MS and ICP/ES). Samples were also analyzed for seven anion species using a deionized water extraction and ion chromatography (table 2).

The free-gas samples were drawn from the Tedlar bags and cartridges with a 5-cc syringe and analyzed for 19 hydrocarbons in the C<sub>1</sub> to C<sub>8</sub> range using the GC-FID instrument (appendix F). Gas from the Tedlar bags and lead-lined cartridges were also analyzed for fixed gases (CO<sub>2</sub>, CO, O<sub>2</sub>, N<sub>2</sub>, He, and H<sub>2</sub>) using a Varian® CP-4900 gas chromatograph with a thermal conductivity detector (GC-TCD).

The precision and accuracy of the hydrocarbon, organic carbon, major/trace element, and anion analyses was between ±10 to 20% for a 95% confidence level based on the analysis of laboratory duplicates and standard reference materials at 10% frequency.

## Interpretation and Mapping

The organic and inorganic chemical data were compiled in an Excel® spreadsheet for interpretation. The hydrocarbon and elemental compositions of near-surface soil gas and soils can reflect the character of subsurface petroleum accumulations and faults. It is important to identify and correlate the numerous near-sur-



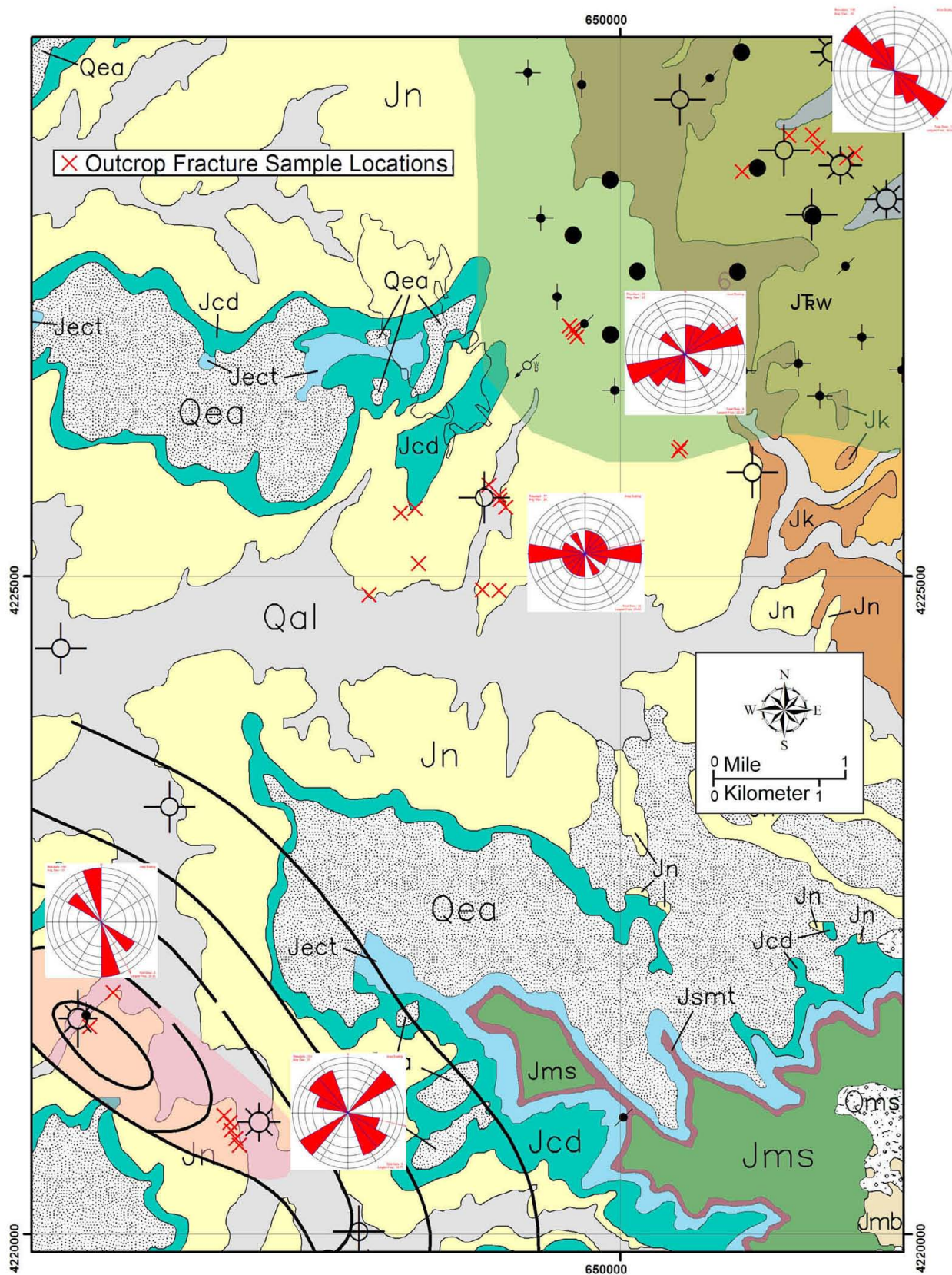


**Figure 17.** Fracture-fill bryophyte, lichen, and soil sample locations over the Lisbon gas cap, oil leg, and water leg, and over the Lightning Draw Southeast field. Dominant joint orientations at sample site areas are also indicated. Surface geology modified from Doelling (2005); see figures 7 and 14 for explanations of well symbols and geologic units. Form line contours based on structure contour map of the Leadville Limestone shown on figure 8. Lisbon and Lightning Draw southeast fields shown in bluish green and pink, respectively.



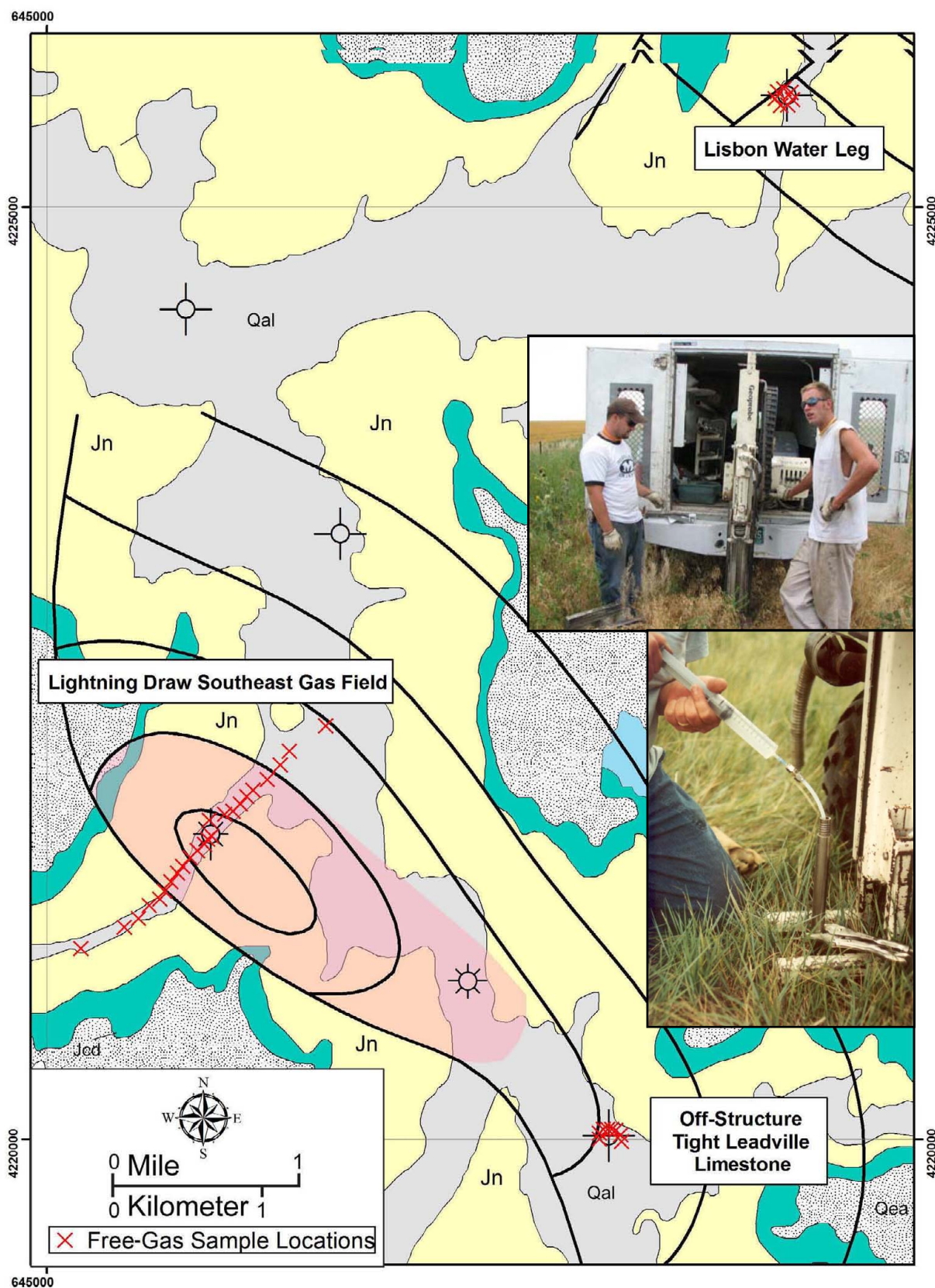
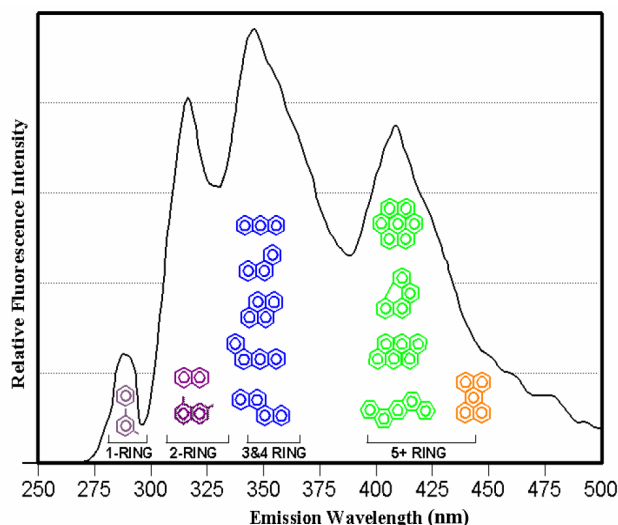


**Figure 18.** Location of 6-foot-deep free-gas samples over and off Lightning Draw Southeast field (shown in pink). The samples were collected with a Geoprobe “Direct-Push” drill and gas was extracted through plastic tubing (inset photos), which was inserted into the 1-inch steel pipes. Surface geology modified from Doelling (2005); see figures 8 and 14 for explanations of well symbols and geologic units. Form line contours based on structure contour map of the Leadville Limestone shown on figure 8.



1 ring (270-290 nm): *benzene, xylenes*

2 rings (310-330 nm): *naphthalene, methyl naphthalene*

3-4 rings (340-380 nm): *phenanthrene, anthracene, benzo(a)anthracene, chrysene, pyrene*

5+ rings (400-500 nm): *anthanthrene, dibenzo(a,h)anthracene, coronene, benzo(g,h,i)fluoranthrene, perylene*

**Figure 19.** Schematic of synchronous scanned fluorescence spectra depicting the aromatic hydrocarbons and corresponding emission wavelengths.

**Table 2.** Components reported by four analytical methods.

| 39 C <sub>1</sub> -C <sub>12</sub> Hydrocarbons                                                                                                                                                                                                                                                                                                                                                                                                                                   | 7 Anions                                                          | 53 Major and Trace Elements                                                                                                                                                                                | Synchronous Scanned Fluorescence                                                                                                                                                        |
|-----------------------------------------------------------------------------------------------------------------------------------------------------------------------------------------------------------------------------------------------------------------------------------------------------------------------------------------------------------------------------------------------------------------------------------------------------------------------------------|-------------------------------------------------------------------|------------------------------------------------------------------------------------------------------------------------------------------------------------------------------------------------------------|-----------------------------------------------------------------------------------------------------------------------------------------------------------------------------------------|
| methane, ethane, ethene, propane, propene, i-butane, n-butane, butene, i-pentane, n-pentane, pentene, i-hexane, n-hexane, hexene, i-heptane, n-heptane, heptene, i-octane, n-octane, benzene, n-butylbenzene, cyclohexane, n-decane, n-dodecane, ethylbenzene, m-ethyltoluene, p-ethyltoluene, indane, naphthalene, n-nonane, n-propylbenzene, 1,2,4,5-tetramethylbenzene, toluene, 1,2,4-trimethylbenzene, 1,3,5-trimethylbenzene, n-undecane, m-xylene, p-xylene, and o-xylene. | fluoride, chloride, bromide, nitrite, nitrate, phosphate, sulfate | Ag, Al, As, Au, B, Ba, Be, Bi, Ca, Cd, Ce, Co, Cr, Cs, Cu, Fe, Ga, Ge, Hf, Hg, In, K, La, Li, Mg, Mn, Mo, Na, Nb, Ni, P, Pb, Pd, Pt, Rb, Re, S, Sb, Sc, Se, Sn, Sr, Ta, Te, Th, Ti, Tl, U, V, W, Y, Zn, Zr | Fluorescence intensities in the 250 to 500 nm range that correspond to condensate, medium-gravity oil, and low-gravity oil. Allows fingerprint matching with produced oils in the area. |

face compounds and elements with their sources—particularly petroleum accumulations. Different accumulations yield different near-surface compositional signatures, which can be used to determine if the accumulation is in the oil or gas range. Factor and discriminant analysis were used in this study to reduce the complex mixtures of organic and inorganic variables to a smaller number of interpretable variables.

Both factor and discriminant analysis are multivariate statistical tools that allow the evaluation of large numbers of data variables simultaneously. Multivariate analysis of the data was performed in Statistica® 8.0. These multivariate tools permit the user to appreciate the existence of particular organic and inorganic associations that may reflect compositionally unique microseepage and mineralizing processes. In oil and gas exploration, this is important because the presence of oil or gas in the subsurface is rarely imaged by one or two variables.

Factor analysis summarizes the data set in a series of mathematical “vectors” or “factors,” which are combinations of co-varying variables in multivariate space. The derived factors (when combined) account for all or most of the variation in the dataset, but in fewer variables than are in the dataset. For example, there may be 15 variables measured in a dataset, but these may be reduced to five factors, which account for most of the variance in the individual variables. Factors are ranked in descending order of the amount of variance they account for in the dataset. Factor 1 accounts for the most variance, factor 2 the second greatest, and so on. For each factor, it is possible to identify the mixture of variables (components) and their relative importance. In oil and gas producing basins, it is common for factor analysis to result in at least one factor reflecting a mixture of light (C<sub>1</sub> to C<sub>4</sub>) hydrocarbons (that can be related to “gas”), and at least one reflecting a mixture of heavy (C<sub>5</sub> to C<sub>x</sub>) hydrocarbons (that can be related to “oil”). Factor loadings are the correlation coefficients

between the variables and the factors. The more a variable is correlated with a particular factor (that is, correlated group of variables in multivariate space), the higher the factor loadings will be for that variable. Factors are plotted spatially as “factor scores,” which represent the degree of correlation of variables in particular samples with the derived factors. In this study, standardized factor scores of 1, 1.5, and 2 above a mean of zero are arbitrarily considered as anomalous for the sake of comparing the various datasets and thereby evaluating the effectiveness of the various geochemical methods and sample media.

Forward, stepwise, discriminant analysis was used to discriminate the compositional character of microseepage over productive and barren areas using the  $C_1$  to  $C_{12}$  hydrocarbon variables from soil samples over known productive and barren areas (that is, training sets). In the case of soil samples, the compositional character of the “adsorbed” microseepage over dry and barren areas reflects an alteration effect on soils as a result of continuous or episodic microseepage and hydrocarbon degradation over long periods of time. In essence, discriminant analysis is used to distinguish between the unique multi-component alteration signature imparted to soils over barren and productive areas from prolonged microseepage. The analysis derives a “discriminant function” or linear combination of variables that separates the compositional character of microseepage between “productive and barren” areas. The form of the discriminant function, also called a *canonical root*, is a latent variable which is created as a linear combination of discriminating (independent) variables, such that  $L = b_1x_1 + b_2x_2 + \dots + b_nx_n + c$ , where the  $b$ 's are discriminant coefficients, the  $x$ 's are discriminating variables, and  $c$  is a constant. The discriminant coefficients are used to assess the relative classifying importance of the independent variables. If microseepage can be distinguished between “productive and barren” areas based on statistical significance tests (for example, Wilk's Lambda, F-tests) and cross-validation, then the discriminant function can be used to classify samples from “unknown” areas into productive or barren categories. The forward, stepwise, discriminant analysis eliminates variables from the function that have minimal influence on the discrimination based on F-test and Wilk's Lambda statistics. These predictions are represented as discriminant scores or probabilities of a particular sample falling into either barren or productive clusters. A discriminant probability of 0.9 was arbitrarily chosen as an anomalous threshold for sake of comparison between the various datasets and to assess the effectiveness of each geochemical method and sample media tested. For example, samples with “Lisbon gas probabilities” over 0.9 have a 90% chance of being correctly classified into the compositional group representing microseepage over the Lisbon gas cap.

In some cases, the absolute concentrations of organic and inorganic variables in soils and free gas can be spatially correlated with underlying hydrocarbon reservoirs, and may actually reflect charge in the reservoir rather than an “alteration-effect” on soils as a result of hydrocarbon microseepage over long periods of time. In the Lisbon study, absolute concentrations of organic and inorganic variables have been transformed to standardized Z-scores to better evaluate contrast in the data. The Z-scores are derived by subtracting the

population mean for a particular variable from the concentration of that variable for a particular sample and then dividing by the population standard deviation. This reduces the data to a mean of zero and the Z-scores then represent standard deviations above a mean of zero (that is, Standard Normal Distribution). In this study, the absolute concentrations of organic and inorganic variables over Lisbon are significantly higher than those over LDSE field, possibly because of more intense microseepage and the presence of exposed uranium mineralization. Z-scores were therefore calculated separately for the Lisbon and LDSE datasets to more fully appreciate the subtle, but significant, anomalies at LDSE. In this study, Z-scores (standard deviations) of 1, 1.5, and 2 above a mean of zero are arbitrarily considered as anomalous for the sake of comparing the various datasets and thereby evaluating the effectiveness of the various geochemical methods and sample media.

The absolute concentrations of hydrocarbons (in parts per billion) and fixed gases (in parts per million) in free gas over LDSE are plotted to emphasize the low concentration of gas species in these samples. In this case, thresholds between anomalous and background samples were selected from frequency distributions of the data (that is probability plots).

Organic and inorganic variable Z-scores, and the factor and discriminant scores and free-gas concentrations are plotted on a geological background as proportional symbols using ArcGIS 9.2™. Only those variables and scores that show a spatial correlation with the Lisbon and/or LDSE fields are presented here. There are several inorganic variables, for instance, that are spatially correlated with specific geological units (for example, rare earth element anomalies in soils over the arkosic Permian Cutler Formation), the meaning of which is beyond the scope of this study.

## RESULTS OF THE GEOCHEMICAL SURVEY

The results of the study are very encouraging in that both organic and inorganic anomalies are spatially associated with parts of Lisbon and LDSE fields (table 3). Although several variables are anomalous over parts of the fields, only those most coherent anomalies are presented. Throughout the presentation of results the number of anomalous samples relative to total number of samples over and off the field structures is given to express the effectiveness of the various techniques for predicting oil and gas potential over Leadville reservoirs.

### Thermally Desorbed Hydrocarbons: Surface Soils

#### Absolute Hydrocarbon Concentrations

Several “live oil” hydrocarbon concentration anomalies are evident over both the Lisbon and LDSE areas relative to background “water-leg” areas (table 3). Toluene, for instance, is anomalous in the central part of the Lisbon field where normal faults are most abundant and closely spaced and also in the northwest part of the field on the west side of a normal fault (figure 20). The anomalies

**Table 3.** Organic and inorganic anomaly types identified in different sample media over Lisbon and Lightning Draw Southeast fields.

|                             | Lisbon Field                                                                                                                                                                                                                                                                                                                                                                                                                                                                                                                                                                      | Lightning Draw Southeast Field                                                                                                                                                                                                                                                                                                                                                                                                                                                                                                                                                                     |
|-----------------------------|-----------------------------------------------------------------------------------------------------------------------------------------------------------------------------------------------------------------------------------------------------------------------------------------------------------------------------------------------------------------------------------------------------------------------------------------------------------------------------------------------------------------------------------------------------------------------------------|----------------------------------------------------------------------------------------------------------------------------------------------------------------------------------------------------------------------------------------------------------------------------------------------------------------------------------------------------------------------------------------------------------------------------------------------------------------------------------------------------------------------------------------------------------------------------------------------------|
| <b>Surface Soils</b>        | <p>methane, ethane, ethene, propane, propene, i-butane, n-butane, butene, i-pentane, n-pentane, pentene, i-hexane, n-hexane, hexene, i-heptane, n-heptane, heptene, i-octane, n-octane, benzene, n-butylbenzene, cyclohexane, n-decane, n-dodecane, ethylbenzene, m-ethyltoluene, p-ethyltoluene, indane, naphthalene, n-nonane, n-propylbenzene, 1,2,4,5-tetramethylbenzene, toluene, 1,2,4-trimethylbenzene, 1,2,5-trimethylbenzene, n-undecane, m-xylene, p-xylene, and o-xylene</p> <p>Bi, Cd, Hg, Mo, Pb, U, V</p> <p>297-305 nm factor scores, 395-470 nm factor scores</p> | <p>methane, ethane, ethene, propane, propene, i-butane, n-butane, butene, i-pentane, n-pentane, pentene, i-hexane, n-hexane, hexene, i-heptane, n-octane, benzene, n-butylbenzene, n-decane, n-dodecane, ethylbenzene, m-ethyltoluene, p-ethyltoluene, indane, naphthalene, n-nonane, n-propylbenzene, 1,2,4,5-tetramethylbenzene, toluene, 1,2,4-trimethylbenzene, 1,3,5-trimethylbenzene, n-undecane, m-xylene, p-xylene, and o-xylene</p> <p>Ag, Al, As, Be, Bi, Co, Cu, Ga, Hf, Hg, La, Li, Mo, Pb, Sc, Sn, Sr, Ti, U, V, Zn, Zr</p> <p>297-305 nm factor scores, 395-470 nm factor scores</p> |
| <b>Bryophyte and Lichen</b> | <p>ethane, ethene, propene, i-butane, butene, pentene, hexene, benzene, n-butylbenzene, n-decane, ethylbenzene, m-ethyltoluene, p-ethyltoluene, indane, naphthalene, n-nonane, n-propylbenzene, 1,2,4,5-tetramethylbenzene, toluene, 1,2,4-trimethylbenzene, 1,2,5-trimethylbenzene, m-xylene, p-xylene, and o-xylene</p> <p>Ag, Al, As, Au, B, Ba, Bi, Co, Cu, Ga, Hf, K, La, Li, Mo, Na, Pb, Re, Sb, Sc, Sn, Sr, Th, Ti, U, V, Y, Zn, Zr</p> <p>305 nm Intensity</p>                                                                                                            | <p>methane, ethane, ethene, propene, i-butane, butene, pentene, hexene, benzene, indane, naphthalene, 1,2,4-trimethylbenzene, 1,2,5-trimethylbenzene, o-xylene</p> <p>Ag, Al, As, B, Ba, Bi, Co, Cu, Ga, Hf, K, Li, Mo, Na, Pb, Sb, Sc, Sr, Th, Ti, Zr</p> <p>305 nm Intensity</p>                                                                                                                                                                                                                                                                                                                 |
| <b>Fracture-fill Soils</b>  | <p>methane, ethane, propane, propene, butene, pentene, hexene, n-octane, n-butylbenzene, m-ethyltoluene, p-ethyltoluene, naphthalene, 1,2,4,5-tetramethylbenzene, 1,2,4-trimethylbenzene, 1,2,5-trimethylbenzene, n-undecane, n-dodecane</p> <p>Ag, Cl, Na, NO<sub>3</sub>, Re, S, Se, SO<sub>4</sub>, U, Y</p> <p>305 and 335 nm Intensity</p>                                                                                                                                                                                                                                   | <p>methane, ethane, ethene, propane, propene, butene, pentene, hexene, n-octane, ethylbenzene, n-butylbenzene, m-ethyltoluene, p-ethyltoluene, indane, naphthalene, 1,2,4,5-tetramethylbenzene, 1,2,4-trimethylbenzene, 1,2,5-trimethylbenzene, n-undecane, m-xylene, p-xylene</p> <p>Ag, As, Co, S, Se, Y</p>                                                                                                                                                                                                                                                                                     |
| <b>Free Gas</b>             | <p>No free gas collected</p>                                                                                                                                                                                                                                                                                                                                                                                                                                                                                                                                                      | <p>ethane, propane, propene, i-butane, n-butane, i-pentane, n-pentane, i-hexane, hydrogen, carbon dioxide</p> <p>helium, carbon dioxide, and hydrogen at margins of reservoirs</p>                                                                                                                                                                                                                                                                                                                                                                                                                 |



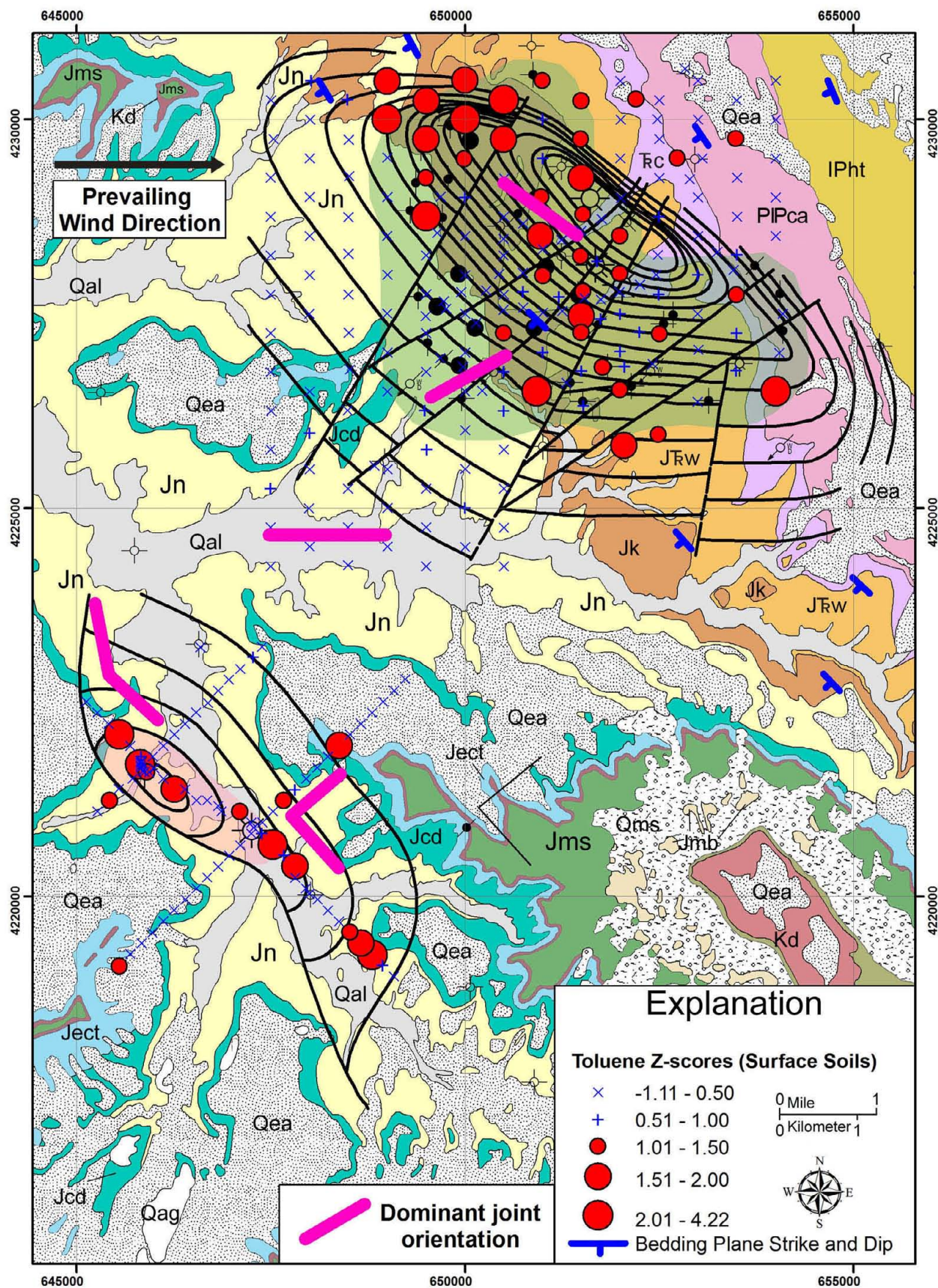


**Figure 20.** Distribution of toluene Z-scores in surface soils over the Lisbon and Lightning Draw Southeast fields. See figure 14 for description of geologic units (geologic base modified from Doelling, 2005) and figure 7 for explanations of well symbols; form line contours based on structure contour maps of the Leadville Limestone shown on figures 7 and 8. Lisbon and Lightning Draw southeast fields shown in bluish green and pink, respectively.



occur mainly over the Triassic-Jurassic Wingate Sandstone and Jurassic Kayenta Formation, but a few anomalous samples are also found over the Permian Cutler Group, Triassic Chinle Formation, and Jurassic Navajo Sandstone (figure 20). The anomalies cover 13% of the total samples over the field, and 6% of samples off the field also report as anomalous.

At LDSE field, toluene anomalies trend parallel to joint sets in Navajo Sandstone and over the reverse fault bounding the field to the southwest (figure 20). Anomalous samples comprise 13% of samples over the field and 12% of samples off the field. Anomalous samples occur over the Navajo ( $n = 10$ ), Quaternary stream alluvium ( $n = 3$ ), and the Slick Rock Member of the Jurassic Entrada Sandstone ( $n = 2$ ).

### Discriminant Analysis Results

Although several hydrocarbons in surface soils are spatially associated with the Leadville oil and gas fields, the anomalies are somewhat sporadic and some fall outside the limits of the fields. Discriminant analysis was therefore used to determine (1) if a linear combination of variables distinguishes microseepage over the oil and gas fields from that over the water legs, (2) which hydrocarbon variables best discriminate between oil, gas, and water production, (3) if discriminant scores (probabilities) better map the surface expression of the two fields, and (4) if separate discriminant functions for the fields predict one another (that is, cross-validate).

### Three-Component Discriminant Analysis

The first discriminant analysis model distinguishes hydrocarbon microseepage between the gas cap (samples at the Lisbon No. D-810 well), oil leg (samples at the Lisbon No. C-99 well), and water leg (several samples) at Lisbon field (figure 21). In this model, the microseepage over the gas cap is distinguished from that over the oil and water legs, and pentane, benzene, and propane are the most important variables for this discrimination (figure 22). The microseepage character of the less productive oil leg shows less distinct separation from the water leg than the

gas cap does (figure 22). Toluene contributes most to the weak discrimination of microseepage between the Lisbon oil and water legs. Soils around the very productive Lisbon No. C-910 gas well (table 1) and other parts of the gas cap predict as gas-prone and dry wells predict as dry.

Soil samples that fall into the “gas” category cluster mainly in the upper part of the Lisbon anticline where most of the gas production occurs (figure 22). Gas-prone samples make up 16% of samples over the field and 7% of samples off the field (table 4, row 1). The anomalies are clustered in the normal-faulted, east-central part of the field, along the northeastern faulted margin of the field, and west of a normal fault in the northwest part of the field (figure 22). The anomalies mainly occur over the Wingate and Kayenta Formations, but sporadic anomalies are also found over the Cutler Group, Chinle Formation, and Navajo Sandstone.

Two samples (4%) over Navajo Sandstone and Quaternary stream alluvium near the top of the LDSE anticline also predict as having “Lisbon gas” type compositional character (figure 22). These comprise a smaller proportion of the samples over the field compared with Lisbon field, but none of the samples off the LDSE field are incorrectly classified as having “Lisbon gas” character (table 4, row 1).

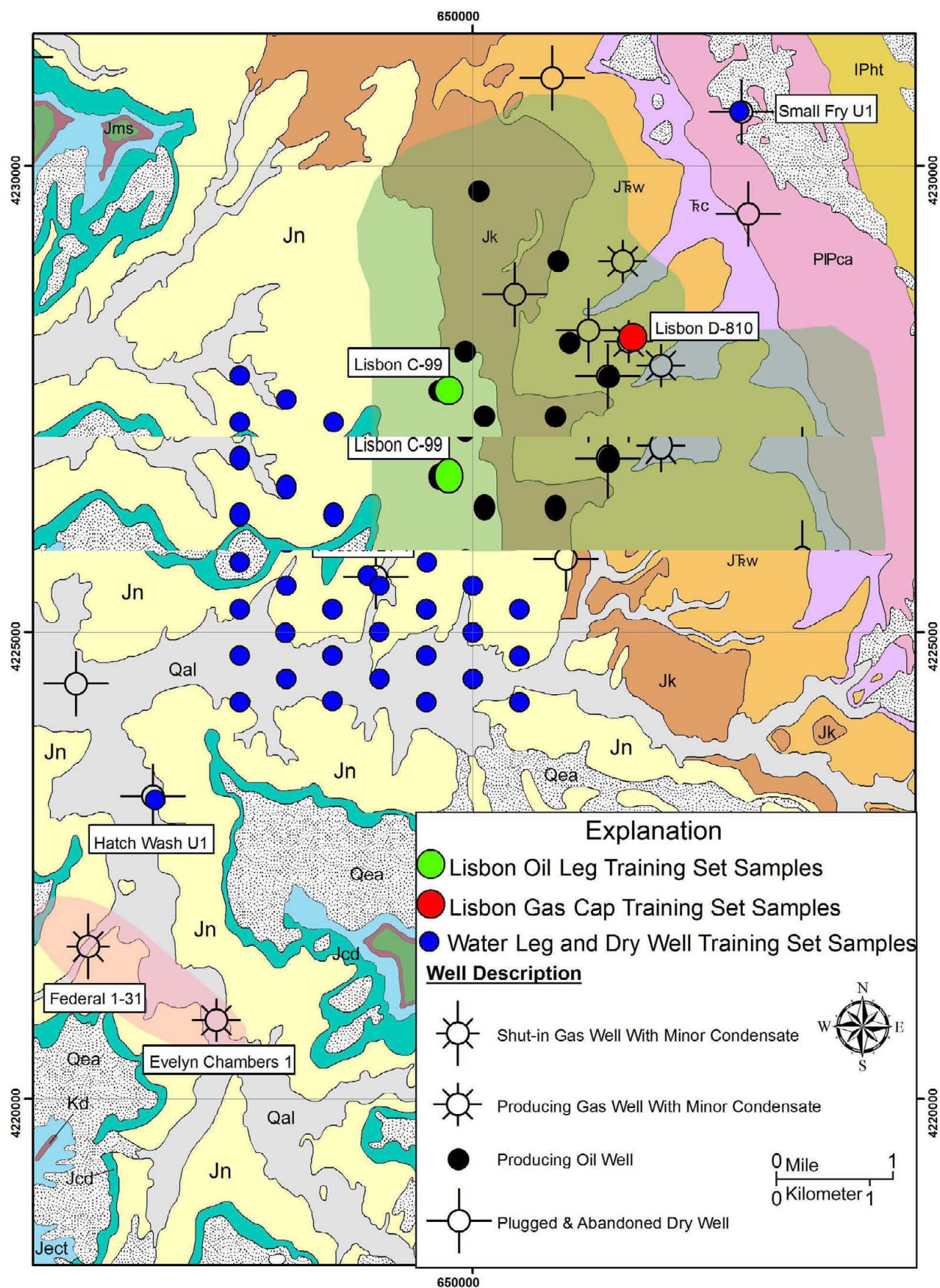
Samples around the Lisbon No. D-716 oil well, Federal No. 1-31 gas well, and Evelyn Chambers No. 1 gas/condensate well are predicted as oil-prone (figure 23). The anomalous samples comprise 7% of the samples over Lisbon field and 8% of the samples over LDSE field, and none of the samples are incorrectly classified over either field (table 4, row 2). Anomalous samples over Lisbon occur over Navajo Sandstone and those over LDSE field are over Quaternary stream alluvium.

### Two-Component Discriminant Analysis

The second discriminant analysis model tests for differences in microseepage between productive “gas/oil” parts of Lisbon field and the water leg (figure 24). Samples around productive wells

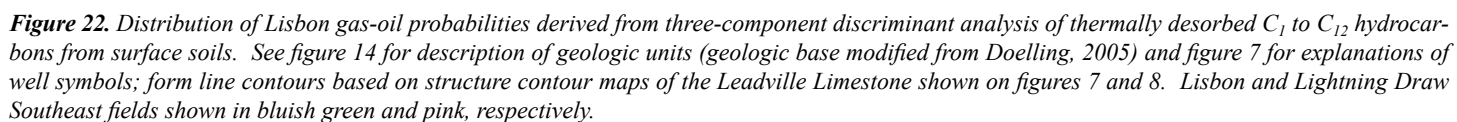
**Table 4.** Correct and incorrect classifications for discriminant models (surface soils). Orange shading represents the field being predicted by the model. The white area represents training set samples that are correctly classified.

| Row Number | Model                             | Correct classification (% of samples over field) |                   | Incorrect classification (% of samples off field) |                   |
|------------|-----------------------------------|--------------------------------------------------|-------------------|---------------------------------------------------|-------------------|
|            |                                   | Lisbon                                           | Lightning Draw SE | Lisbon                                            | Lightning Draw SE |
| 1          | Lisbon Gas Probability            | 16                                               | 4                 | 7                                                 | 0                 |
| 2          | Lisbon Oil Probability            | 7                                                | 8                 | 0                                                 | 0                 |
| 3          | Lisbon Gas/Oil Probability        | 20                                               | 26                | 12                                                | 5                 |
| 4          | Lightning Draw SE Gas Probability | 3                                                | 38                | 2                                                 | 3                 |



**Figure 21.** Surface soil training set samples used for three-component Lisbon gas cap versus oil leg versus water leg discriminant analysis model. See figure 14 for description of geologic units (geologic base modified from Doelling, 2005). Lisbon and Lightning Draw Southeast fields shown in bluish green and pink, respectively.







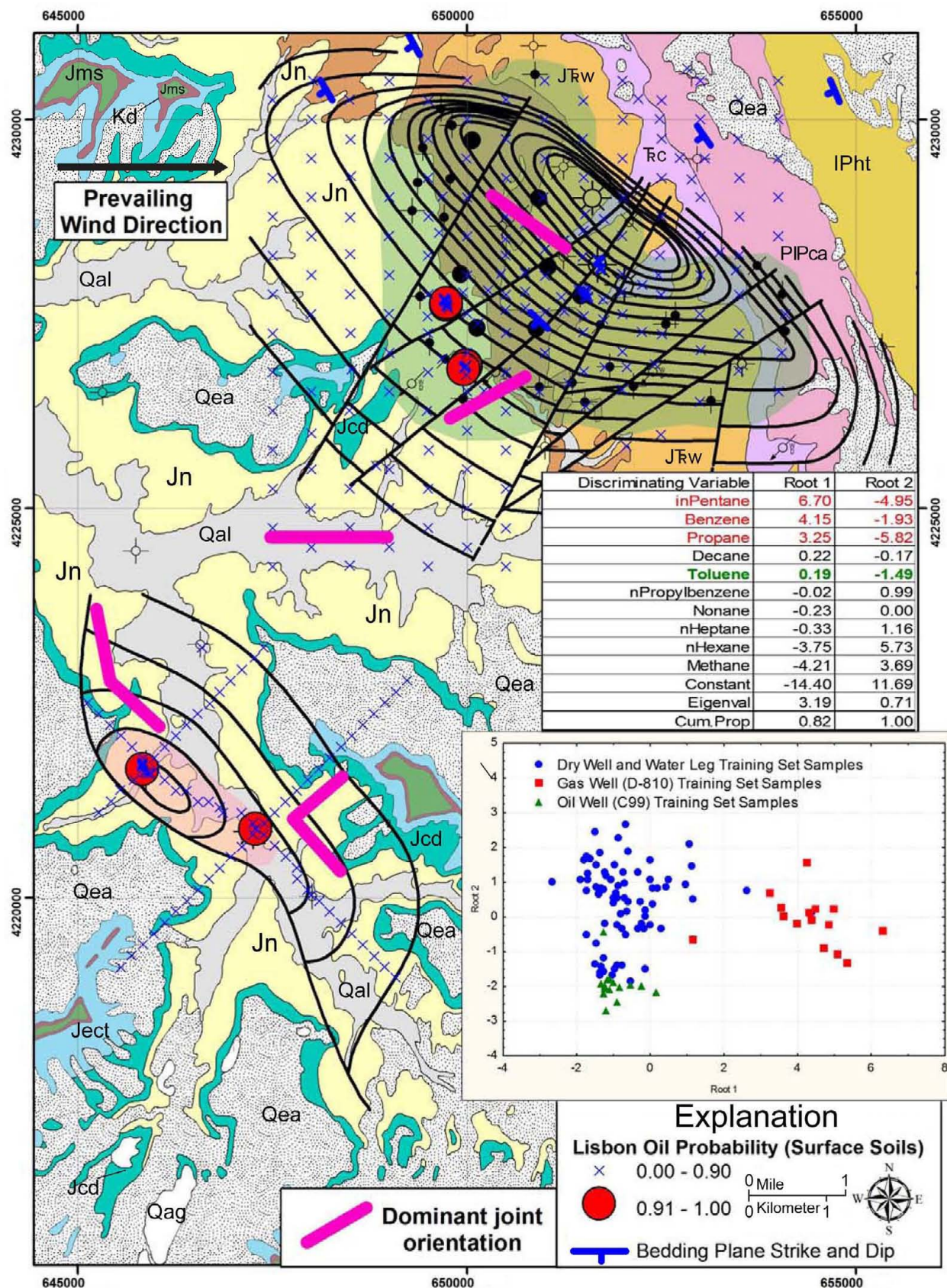


**Figure 23.** Distribution of Lisbon oil probabilities derived from three-component discriminant analysis of thermally desorbed  $C_1$  to  $C_{12}$  hydrocarbons from surface soils. See figure 14 for description of geologic units (geologic base modified from Doelling, 2005) and figure 7 for explanations of well symbols; form line contours based on structure contour maps of the Leadville Limestone shown on figures 7 and 8. Lisbon and Lightning Draw Southeast fields shown in bluish green and pink, respectively.



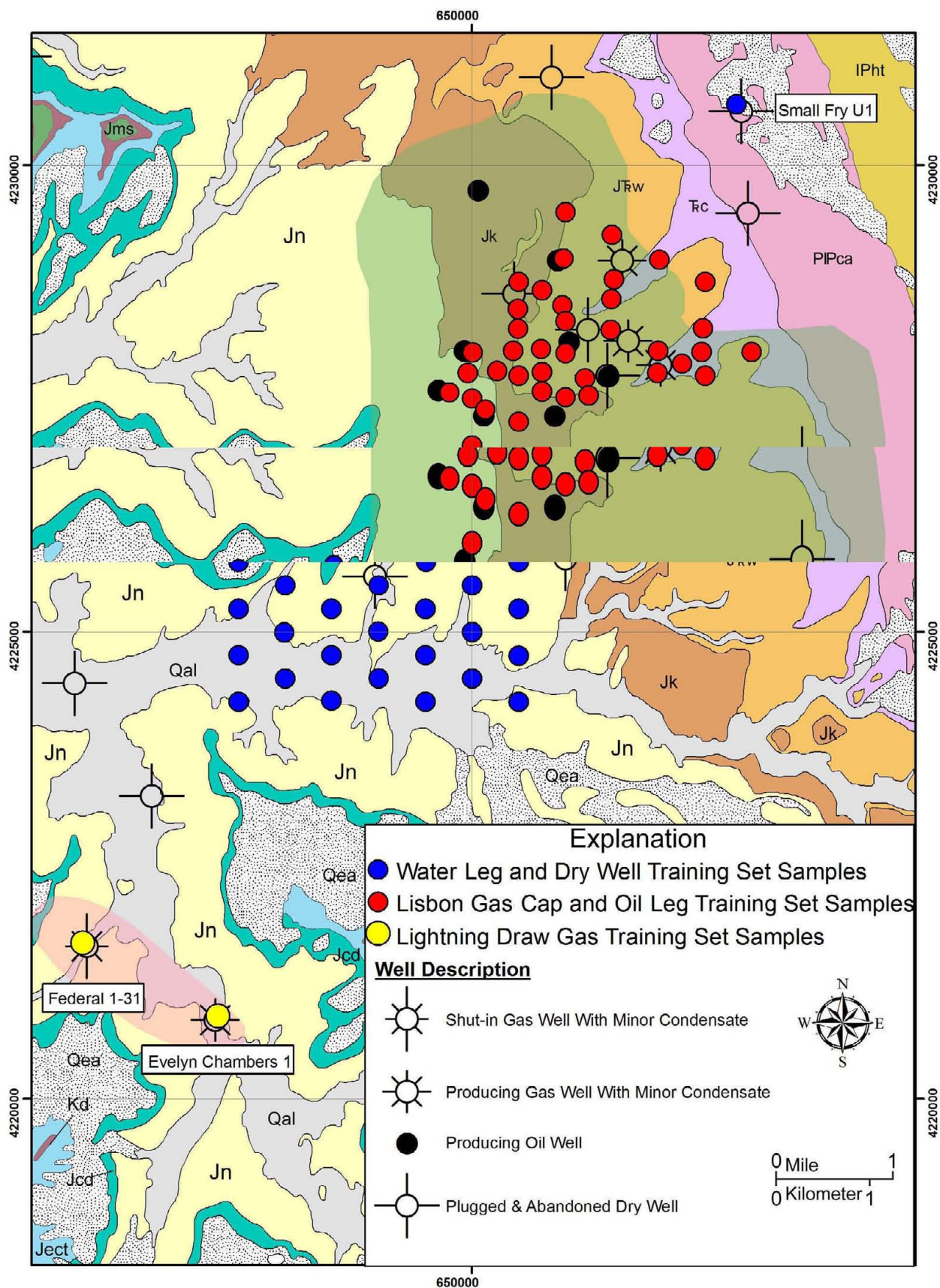


**Figure 24.** Surface soil training set samples used for two component Lisbon gas cap/oil leg versus water leg and Lightning Draw Southeast gas versus Lisbon water leg discriminant analysis models. See figure 14 for description of geologic units (geologic base modified from Doelling, 2005). Lisbon and Lightning Draw Southeast fields shown in bluish green and pink, respectively.

(Federal No. 1-31 and Evelyn Chambers No. 1) in LDSE field are also compared with the Lisbon water-leg samples (figure 24). Ethane and *n*-butane are important variables for discriminating between the productive part of Lisbon and the water leg.

Samples with anomalous Lisbon gas/oil probabilities (that is, samples with similar compositional character to productive parts of Lisbon field) comprise 20% of Lisbon field samples and there is a clustering of anomalies in the central, northwest, and southeast parts of the field (figure 25; table 4, row 3). A smaller proportion of anomalous samples (12%) fall outside of the productive limits of the field. The majority of anomalous samples within the field are over the Wingate and Kayenta Formations and isolated anomalies within and outside the field occur over Quaternary stream and eolian deposits, and the Cutler Group, Chile Formation, and Navajo Sandstone. At LDSE, 26% of samples over the field are predicted as having productive “Lisbon-like” compositional character (figure 25; table 4, row 3). Three anomalous samples (5% of samples off the field) are also evident off the field to the northeast (figure 25; table 4, row 3). Two of the 17 anomalous samples occur over Navajo Sandstone and the remainder are over Quaternary stream alluvium.

The microseepage over the productive part of LDSE field is distinct from that over the Lisbon water leg, and ethane and *n*-butane again are the most influential discriminating variables (figure 26). Ethylene, methane, pentane, and propane are also important variables for discrimination. Samples with anomalous LDSE gas probability comprise 38% of samples over the field and 3% of samples off the field (figure 26; table 4, row 4). One of the 20 anomalous samples occurs over Navajo Sandstone, and the remaining samples are situated over Quaternary stream alluvium. A smaller proportion of samples over and off Lisbon field predict as having “LDSE-like” compositional character (figure 26; table 4, row 4). Anomalies over the field are mainly over Wingate and Kayenta Formations with one sample situated over Navajo Sandstone. The two samples outside the productive limits of the field occur over the Wingate and Chinle Formations.

## Thermally Desorbed Hydrocarbons: Fracture-Fill Bryophyte, Lichen, and Soils

Several hydrocarbons are anomalous in outcrop fracture-fill bryophyte, lichen, and soils over Lisbon and LDSE fields as opposed to the Lisbon water-leg (table 3). As was done for the surface soils, discriminant analysis was performed on thermally desorbed  $C_1$  to  $C_{12}$  data from the outcrop bryophyte, lichen, and soils to determine if the microseepage over Lisbon and LDSE fields is compositionally distinct from that over the Lisbon water leg and, if so, to identify which variables contribute most to the discrimination. It is also important to determine if discriminant functions developed for both fields predict each other (that is, cross-validation). The discriminant scores (probabilities) are again plotted to evaluate the spatial association of anomalies with productive and non-productive areas.

### Fracture-Fill Bryophyte and Lichen

Fracture-fill bryophyte and lichen samples over the gas cap, oil leg, and water leg at Lisbon field were analyzed for compositional differences in a three-component discriminant model, and then samples over LDSE field were compared with those over the Lisbon water leg (figure 27). Bryophyte and lichen samples over the Lisbon gas cap, oil leg, and water leg are clearly different in terms of their compositional character as shown on the canonical score plot in figure 28. The canonical scores for each sample in the plot are derived by inserting the hydrocarbon concentrations into the two discriminant functions (that is, Roots 1 and 2). In the case of fracture-fill bryophyte and lichen, methane contributes most to the discrimination of the gas cap from the oil and water legs, and propane is the most important variable for separating the oil leg from the gas cap and water leg (figure 28). Seven bryophyte and lichen samples were taken over the LDSE anticline. One of the seven samples (14%) falls into the productive Lisbon gas cap category (figure 28; table 5, row 1). This sample was from the crest of the anticline near the Federal No. 1-31 gas well. Three out of seven (43%) samples at a lower structural level on the anticline (that is, near the Evelyn Chambers No. 1 gas/condensate well) predict to have Lisbon oil leg compositional character (figure 29; table 5).

**Table 5.** Correct and incorrect classifications for discriminant models (fracture-fill bryophyte and lichen). Orange shading represents the field being predicted by the model. The white area represents training set samples that are correctly classified.

| Row Number | Model                             | Correct Classification<br>(% of samples over field) |                   | Incorrect Classification<br>(% of samples off field) |                   |
|------------|-----------------------------------|-----------------------------------------------------|-------------------|------------------------------------------------------|-------------------|
|            |                                   | Lisbon                                              | Lightning Draw SE | Lisbon                                               | Lightning Draw SE |
| 1          | Lisbon Gas Probability            | 100                                                 | 14                | 0                                                    | 0                 |
| 2          | Lisbon Oil Probability            | 100                                                 | 28                | 0                                                    | 0                 |
| 3          | Lightning Draw SE Gas Probability | 75                                                  | 100               | 0                                                    | 0                 |



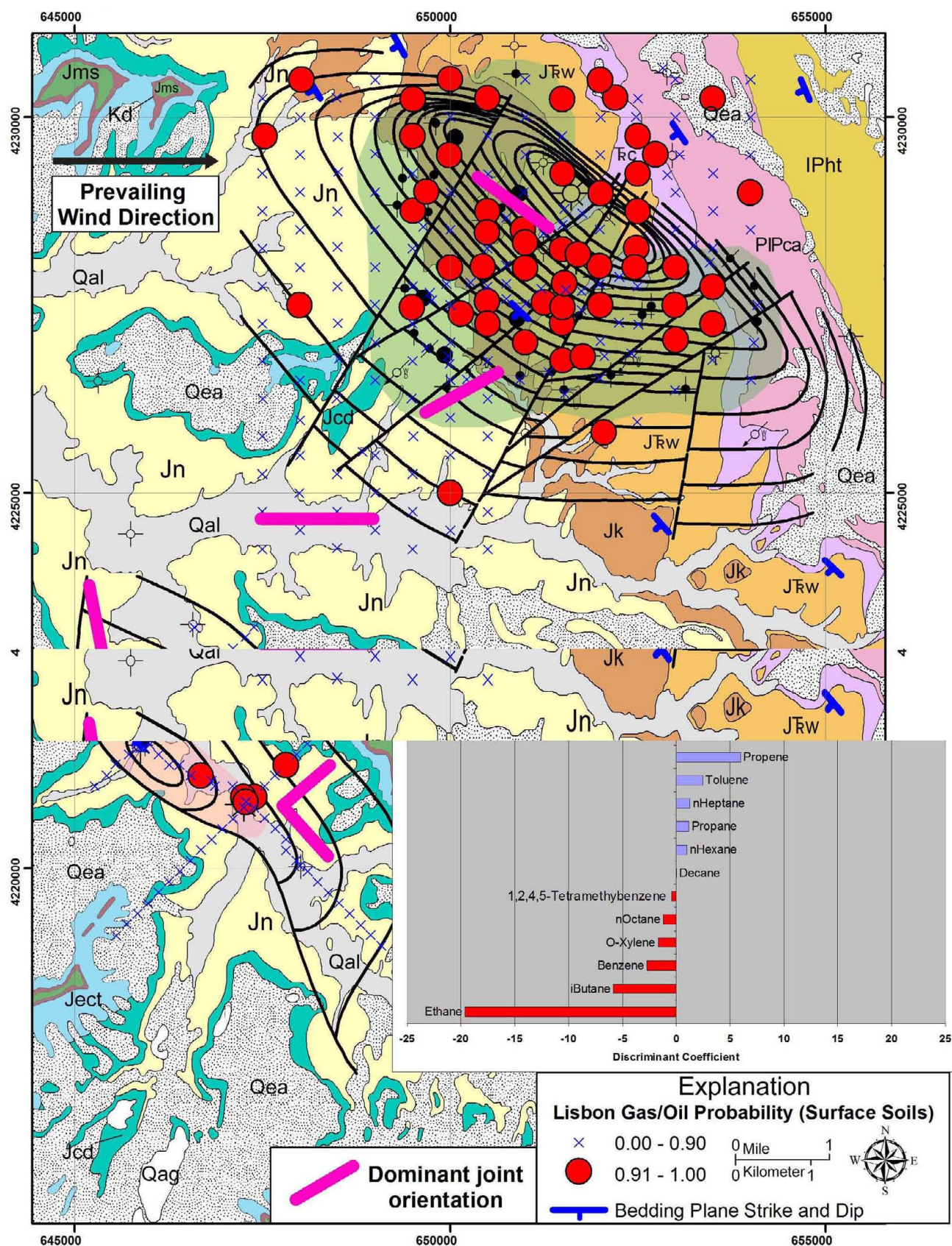


**Figure 25.** Distribution of Lisbon gas-oil probabilities derived from two-component discriminant analysis of thermally desorbed  $C_1$  to  $C_{12}$  hydrocarbon from surface soils. See figure 14 for description of geologic units (geologic base modified from Doelling, 2005) and figure 7 for explanations of well symbols; form line contours based on structure contour maps of the Leadville Limestone shown on figures 7 and 8. Lisbon and Lightning Draw South-east fields shown in bluish green and pink, respectively.



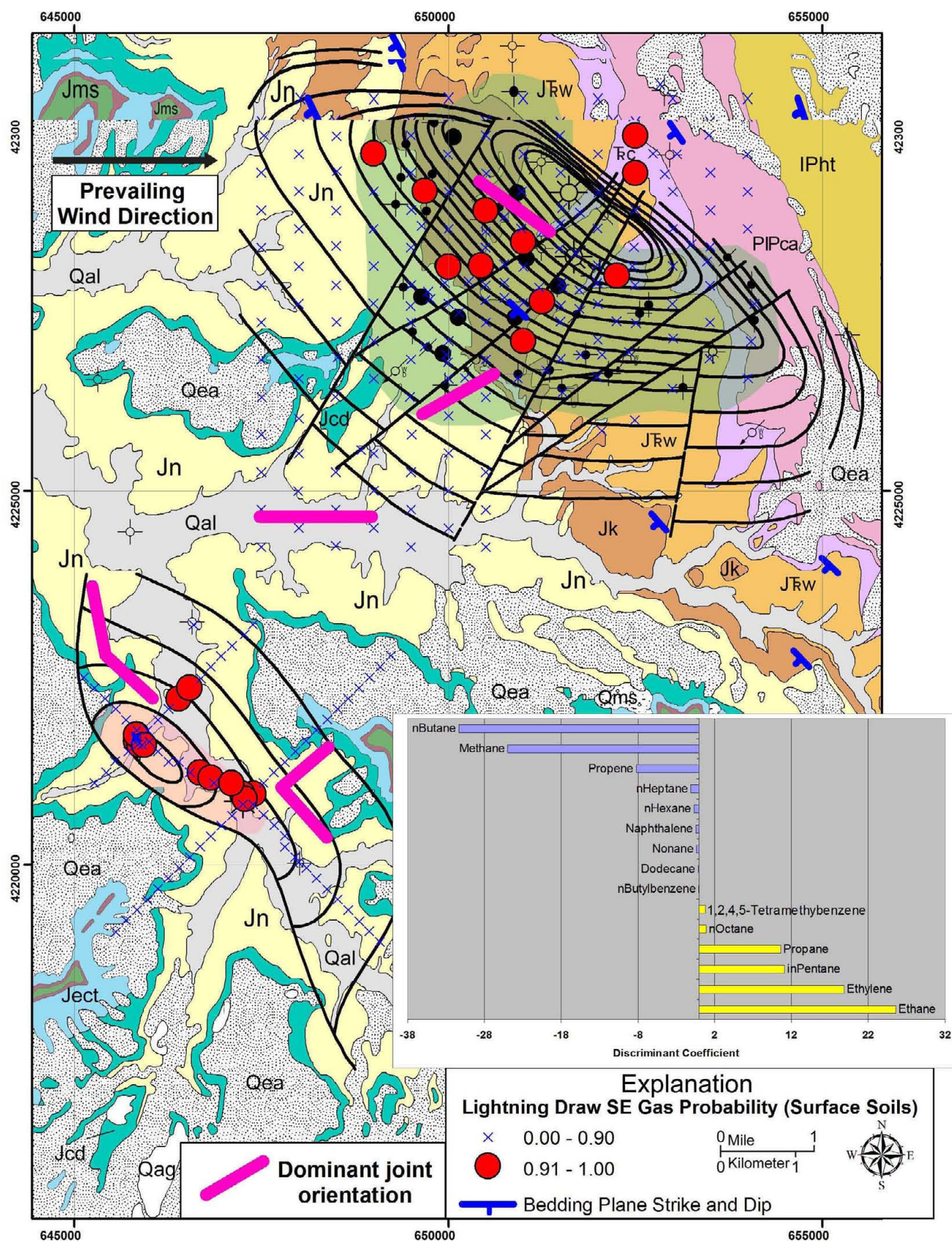


**Figure 26.** Distribution of Lightning Draw Southeast gas probabilities derived from two-component discriminant analysis of thermally desorbed  $C_1$  to  $C_{12}$  hydrocarbon from surface soils. See figure 14 for description of geologic units (geologic base modified from Doelling, 2005) and figure 7 for explanations of well symbols; form line contours based on structure contour maps of the Leadville Limestone shown on figures 7 and 8. Lisbon and Lightning Draw Southeast fields shown in bluish green and pink, respectively.



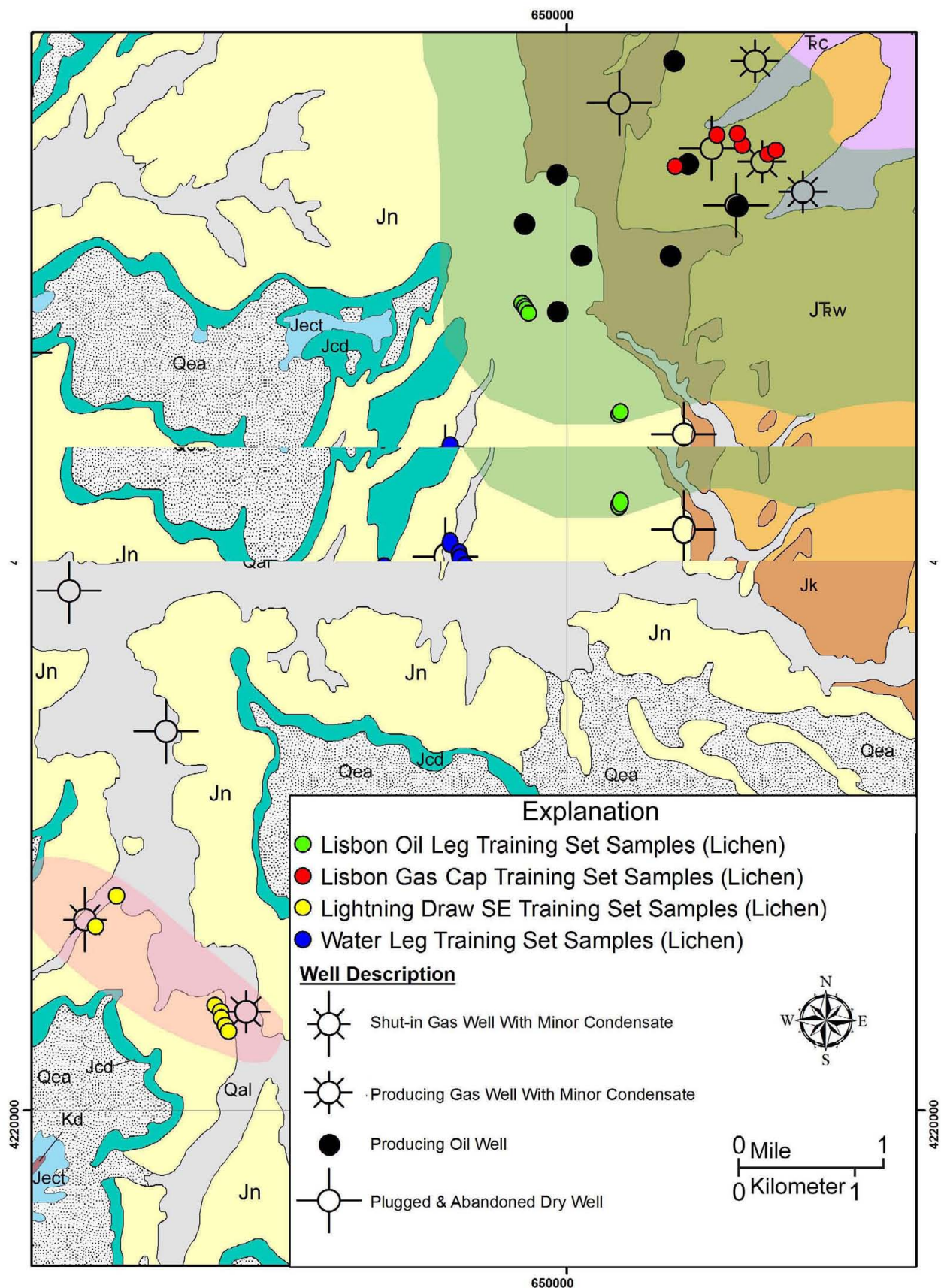


**Figure 27.** Bryophyte and lichen training set samples used for three-component Lisbon gas cap versus oil leg versus water leg and two-component Lightning Draw Southeast gas versus Lisbon water leg discriminant analysis models. See figure 14 for description of geologic units (geologic base modified from Doelling, 2005). Lisbon and Lightning Draw Southeast fields shown in bluish green and pink, respectively.



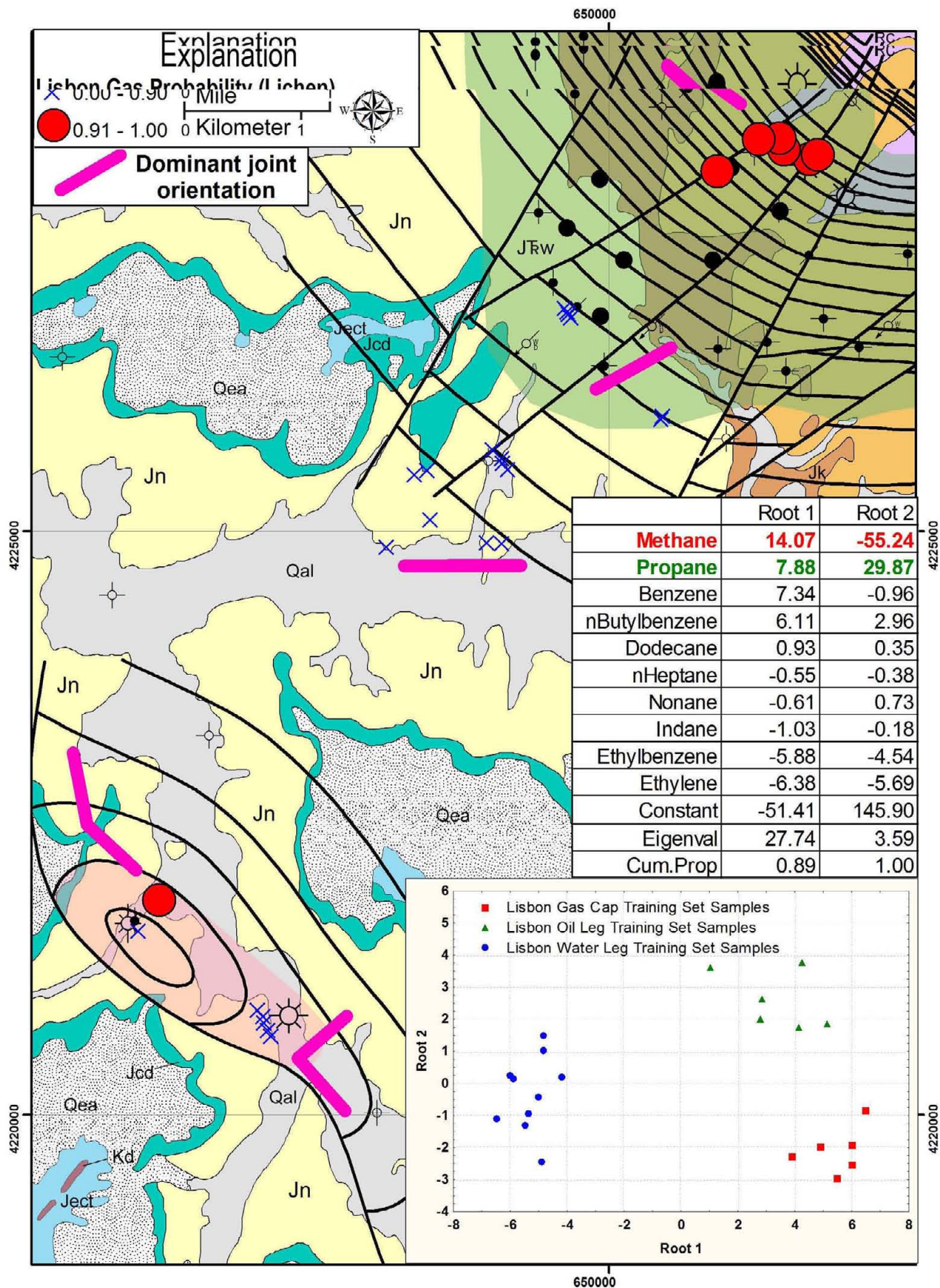


**Figure 28.** Distribution of Lisbon gas probability derived from three-component discriminant analysis of thermally desorbed C<sub>1</sub> to C<sub>12</sub> hydrocarbon from bryophyte and lichen samples. See figure 14 for description of geologic units (geologic base modified from Doelling, 2005) and figure 7 for explanations of well symbols; form line contours based on structure contour maps of the Leadville Limestone shown on figures 7 and 8. Lisbon and Lightning Draw Southeast fields shown in bluish green and pink, respectively.



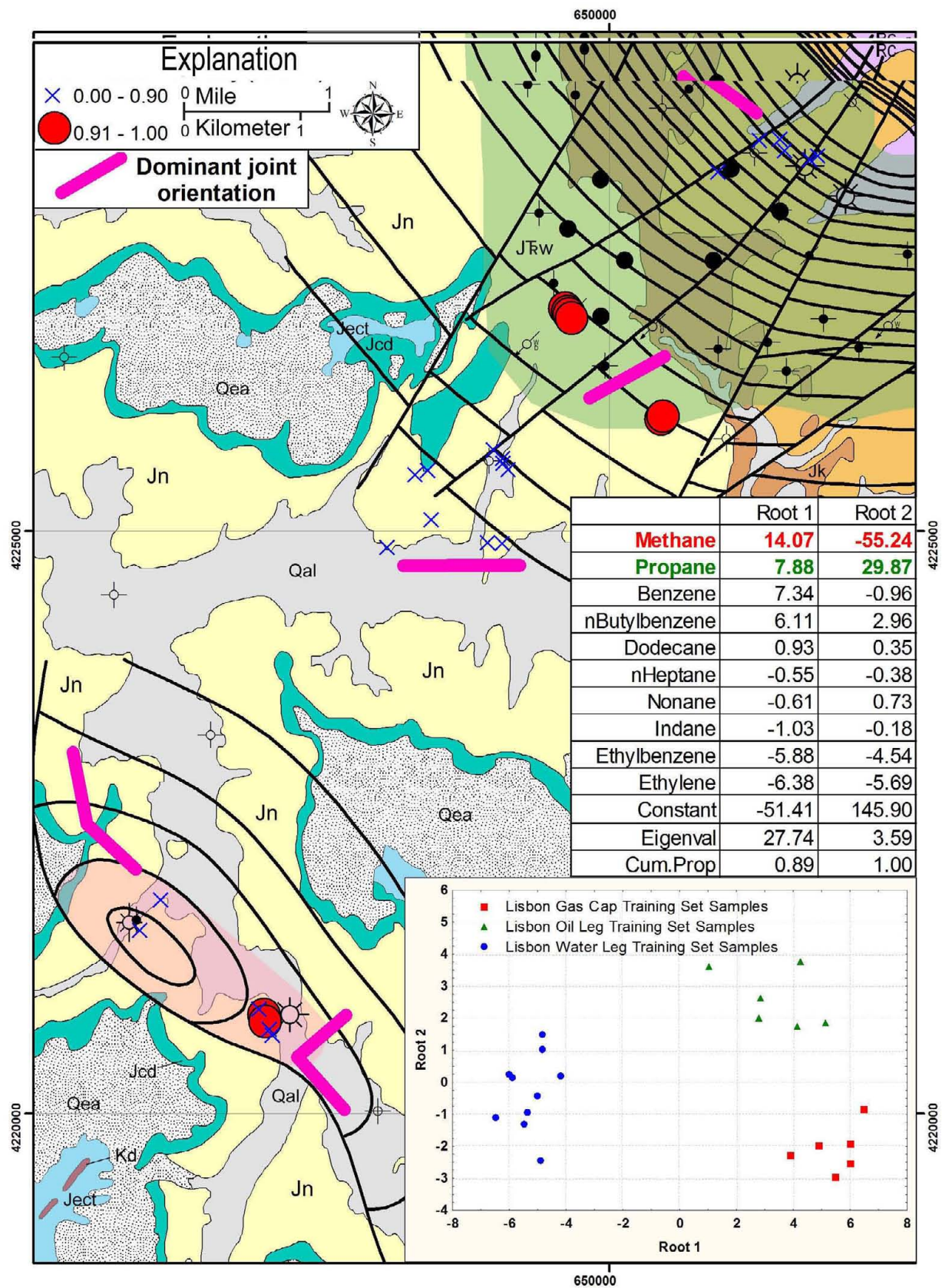


**Figure 29.** Distribution of Lisbon oil probability derived from three-component discriminant analysis of thermally desorbed  $C_1$  to  $C_{12}$  hydrocarbon from bryophyte and lichen samples. See figure 14 for description of geologic units (geologic base modified from Doelling, 2005) and figure 7 for explanations of well symbols; form line contours based on structure contour maps of the Leadville Limestone shown on figures 7 and 8. Lisbon and Lightning Draw Southeast fields shown in bluish green and pink, respectively.

When the bryophyte and lichen samples over LDSE gas field are compared with those over the Lisbon water leg, nine of twelve (75%) samples over the productive parts of the Lisbon field are predicted as having LDSE gas potential (figure 30; table 5). Important variables that contribute to the distinction between samples over LDSE field and the Lisbon water leg are ethane, *n*-hexane, propane, ethylene, *n*-butylbenzene, and ethylbenzene (figure 30).

### Fracture-Fill Soils

The same discriminant models were tested on C<sub>1</sub> to C<sub>12</sub> data from fracture-fill soils collected over the Lisbon gas cap, oil leg, and water leg, and LDSE field with the only difference being that more soils were available over the Lisbon gas cap than were bryophyte and lichen samples (compare figures 27 and 31). The compositional character of microseepage between the Lisbon gas cap, oil leg, and water leg is even more distinct (that is, more separation between canonical score clusters) than that shown by the bryophyte and lichen training set samples (compare figures 28 and 32). Like the bryophyte and lichen samples, variables in fracture-fill soils that contribute most to the discrimination of the gas cap and oil leg are methane and propane, respectively. A higher percentage of the fracture-fill soils over the LDSE field (71%) predict as Lisbon gas-prone as compared with that predicted by the bryophyte and lichen samples (14%). None of the fracture-fill soils over LDSE fall into the Lisbon oil leg category (figure 33; table 6, row 2).

Fracture-fill soils over LDSE field are compositionally distinct from the Lisbon water leg, but fewer of the Lisbon field soils (40%) predict as LDSE gas as compared with the 75% of the Lisbon bryophyte and lichen samples that predicted as LDSE gas-prone (figure 34). Variables that significantly contribute to the discrimination of microseepage in fracture-fill soils over LDSE field and the Lisbon water leg are *n*-pentane, *n*-butane, and ethylbenzene.

### Fluorescence of Solvent-Extractable Aromatic Hydrocarbons (Surface Soils)

Lisbon oil samples (from Lisbon No. C-99 and Lisbon No. D-716 wells) have condensate to medium gravity oil fluorescence spectral

patterns, and they can therefore be classified as “light oils” (figures 35a and 35b). Background and anomalous fluorescence patterns are clearly distinguished in surface soils. In background areas, peak wavelengths are low intensity and below the 300 nm single-ring aromatic wavelength (figures 19 and 35c). Synchronous scanned fluorescence spectra in anomalous areas are more intense and extend to longer, multi-ring aromatic wavelengths (figures 35d and 35e). Soil samples with these anomalous spectra contain light oil that has been weathered through chemical and biological oxidation processes. As weathering progresses, the once fresh light oil (as in figures 35a and 35b) gradually loses its light single and double ring aromatic compounds leaving a residue of 3- to 6-ring aromatics that fluoresce in the 395 to 470 nm range (figures 35d and 35e). Asphalt dust from paved roads can add intensity to peaks in the 350 to 450 nm range thereby producing false anomalies (figure 35f). Soil samples collected near paved roads in this study were therefore removed from the database prior to interpreting the SSF data.

Factor analysis reveals high loadings for the 395 nm, 431 nm, and 470 nm peaks (that is, heavy 4- to 6-ring aromatic residue in weathered light oil). Samples with high correlation of these fluorescence peaks (that is, high 395 to 470 nm factor scores) are clustered in the central and eastern part of Lisbon field where closely spaced normal faults are most abundant (figure 36). One anomaly cluster, in the central part of the field, is parallel to a northeast-oriented normal fault in the Lisbon anticline and the joint set in the oil leg (figure 36). Most anomalies occur over Wingate Sandstone, but isolated anomalies are also found over the Chinle, Kayenta, and Navajo Formations. Anomalous samples comprise 10% and 3% of the samples over and off the field, respectively.

Anomalous 395 to 470 nm factor scores are also evident in 17% of the samples over LDSE field, and the orientation of the 0.6-mile-long (1-km) anomaly in the southeast part of the field is sub-parallel to joint sets in Navajo Sandstone (figure 36). They occur mainly over Quaternary stream alluvium with the exception of the southeasternmost anomaly, which is situated over Navajo Sandstone (figure 36).

**Table 6.** Correct and incorrect classifications for discriminant models (fracture-fill soils). Orange shading represents the field being predicted by the model. The white area represents training set samples that are correctly classified.

| Row Number | Model                             | Correct Classification (% of samples over field) |                   | Incorrect Classification (% of samples off field) |                   |
|------------|-----------------------------------|--------------------------------------------------|-------------------|---------------------------------------------------|-------------------|
|            |                                   | Lisbon                                           | Lightning Draw SE | Lisbon                                            | Lightning Draw SE |
| 1          | Lisbon Gas Probability            | 100                                              | 71                | 0                                                 | 0                 |
| 2          | Lisbon Oil Probability            | 83                                               | 0                 | 0                                                 | 0                 |
| 3          | Lightning Draw SE Gas Probability | 50                                               | 100               | 0                                                 | 0                 |



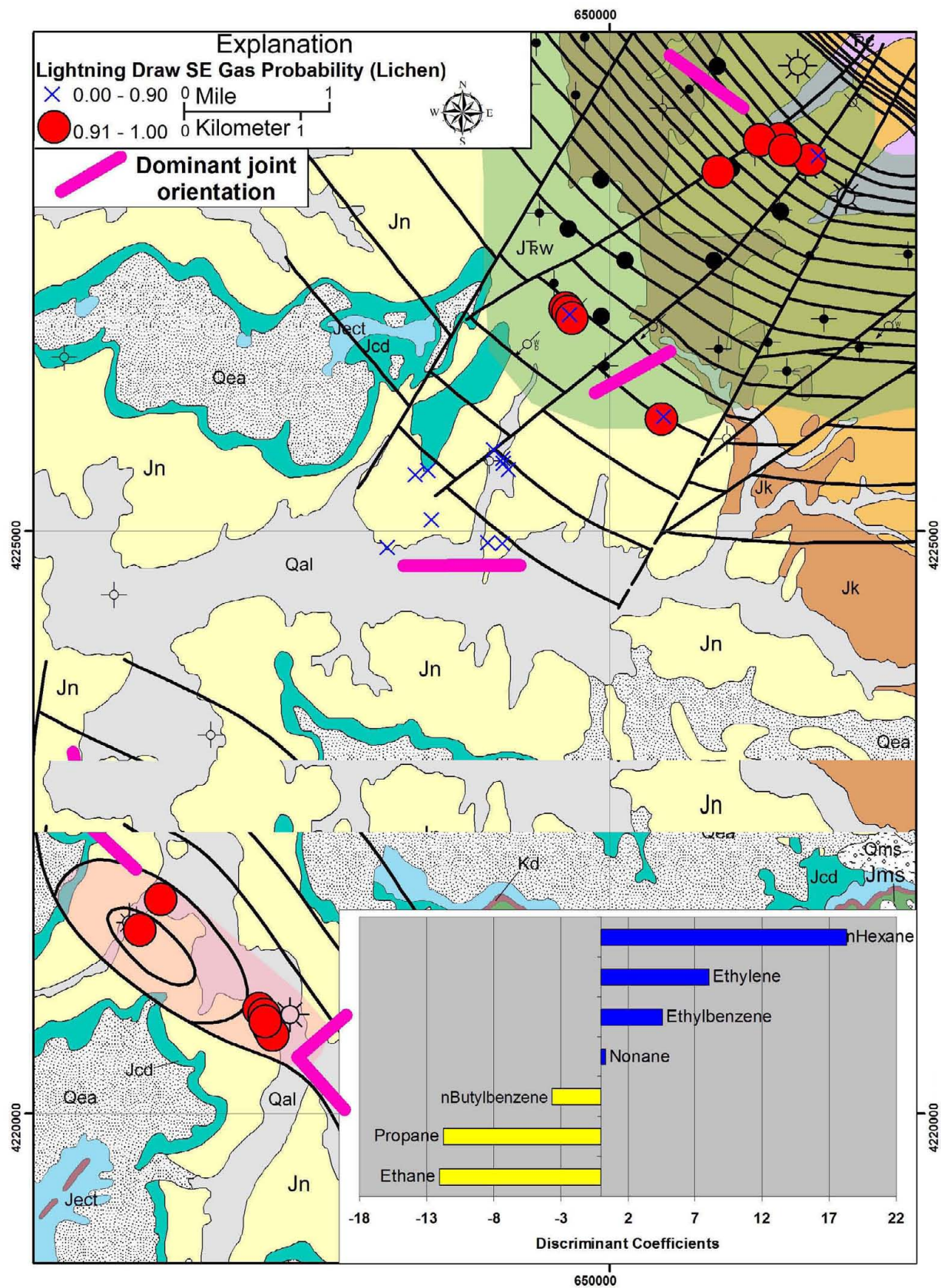


**Figure 30.** Distribution of Lightning Draw Southeast gas probabilities derived from two-component discriminant analysis of thermally desorbed  $C_1$  to  $C_{12}$  hydrocarbon from bryophyte and lichen samples. See figure 14 for description of geologic units (geologic base modified from Doelling, 2005) and figure 7 for explanations of well symbols; form line contours based on structure contour maps of the Leadville Limestone shown on figures 7 and 8. Lisbon and Lightning Draw Southeast fields shown in bluish green and pink, respectively.

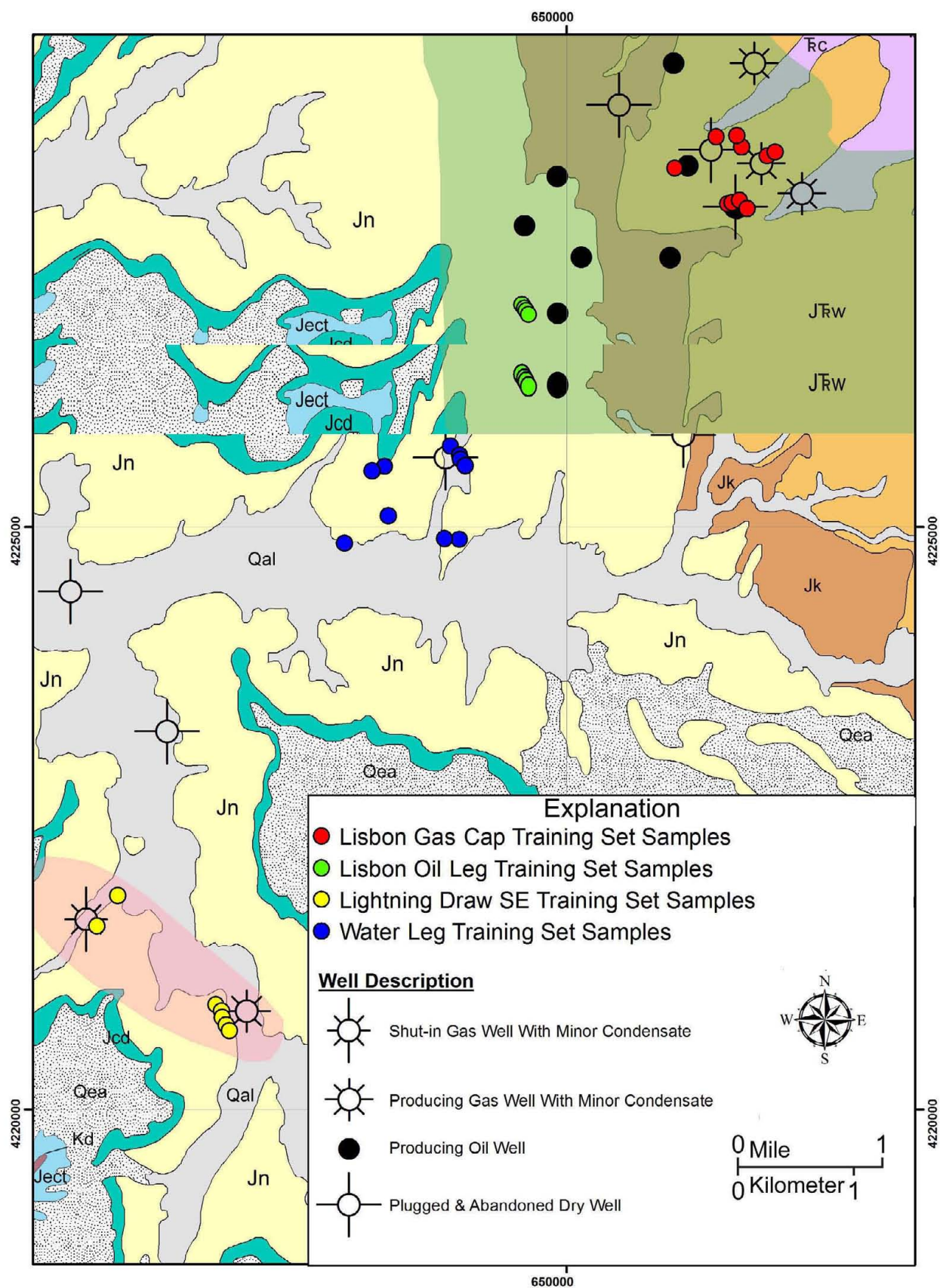


**Figure 31.** Fracture-fill soil training set samples used for three-component Lisbon gas cap versus oil leg versus water leg and two-component Lightning Draw Southeast gas versus Lisbon water leg discriminant analysis models. See figure 14 for description of geologic units (geologic base modified from Doelling, 2005). Lisbon and Lightning Draw Southeast fields shown in bluish green and pink, respectively.



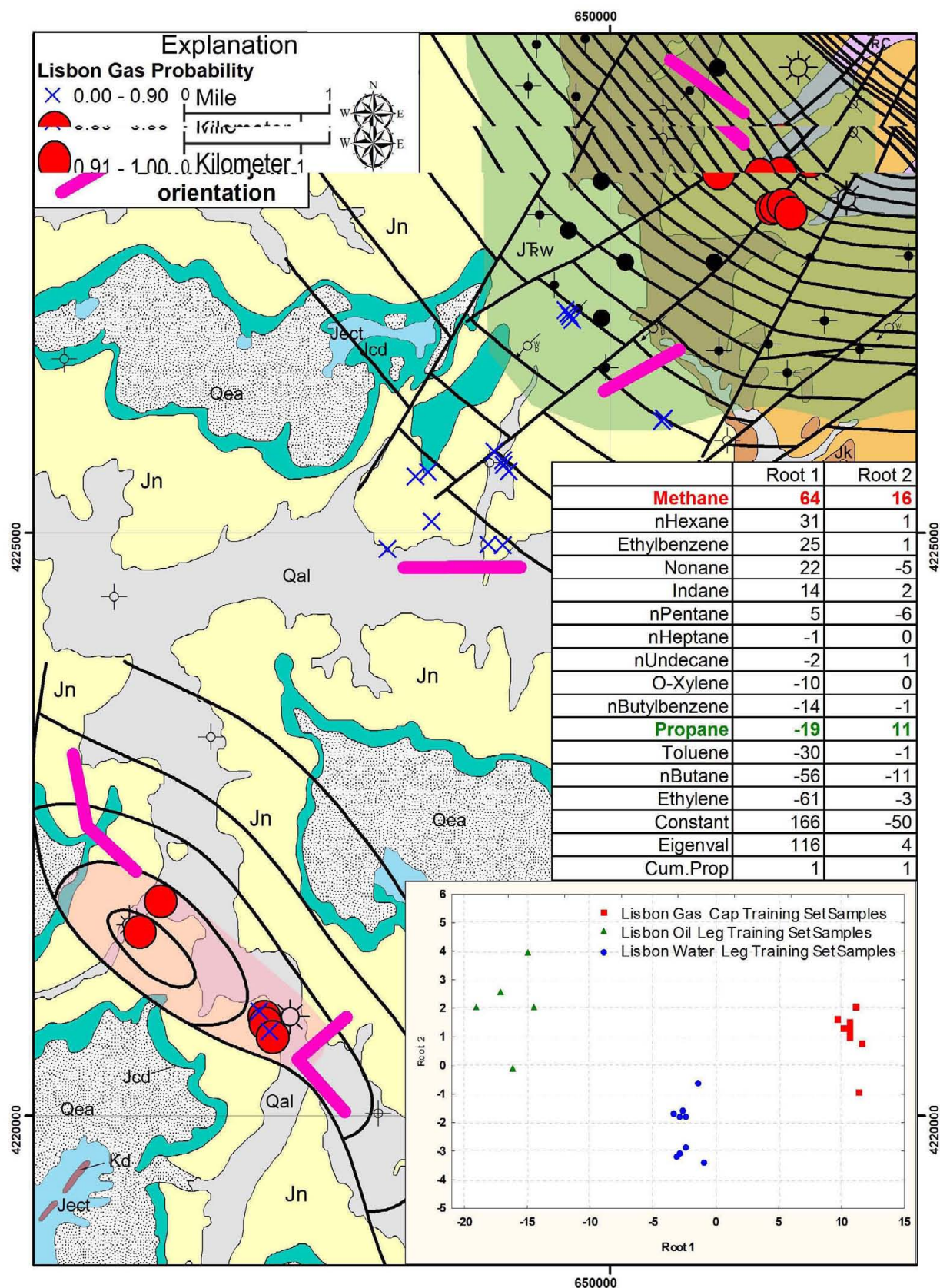


**Figure 32.** Distribution of Lisbon gas probability derived from three-component discriminant analysis of thermally desorbed  $C_1$  to  $C_{12}$  hydrocarbon from fracture-fill soil samples. See figure 14 for description of geologic units (geologic base modified from Doelling, 2005) and figure 7 for explanations of well symbols; form line contours based on structure contour maps of the Leadville Limestone shown on figures 7 and 8. Lisbon and Lightning Draw Southeast fields shown in bluish green and pink, respectively.



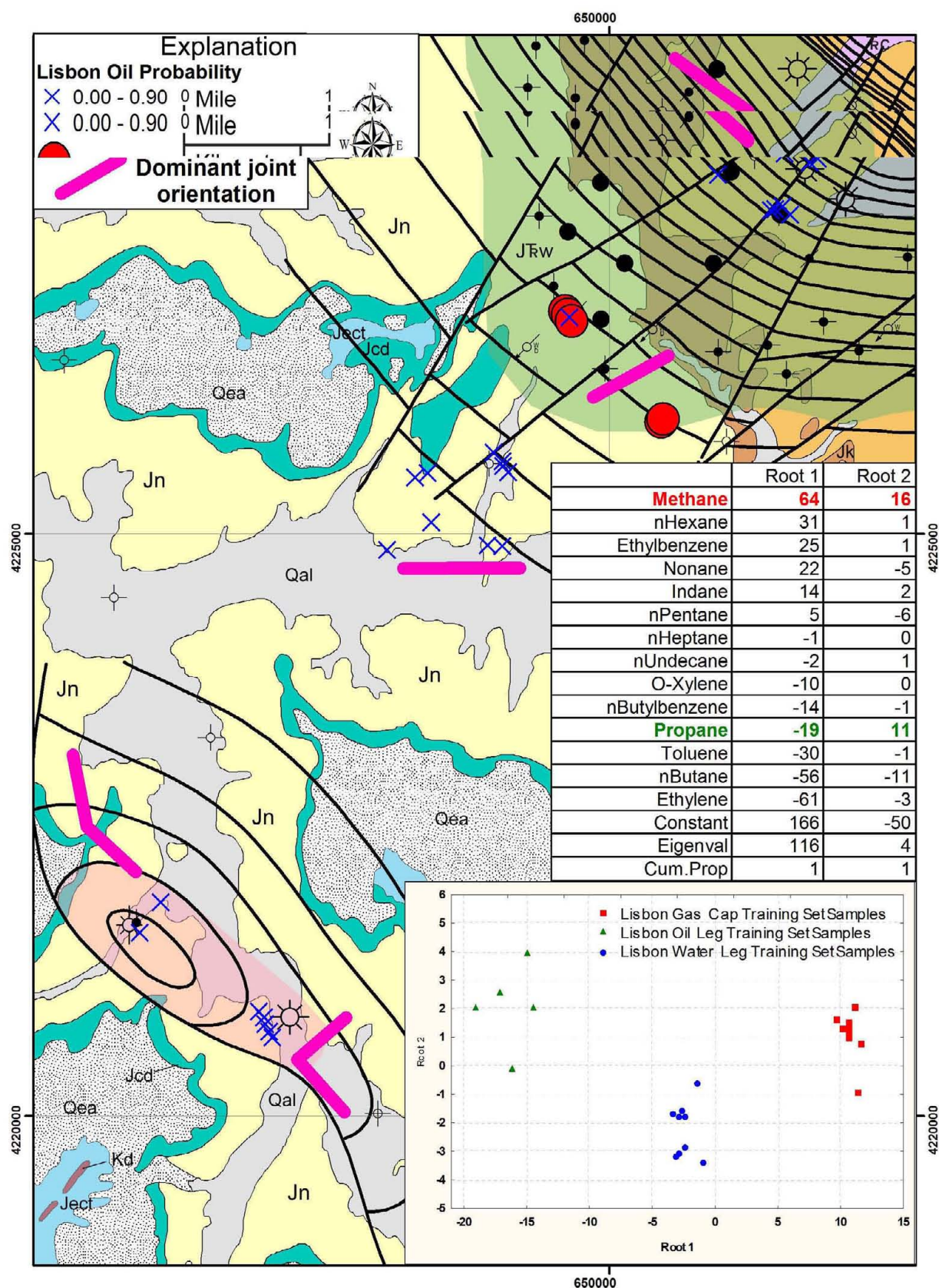


**Figure 33.** Distribution of Lisbon oil probability derived from three-component discriminant analysis of thermally desorbed  $C_1$  to  $C_{12}$  hydrocarbon from fracture-fill soil samples. See figure 14 for description of geologic units (geologic base modified from Doelling, 2005) and figure 7 for explanations of well symbols; form line contours based on structure contour maps of the Leadville Limestone shown on figures 7 and 8. Lisbon and Lightning Draw Southeast fields shown in bluish green and pink, respectively.



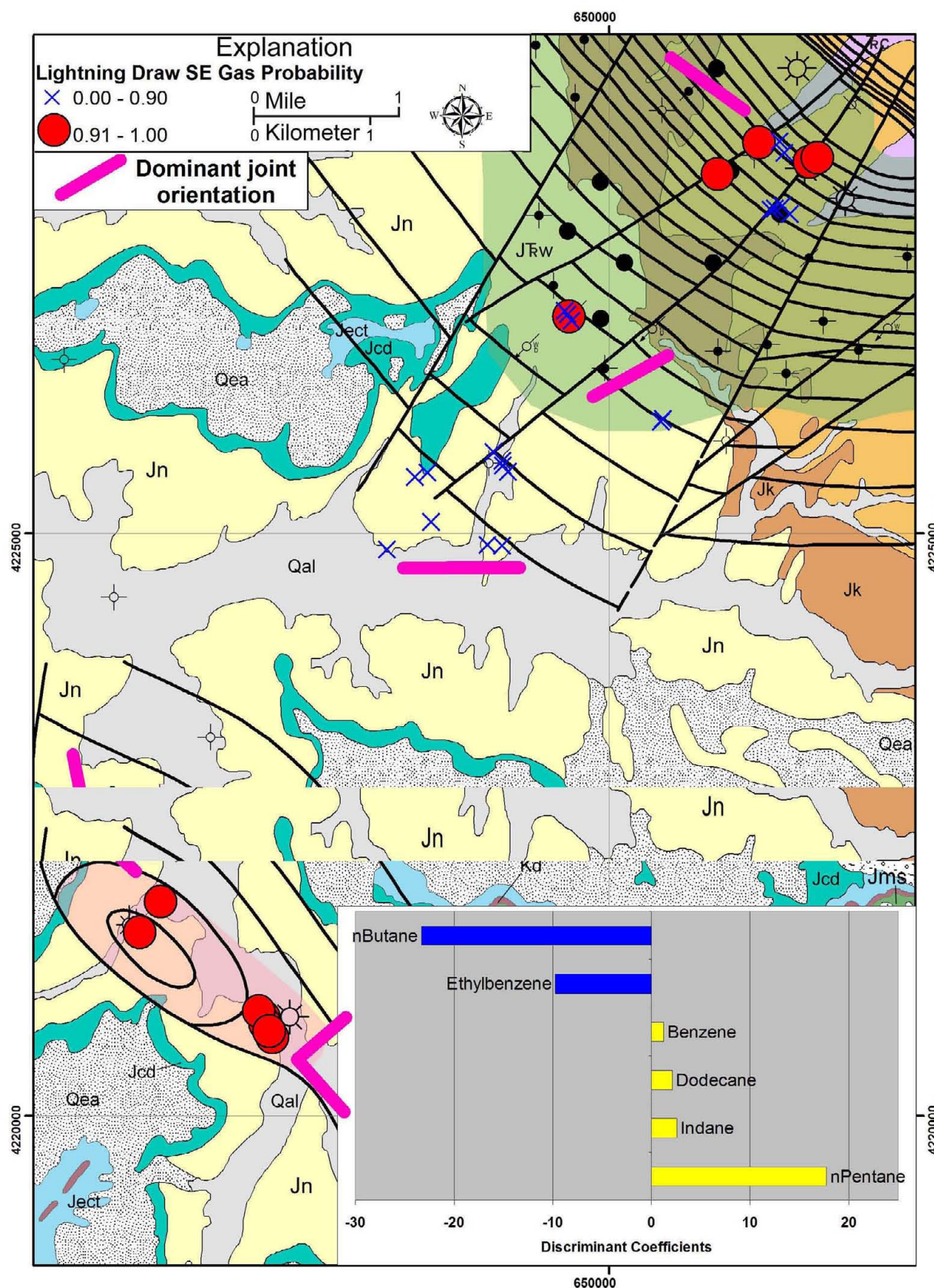


**Figure 34.** Distribution of Lightning Draw Southeast gas probabilities derived from two-component discriminant analysis of thermally desorbed  $C_1$  to  $C_{12}$  hydrocarbon from fracture-fill soil samples. See figure 14 for description of geologic units (geologic base modified from Doelling, 2005) and figure 7 for explanations of well symbols; form line contours based on structure contour maps of the Leadville Limestone shown on figures 7 and 8. Lisbon and Lightning Draw Southeast fields shown in bluish green and pink, respectively.

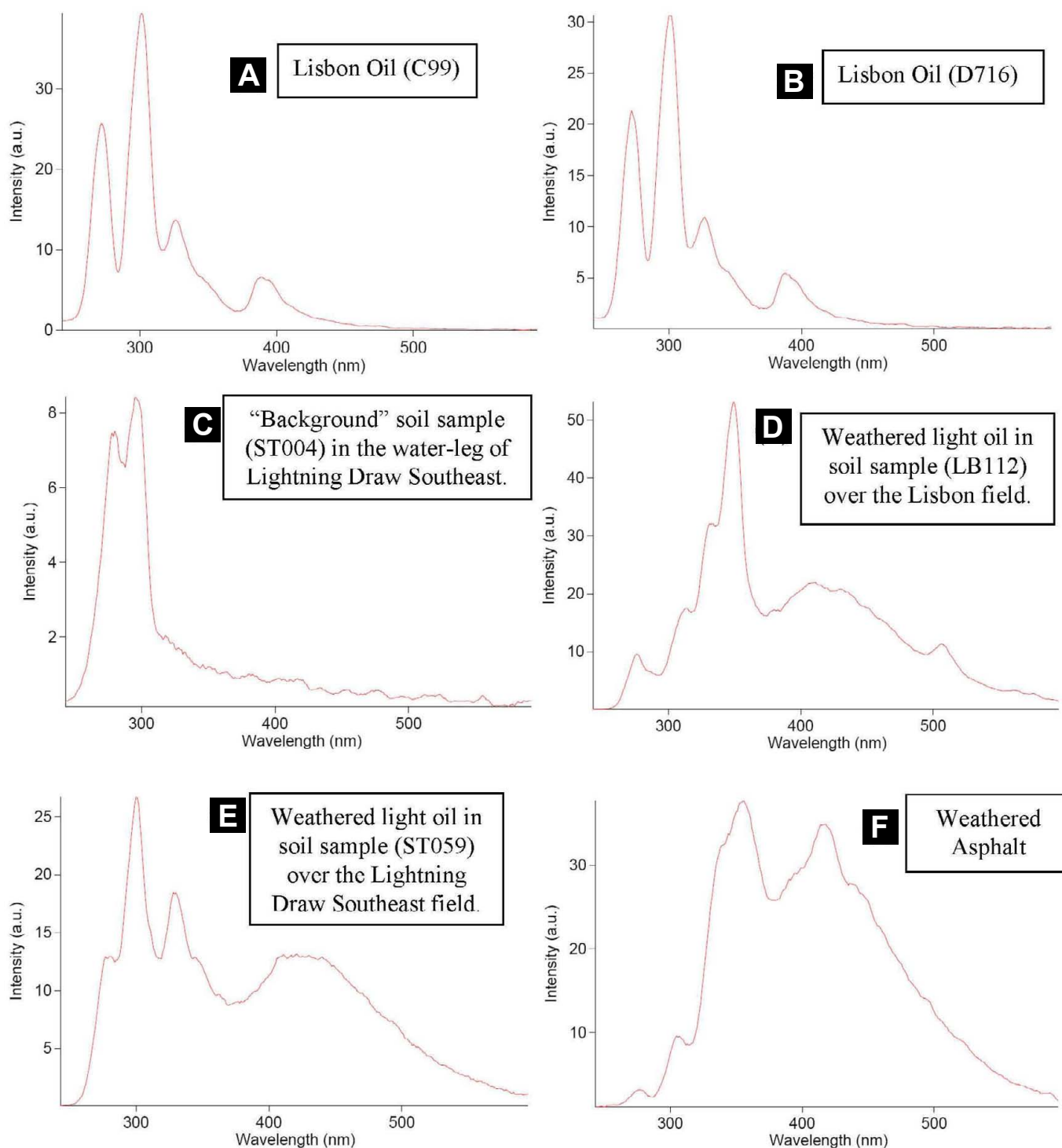


**Figure 35.** Synchronous scanned fluorescence spectra for Lisbon oil (a and b), background soil sample (c), weathered oil in soil over Lisbon field (d), weathered oil in soil over Lightning Draw Southeast field (e), and weathered asphalt (f).

### Hydrocarbons and Fixed Gases (Free-Gas Samples)

Hydrocarbon concentration anomalies in free-gas samples show a distinct spatial correlation with productive parts of LDSE gas field. For example, high-contrast propane anomalies are evident in three samples (19%) over a distance of 600 feet (200 m) (figure 37, table 7). Isohexane is also anomalous in two adjacent samples over a

distance of 450 feet (150 m) and in one isolated sample over the gas field (figure 38). None of the free-gas samples off-structure are anomalous in hydrocarbons (figures 37 and 38). Hydrogen is anomalous in six (38%) samples for a distance of 1200 ft (400 m) over the top of the LDSE anticline and in one (7%) sample off-structure (figure 39, table 7). Carbon dioxide, which is a significant component of the produced gas (table 1), is anomalous in eight (50%) free-gas samples for a distance of 1500 feet (500 m)



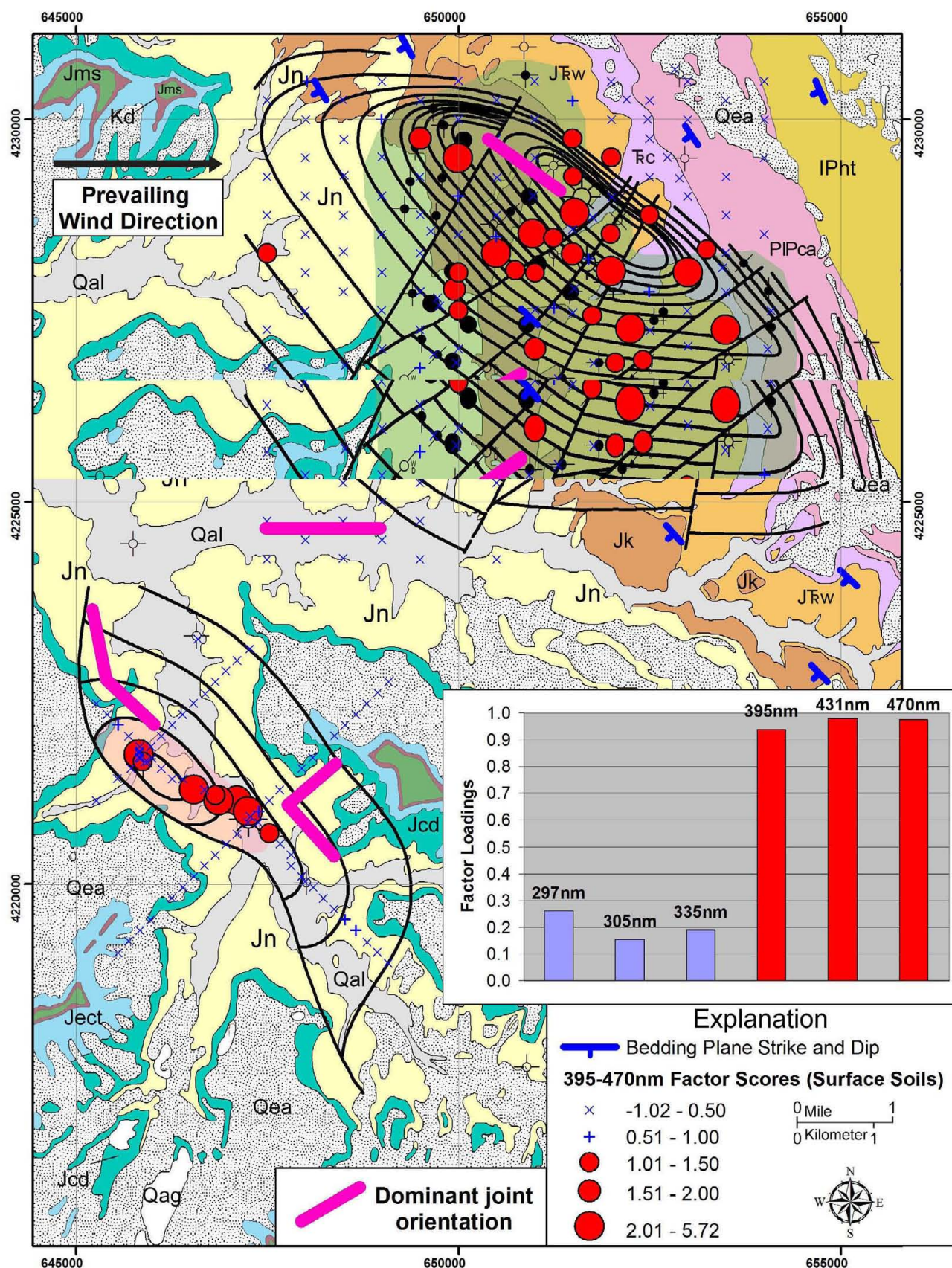


**Figure 36.** Distribution of 395 to 470 nm factor scores (3- to 6-ring aromatics) in surface soils over Lisbon and Lightning Draw Southeast fields (shown in bluish green and pink, respectively). See figure 14 for description of geologic units (geologic base modified from Doelling, 2005) and figure 7 for explanations of well symbols; form line contours based on structure contour maps of the Leadville Limestone shown on figures 7 and 8.

over the LDSE anticline and in four (27%) samples off-structure (figure 40, table 7). Helium, which is also concentrated in the produced gas (table 1), is above ambient levels ( $>5.2$  parts per million [ppm]) in six samples off-structure at LDSE field and in three samples over the water leg of Lisbon field (figure 41). This represents 60% of the samples collected off the LDSE field (table 7).

### Acid-Extractable Metals (Soils and Fracture-Fillings)

Major and trace element anomalies in soils, fracture-fillings, bryophyte, and lichen are evident over both Lisbon and LDSE fields (table 3). A larger variety of trace metals are anomalous in surface soils over LDSE compared with soils over Lisbon. Elements that show a distinct spatial correlation with Lisbon and/or LDSE fields are cadmium, uranium, molybdenum, vanadium, manganese, lead, mercury, and organic carbon (table 8).

Factor analysis reveals two heavy metal element associations that are spatially associated with Lisbon and LDSE fields. The first factor has high loadings for cadmium, uranium, and molybdenum, and moderate loadings for vanadium, manganese, and lead (figure 42). Samples that show correlation of these elements form a 1.2-miles-long (2 km), northeast-trending anomaly cluster mainly over the Chinle Formation along a canyon in the east-central part of Lisbon field (figure 42). The canyon has a similar orientation to the dominant joint set in Navajo Sandstone over the

Lisbon oil leg (figure 42). These anomalous samples comprise 3% and 2% of the samples over and off Lisbon field, respectively. A higher proportion of anomalous samples are evident in Quaternary stream alluvium over LDSE field (figure 42, table 8). The 0.6-mile-long (1 km) anomaly over the southeast half of the field is subparallel to joint sets in Navajo and it is spatially correlated with heavy aromatic hydrocarbon anomalies shown in figure 36. Only 3% of samples off the field report as anomalous and these occur over Quaternary stream alluvium and Navajo Sandstone (figure 42; table 8).

The second factor shows high loadings for mercury, organic carbon, and lead. These elements are correlated (that is, factor scores  $>1$ ) in 12% and 8% of samples over and off Lisbon field, respectively (figure 43, table 8). Anomalies are evident mainly over the Wingate and Kayenta Formations in the upper part of the Lisbon anticline (figure 43). Although the anomalies are clustered in the northwest, central, and southeast parts of the field, their overall trend is northwest, which is similar to the joint set in Wingate sandstones. A higher proportion of anomalous samples are evident over LDSE field and, as for the heavy aromatic hydrocarbons and cadmium-uranium-molybdenum-vanadium-manganese-lead (Cd-U-Mo-V-Mn-Pb) element association, the anomalies cluster over the southeast half of the field (figure 43, table 8). The majority of the anomalous samples occur over alluvium, but two anomalies are also situated over Navajo Sandstone. The trend of

**Table 7.** Percent of anomalous free-gas samples over and off Lightning Draw Southeast field.

| Variable       | % of anomalous samples over field | % of anomalous samples off field |
|----------------|-----------------------------------|----------------------------------|
| Propane        | 19                                | 0                                |
| Iso-Hexane     | 19                                | 0                                |
| Hydrogen       | 38                                | 7                                |
| Carbon Dioxide | 50                                | 27                               |
| Helium         | 0                                 | 60                               |

**Table 8.** Percent of anomalous soil samples over and off Lisbon and Lightning Draw Southeast fields.

| Variable                           | % anomalous samples over field |                   | % anomalous samples off field |                   |
|------------------------------------|--------------------------------|-------------------|-------------------------------|-------------------|
|                                    | Lisbon                         | Lightning Draw SE | Lisbon                        | Lightning Draw SE |
| Cd-U-Mo-V-Mn-Pb Factor Scores      | 3                              | 21                | 2                             | 3                 |
| Hg-Organic Carbon-Pb Factor Scores | 12                             | 23                | 8                             | 6                 |
| Fluoride Z-scores                  | 1                              | 38                | 6                             | 4                 |
| Arsenic Z-scores                   | 1                              | 49                | 0                             | 15                |



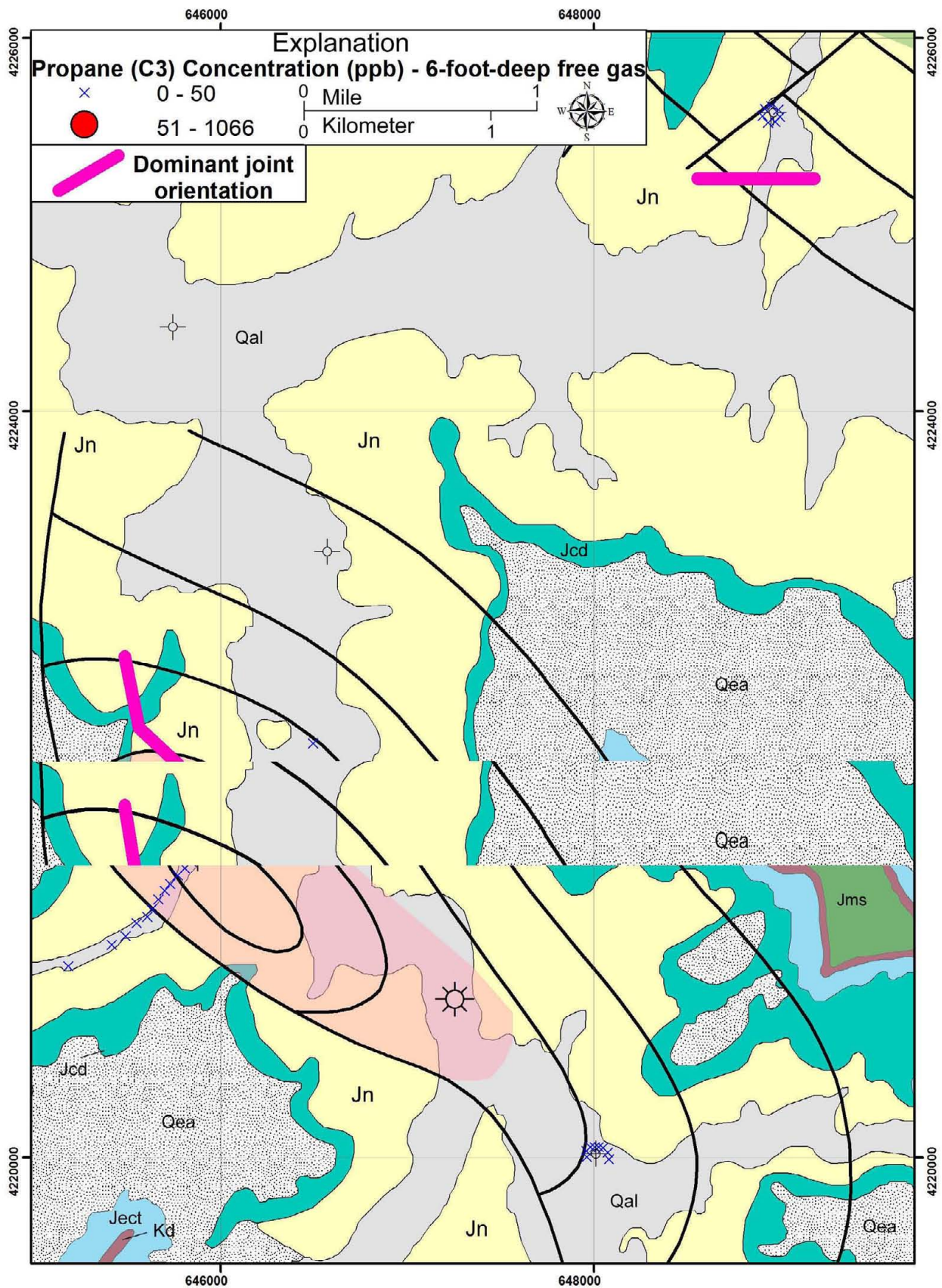


**Figure 37.** Distribution of propane concentrations in 6-foot-deep free gas over Lightning Draw Southeast field (shown in pink) and background areas. See figure 14 for description of geologic units (geologic base modified from Doelling, 2005) and figure 8 for explanations of well symbols; form line contours based on structure contour map of the Leadville Limestone shown on figure 8.



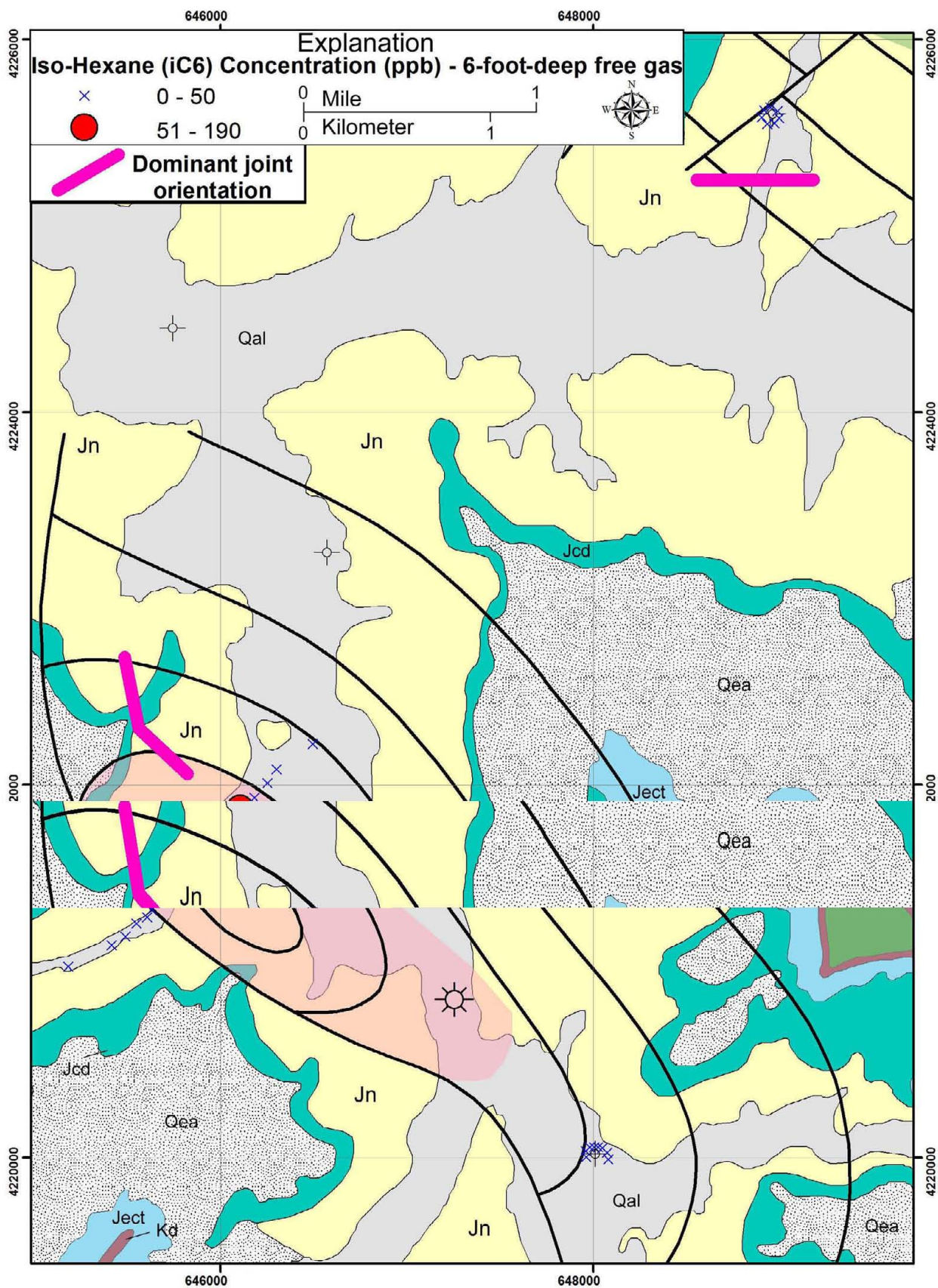


**Figure 38.** Distribution of isohexane concentrations in 6-foot-deep free gas over Lightning Draw Southeast field (shown in pink) and background areas. See figure 14 for description of geologic units (geologic base modified from Doelling, 2005) and figure 8 for explanations of well symbols; form line contours based on structure contour map of the Leadville Limestone shown on figure 8.



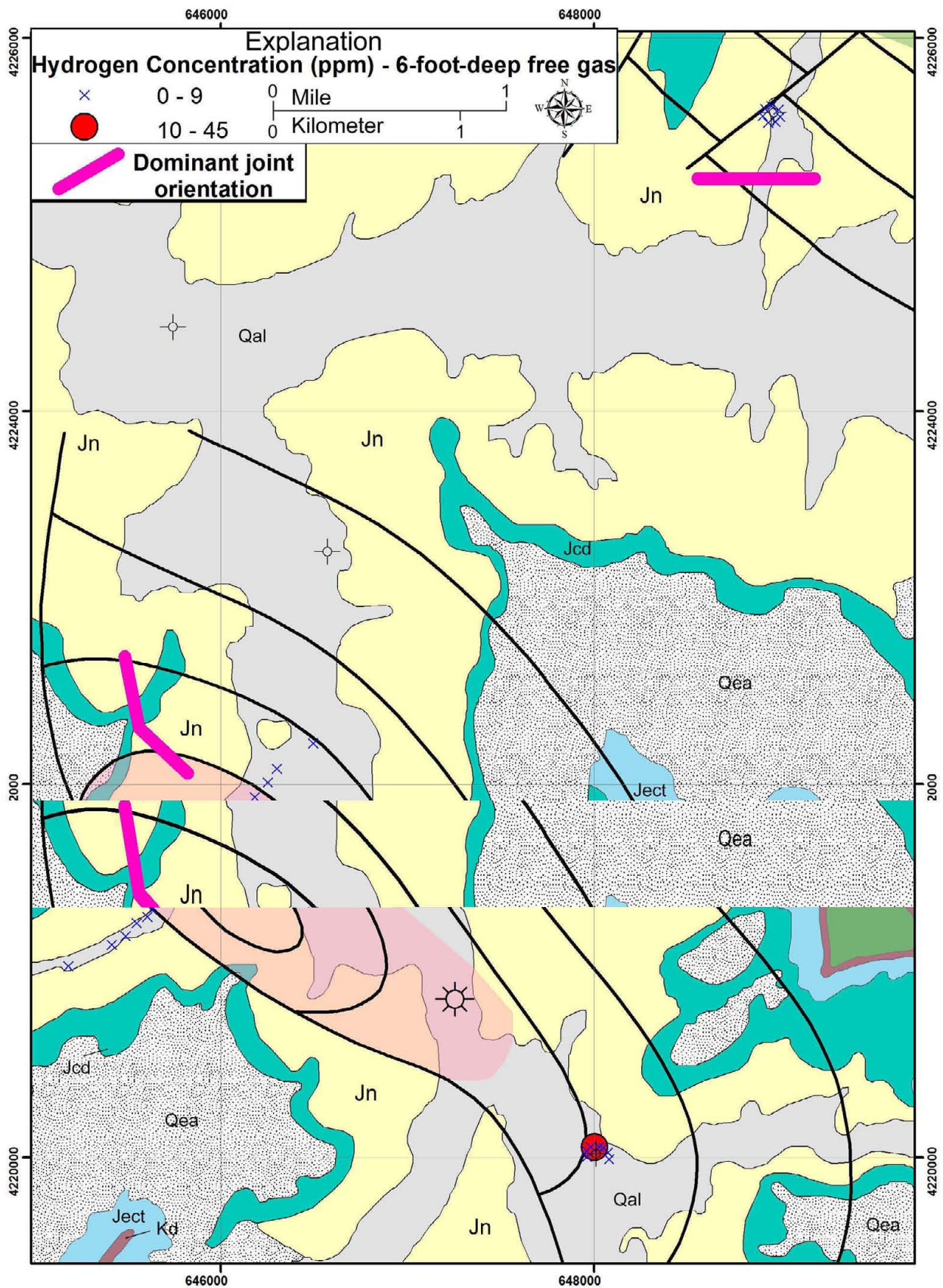


**Figure 39.** Distribution of hydrogen concentrations in 6-foot-deep free gas over Lightning Draw Southeast field (shown in pink) and background areas. See figure 14 for description of geologic units (geologic base modified from Doelling, 2005) and figure 8 for explanations of well symbols; form line contours based on structure contour map of the Leadville Limestone shown on figure 8.



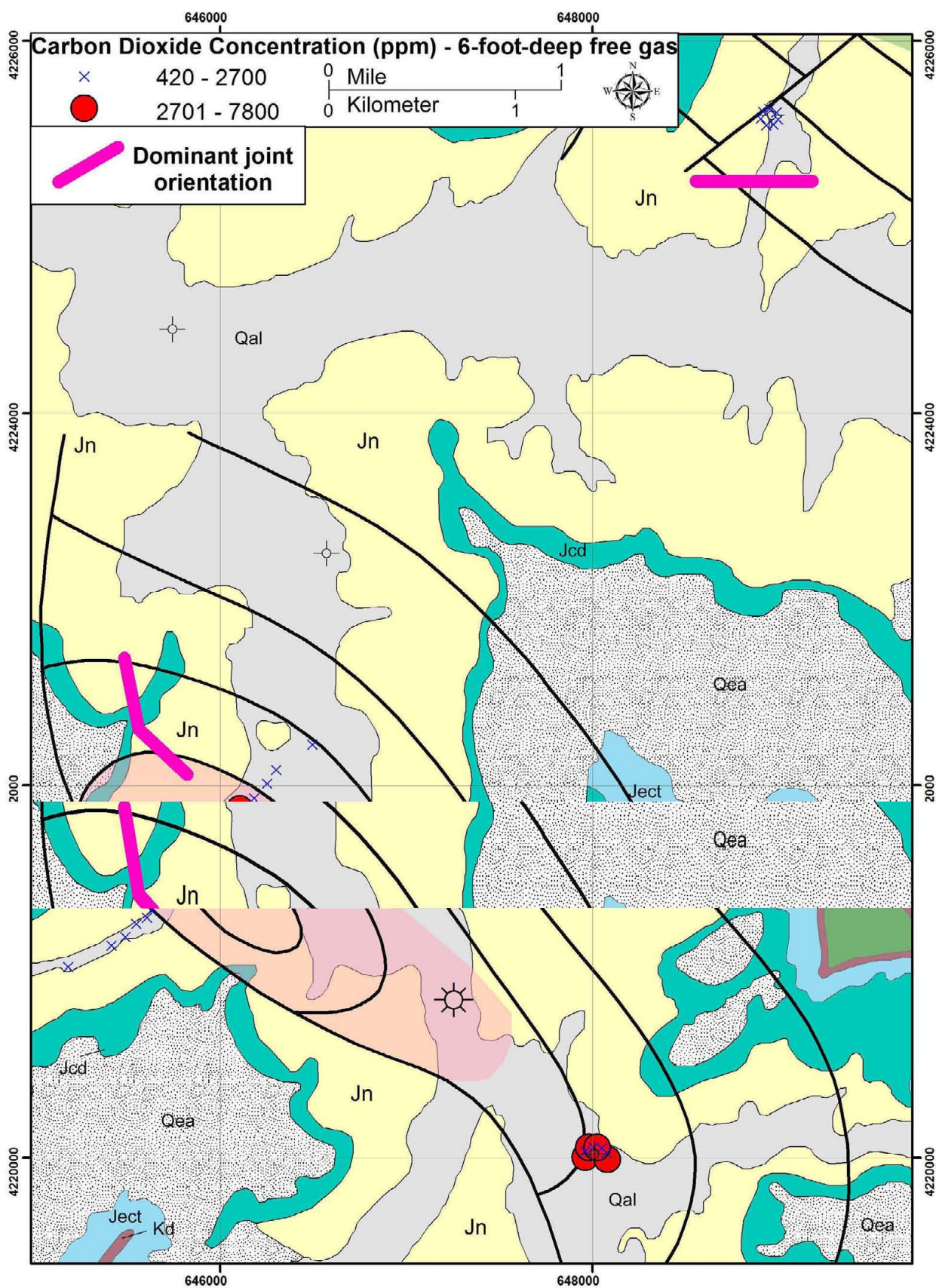


**Figure 40.** Distribution of carbon dioxide concentrations in 6-foot-deep free gas over Lightning Draw Southeast field (shown in pink) and background areas. See figure 14 for description of geologic units (geologic base modified from Doelling, 2005) and figure 8 for explanations of well symbols; form line contours based on structure contour map of the Leadville Limestone shown on figure 8.



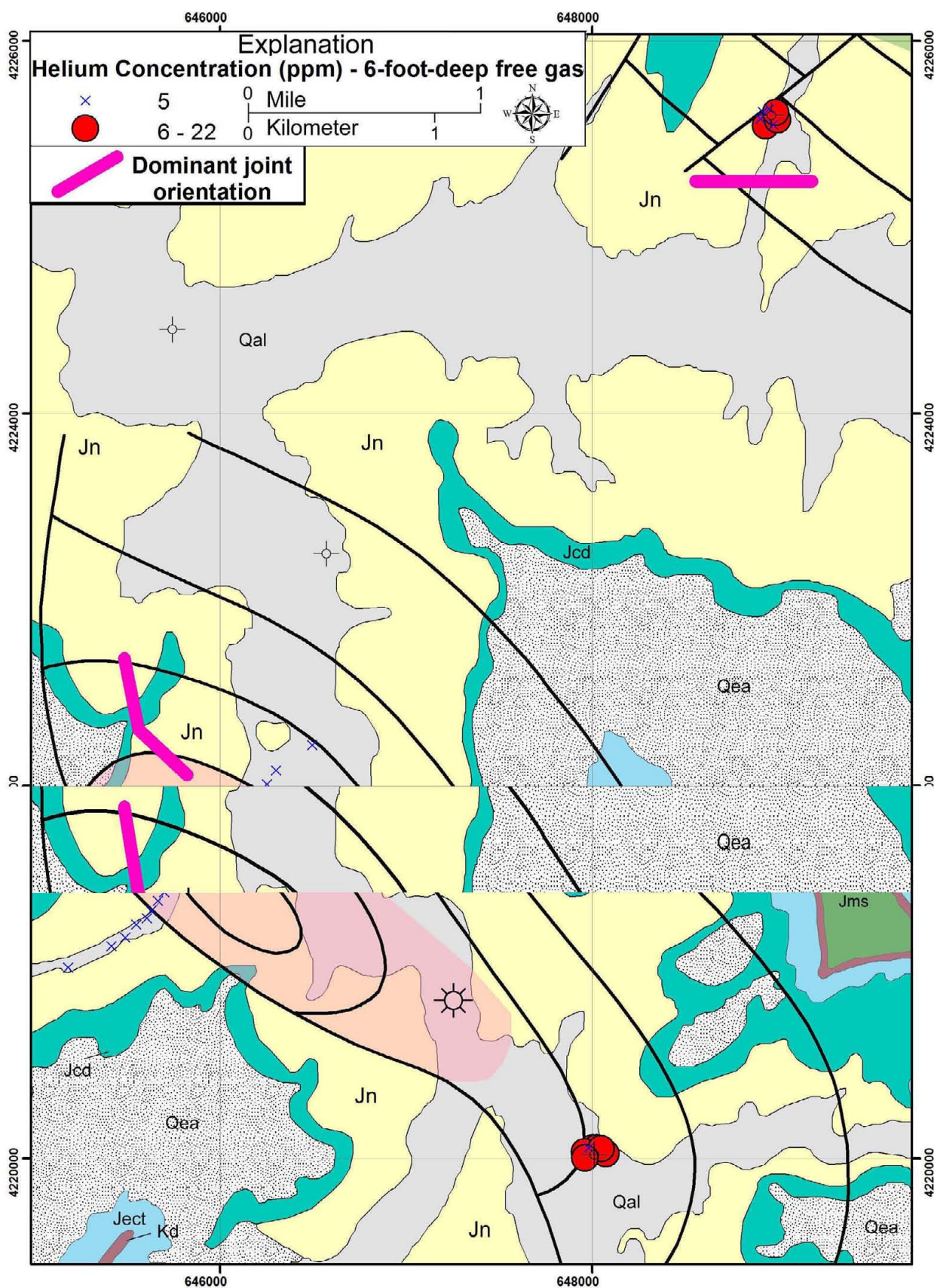


**Figure 41.** Distribution of helium concentrations in 6-foot-deep free gas over Lightning Draw Southeast field (shown in pink) and background areas. See figure 14 for description of geologic units (geologic base modified from Doelling, 2005) and figure 8 for explanations of well symbols; form line contours based on structure contour map of the Leadville Limestone shown on figure 8.



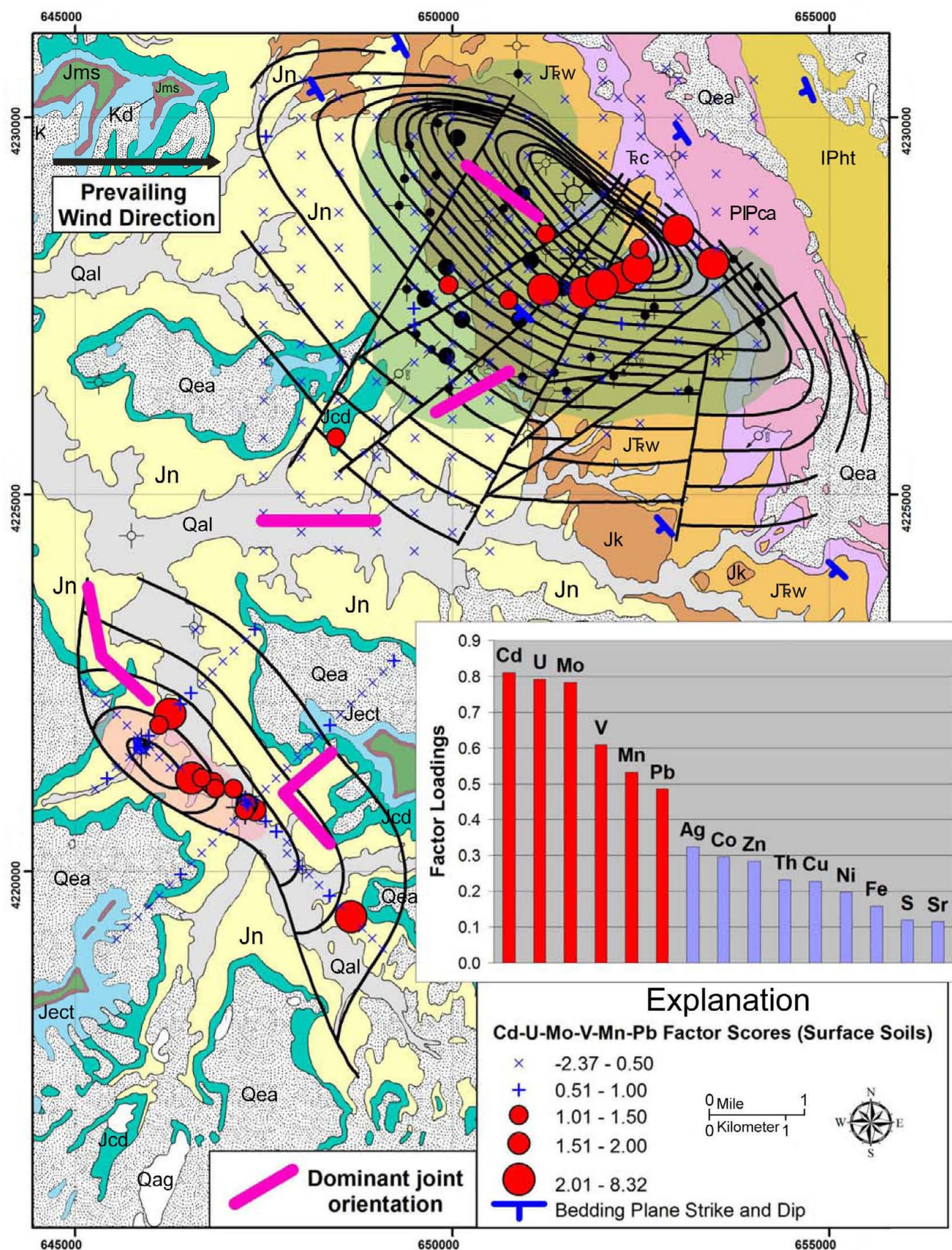


**Figure 42.** Distribution of cadmium-uranium-molybdenum-vanadium-manganese-lead factor scores in surface soils over Lisbon and Lightning Draw Southeast fields (shown in bluish green and pink, respectively). See figure 14 for description of geologic units (geologic base modified from Doelling, 2005) and figure 7 for explanations of well symbols; form line contours based on structure contour maps of the Leadville Limestone shown on figures 7 and 8.



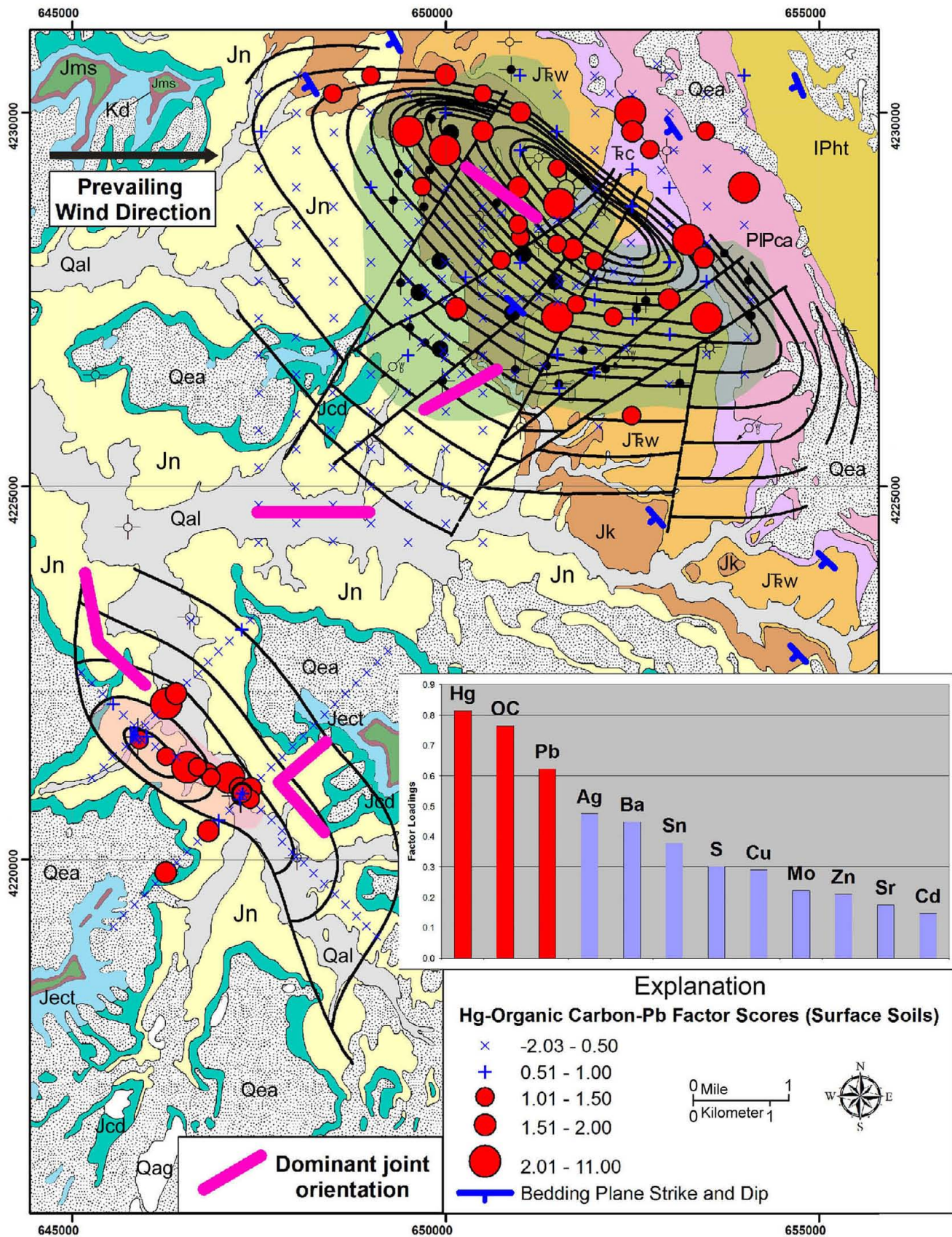


**Figure 43.** Distribution of mercury-organic carbon-lead factor scores in surface soils over Lisbon and Lightning Draw Southeast fields (shown in bluish green and pink, respectively). See figure 14 for description of geologic units (geologic base modified from Doelling, 2005) and figure 7 for explanations of well symbols; form line contours based on structure contour maps of the Leadville Limestone shown on figures 7 and 8.

the anomalies is similar to the joint sets in Navajo outcrops. A small proportion of the anomalous samples fall outside of LDSE field (table 8).

Fluoride is anomalous in 38% of surface soils over LDSE field and 4% of soils off the field. The anomalies, which roughly parallel the northwest joint sets, are confined to Quaternary alluvium and cluster near the Federal No. 1-31 and Evelyn Chambers No. 1 wells and in the central part of the field. In comparison, only a small proportion of samples on and off the Lisbon field are anomalous in fluoride (figure 44, table 8). Anomalies at Lisbon field occur over Quaternary stream and eolian deposits and the Cutler Group, Wingate Sandstone, Kayenta Formation, and Navajo Sandstone.

Arsenic is anomalous in 49% of surface soils over LDSE field and 15% of soils off the field. The anomalies occur over Quaternary stream and eolian alluvium deposits and the Navajo Sandstone and Carmel Formation. The anomalies trend both northwest and northeast, which is parallel to the major joint sets. In comparison, only one sample over the Chinle Formation on Lisbon field is anomalous in arsenic (figure 45).

## DISCUSSION

The main objective of this study was to determine if low cost, surface geochemical methods are applicable to Leadville Limestone hydrocarbon exploration. Our data show that all of the methods tested result in anomalies that are spatially correlated with Lisbon and LDSE fields. Before any conclusions can be drawn, however, further discussion of the results is necessary to explore possible origins for the observed anomalies. The following observations in particular require further discussion.

### Hydrocarbon Anomalies

Aromatic and alkane hydrocarbon anomalies are spatially correlated with both Lisbon and LDSE fields. There is a clustering of anomalies in the central part of Lisbon where normal faults are more abundant and clusters are also evident west of a normal fault at the northwest end of the field. At LDSE, the anomalies trend parallel to the field-bounding reverse fault and anomaly clusters are evident near the Federal No. 1-31 and Evelyn Chambers No. 1 wells, and also off structure. The fluorescence spectral pattern of aromatic hydrocarbon anomalies suggests the presence of weathered light oil in the soil samples. These hydrocarbon anomalies could represent (1) surface contamination developed over past and present production at Lisbon and LDSE fields, and/or (2) the surface expression of past and present hydrocarbon microseepage along joints in sub-cropping sandstones. Factors that favor surface contamination as a source of the anomalies are that anomalies are found in proximity to producing and shut-in well sites and some anomalies are situated downwind of producing well sites. Factors that preclude surface contamination as a source of the anomalies are:

1. While some anomalies occur near production, there are several productive and shut-in wells without hydrocarbon anomalies in soils.
2. There are strong toluene anomalies in soils over the northwest part of Lisbon field that are upwind of production.
3. The heavy aromatic (3- to 6-ring) hydrocarbon anomaly over the southeast half of LDSE field extends for 0.6 mile (1 km) upwind of the Evelyn Chambers No. 1 gas/condensate well.

Therefore, the anomalies most likely represent volatile and liquid hydrocarbon seeps that ascended along joints in outcrop and subcrop sandstones with possible control by the crosscutting normal faults at Lisbon field and the bounding reverse fault and joint sets at LDSE field. The hydrocarbon anomalies are subparallel to preferred joint orientations and the majority of anomalies are found in northwest-trending stream alluvium. This northwest-trending channel is a major topographic feature in the area, which may reflect an underlying fault.

### Discriminant Analysis Models

Discriminant analysis is a useful tool for distinguishing the microseepage over Lisbon and LDSE fields from that of the Lisbon water leg. There is a compositional link between microseepage at Lisbon and Lightning Draw Southeast as demonstrated by the various discriminant models using different sample media. Variables that most influence the distinction between productive and water-wet areas are mainly light hydrocarbons in the  $C_1$  to  $C_6$  range, and this is not surprising considering the composition of the produced gas and that lighter volatile hydrocarbons have a better chance of making it to the surface. The three-component discriminant model for Lisbon field, which compares samples around individual gas and oil wells with those over the water leg, correctly predicts a few samples over LDSE field as having gas or oil potential. The two-component model, which compares an array of samples over the gas cap and oil leg of Lisbon with the water leg, predicts hydrocarbon potential in significantly more samples over LDSE. Rather than only using samples collected at well sites as training sets, a better approach is therefore to use an array of samples that are more representative of microseepage over the productive area. This is important from an exploration standpoint because small targets like LDSE are easier to find if more samples predict hydrocarbon potential. In the subsequent model, which compares samples over LDSE field with those over the Lisbon water leg, several samples over Lisbon field predict hydrocarbon potential. The fact that both Leadville fields predict one another adds confidence to the discriminant models and implies that they can be used in untested areas of the Paradox Basin to assess hydrocarbon potential in Leadville Limestone.

The fracture-fill soils, bryophyte, and lichen better discriminate between the Lisbon gas cap, oil leg, and water leg than do the surface soils. In bryophyte, lichen, and fracture-fill soils, the most



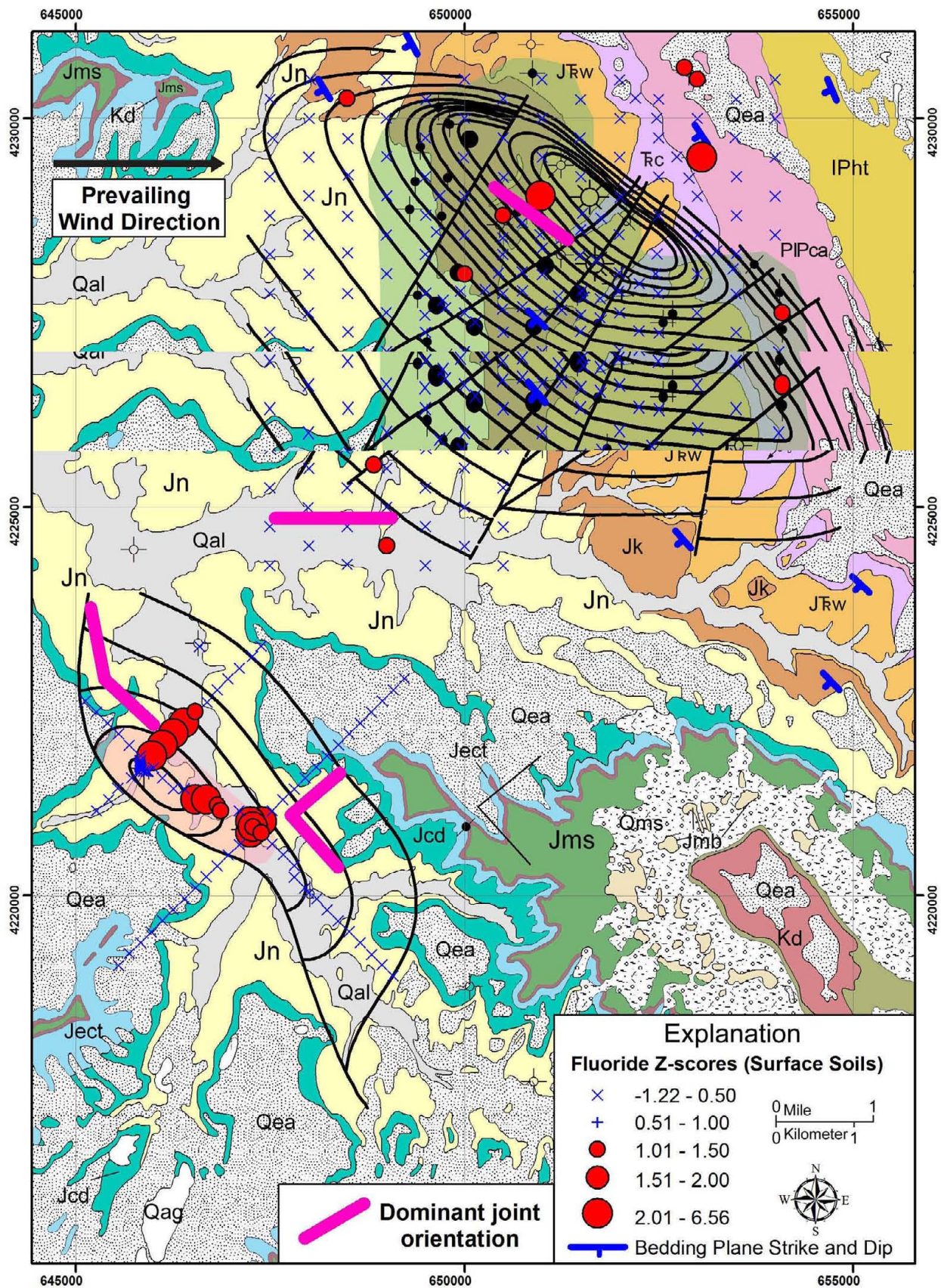


**Figure 44.** Distribution of fluoride Z-scores in surface soils over Lisbon and Lightning Draw Southeast fields (shown in bluish green and pink, respectively). See figure 14 for description of geologic units (geologic base modified from Doelling, 2005) and figure 7 for explanations of well symbols; form line contours based on structure contour maps of the Leadville Limestone shown on figures 7 and 8.



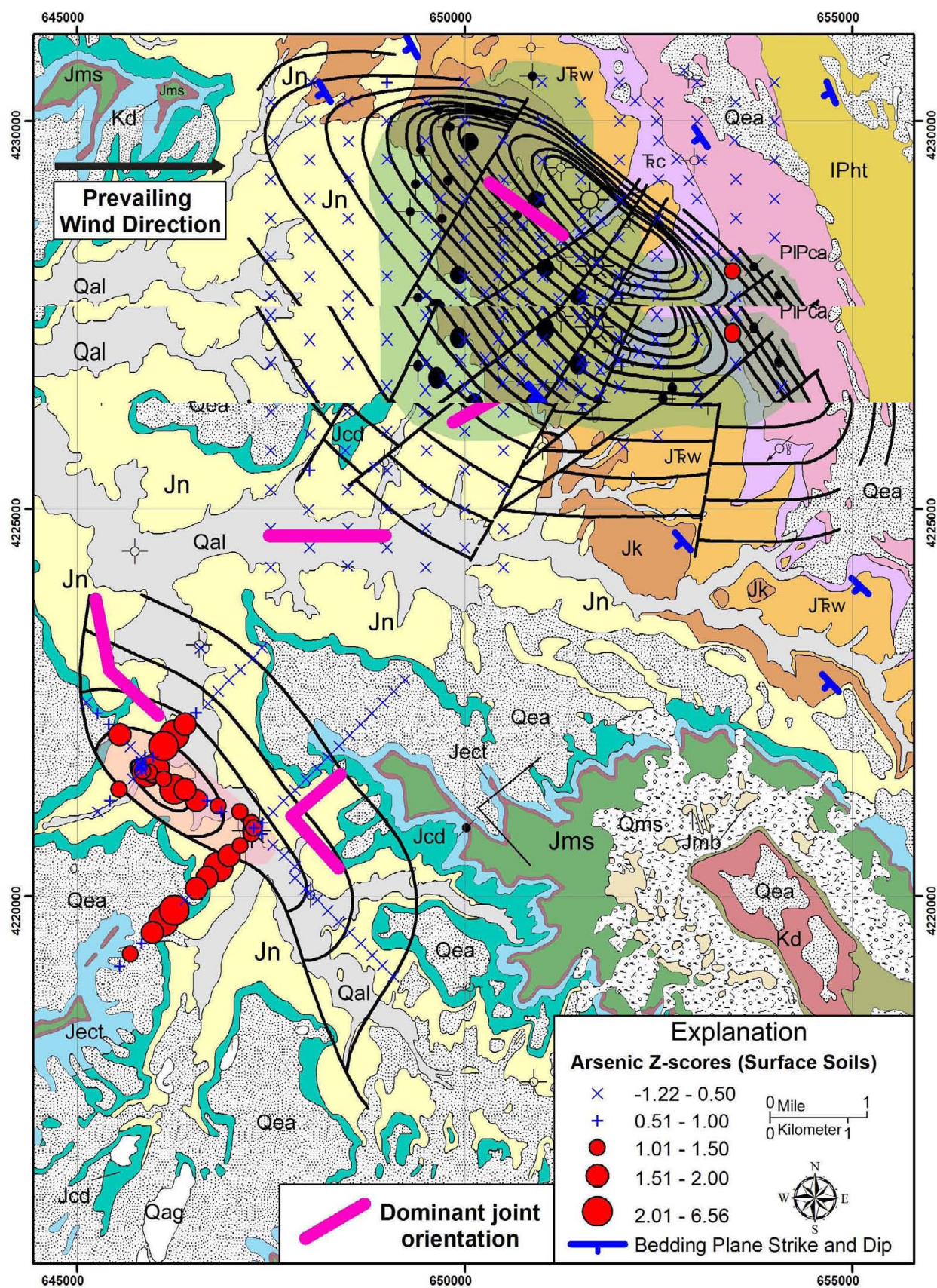


**Figure 45.** Distribution of arsenic Z-scores in surface soils over Lisbon and Lightning Draw Southeast fields (shown in bluish green and pink, respectively). See figure 14 for description of geologic units (geologic base modified from Doelling, 2005) and figure 7 for explanations of well symbols; form line contours based on structure contour maps of the Leadville Limestone shown on figures 7 and 8.



important variables for predicting gas and oil are methane and propane, respectively. The better discrimination power of these sample media probably reflects the fact that they are situated directly on the avenues for ascending microseepage. The fracture-fill soils better predict the gas-prone nature of LDSE field using Lisbon gas-cap samples as a training set. On the other hand, the fracture-fill bryophyte and lichen better predict the productive gas cap at Lisbon using LDSE samples as a training set.

### Free Gas Results

More direct evidence of current-day hydrocarbon seepage over LDSE field is provided by the high contrast, light ( $C_2$  to  $C_6$ ) alkane hydrocarbon anomalies in free-gas samples. These hydrocarbon anomalies are encompassed by more extensive hydrogen and carbon dioxide anomalies (figure 46). Anomalous helium ( $\pm CO_2$  and  $H_2$ ) concentrations in free-gas samples are only found outside the productive limits of LDSE and Lisbon fields (figure 46).

The source of the hydrocarbons, carbon dioxide, and hydrogen anomalies over LDSE field could be (1) weakly productive intervals in the upper and lower Ismay zone, (2) very productive intervals within the Leadville Limestone, or (3) a combination of both reservoirs. The anomalous carbon dioxide over the reservoir could reflect input from the oxidation of Pennsylvanian and/or Mississippian hydrocarbons and Mississippian carbon dioxide. The fact that the carbon dioxide anomaly is wider than the hydrocarbon anomaly favors input from an additional Mississippian source. Hydrogen is actually a common constituent of oil and gas reservoirs (Zinger, 1962), and it could therefore be derived from the Ismay and/or Leadville reservoirs. Hydrogen could certainly come from the Leadville considering its small molecular size and mobility in the subsurface. Helium, which is strongly enriched in produced Leadville gas, is only anomalous over the margins of the LDSE and Lisbon reservoirs. This fact could imply that the hydrocarbons, carbon dioxide, and hydrogen over the productive part of LDSE field are mainly sourced in the Ismay zone. The helium ( $+CO_2$ ) at the margins of the reservoirs may ascend along fractured zones at the margins of salt diapirs formed as a result of subsidence. Helium anomalies in free gas around the Red Wing Creek oil field in North Dakota were documented by Pogorski and Quirt (1981). Fracture zones at the margins of oil and gas reservoirs have also been implicated as a source of the halo anomalies around oil and gas fields (Duchscherer, 1984, 1986).

### Trace Metal and Anion Results

The Cd-U-Mo-V-Mn-Pb element association observed over productive parts of Lisbon and LDSE fields may have separate origins and emplacement mechanisms. Anomalies in the canyon with exposed Chinle Formation and the historic uranium mine workings (Wood, 1968; Chenoweth, 1990, 1996) are probably sourced from the Chinle and mine tailings (figure 47). This is supported by the fact that the strongest uranium anomalies (up to 43.4 ppm) are spatially correlated with abandoned mine shafts and adits and exposed Chinle in the canyon (figure 47).

The anomalous element association is also evident in Quaternary stream alluvium over LDSE field where it also correlates with anomalous heavy aromatic hydrocarbons. The source of this anomaly could be (1) mechanical and chemical dispersion of these elements from abandoned uranium mines in the Salt Wash Member of the Jurassic Morrison Formation 3 miles (5 km) to the east (figure 47) or (2) from the underlying Chinle Formation. Factors in support of chemical dispersion from Salt Wash uranium deposits are (1) the anomalies are in a stream channel that accesses exposed uranium mineralization and oil workings, (2) there is one anomaly off structure and up drainage of LDSE field, and (3) there is an organic carbon build-up (high LOI and heavy aromatics) over the southeast part of the field, which would act as a sink for mechanically and chemically dispersed metals. Factors that negate the Salt Wash uranium deposits as a source of the anomalies in stream alluvium are (1) the uranium contents of the soils are very low ( $<1.1$  ppm), (2) it is unlikely that all of these elements would chemically disperse and precipitate together to form anomalies that are compositionally similar to the Chinle, and (3) there should be more anomalies in upstream areas if the elements were mechanically and chemically dispersed from the Salt Wash deposits on Deerhead Mesa to the south.

A more likely source of the multi-element anomaly is the underlying Chinle. The Evelyn Chambers No. 1 well intersected 98 feet (30 m) of the Chinle. Hydrocarbon and brine fluids that ascended a probable fault underlying the northwest-trending channel probably leached and transported these heavy metals to the surface. Mercury, lead, and fluoride are also spatially associated with the anomaly over the southeast part of the field and a similar origin is therefore invoked. The fluoride anomalies could reflect ascending brines, and the mercury and lead could be derived from the oil seep itself or perhaps the organic-rich black shales of the Paradox Formation it ascends through. The source of the wider dispersed arsenic anomaly over and around LDSE field is unclear. Trace amounts of arsenic are present in crude oil samples, so perhaps this is its source.

## SUMMARY AND RECOMMENDATIONS

Surface geochemical surveys help identify areas of poorly drained or by-passed oil in other basins. Lisbon field was ideal for a surface geochemical survey because proven hydrocarbons underlie the area, sample sites are relatively easily accessible, and the surface geology is similar to the structure of the field. To the southwest, the recently discovered LDSE field has similar geology to Lisbon field in terms of Leadville reservoir lithology, structure, and gas composition. LDSE consists of two wells, producing primarily gas and condensate, along with barren dry wells off structure. However, the field is still near original reservoir pressure and therefore hydrocarbon microseepage to the surface may be more significant than at Lisbon field. The success of relatively low-cost geochemical surveys at Lisbon and LDSE field allows independent operators to reduce risks and

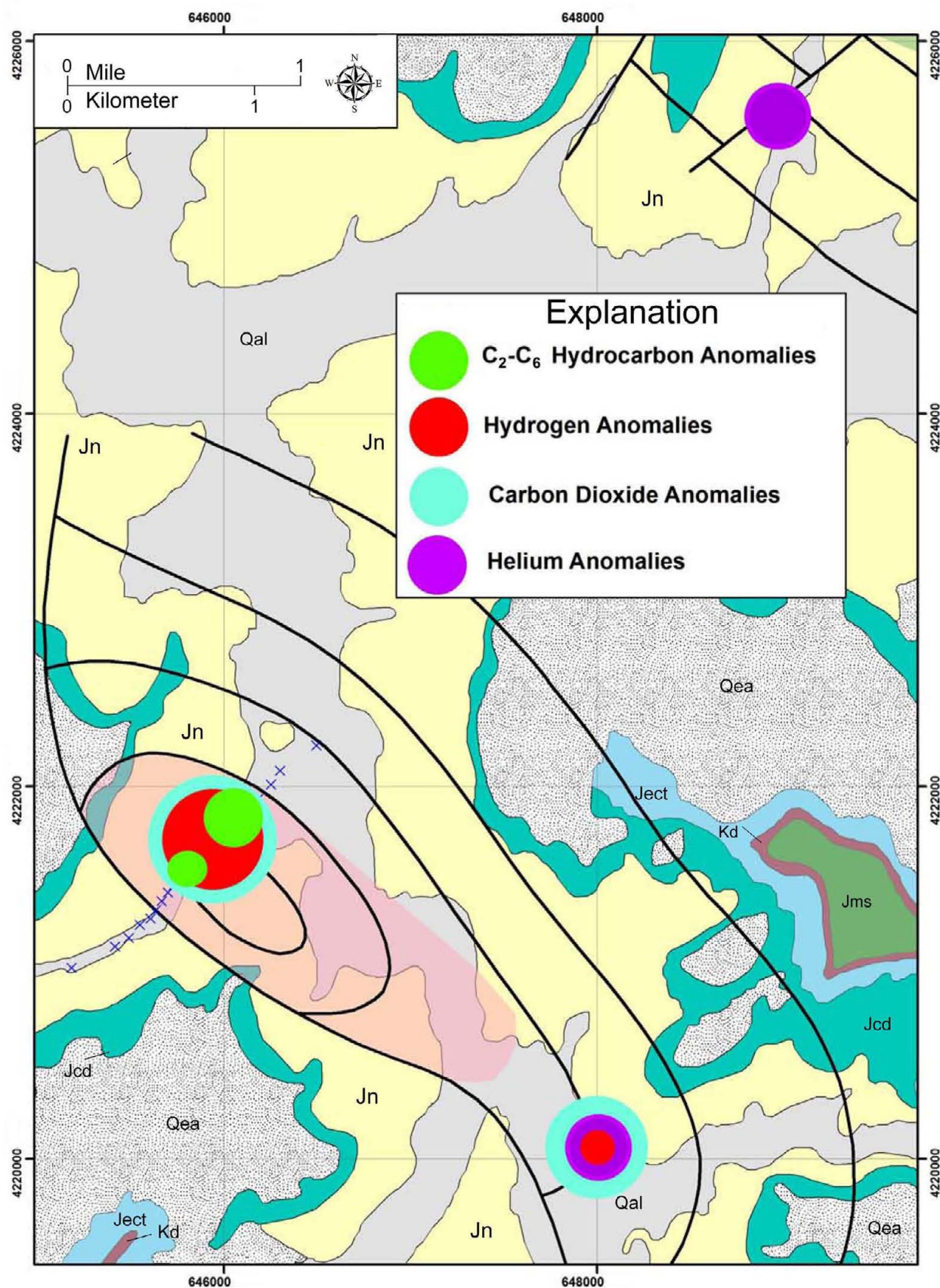


**Figure 46.** Distribution of hydrocarbon and fixed-gas anomalies in free gas over Lightning Draw Southeast field (shown in pink). See figure 14 for description of geologic units (geologic base modified from Doelling, 2005). Form line contours based on structure contour map of the Leadville Limestone shown on figure 8.



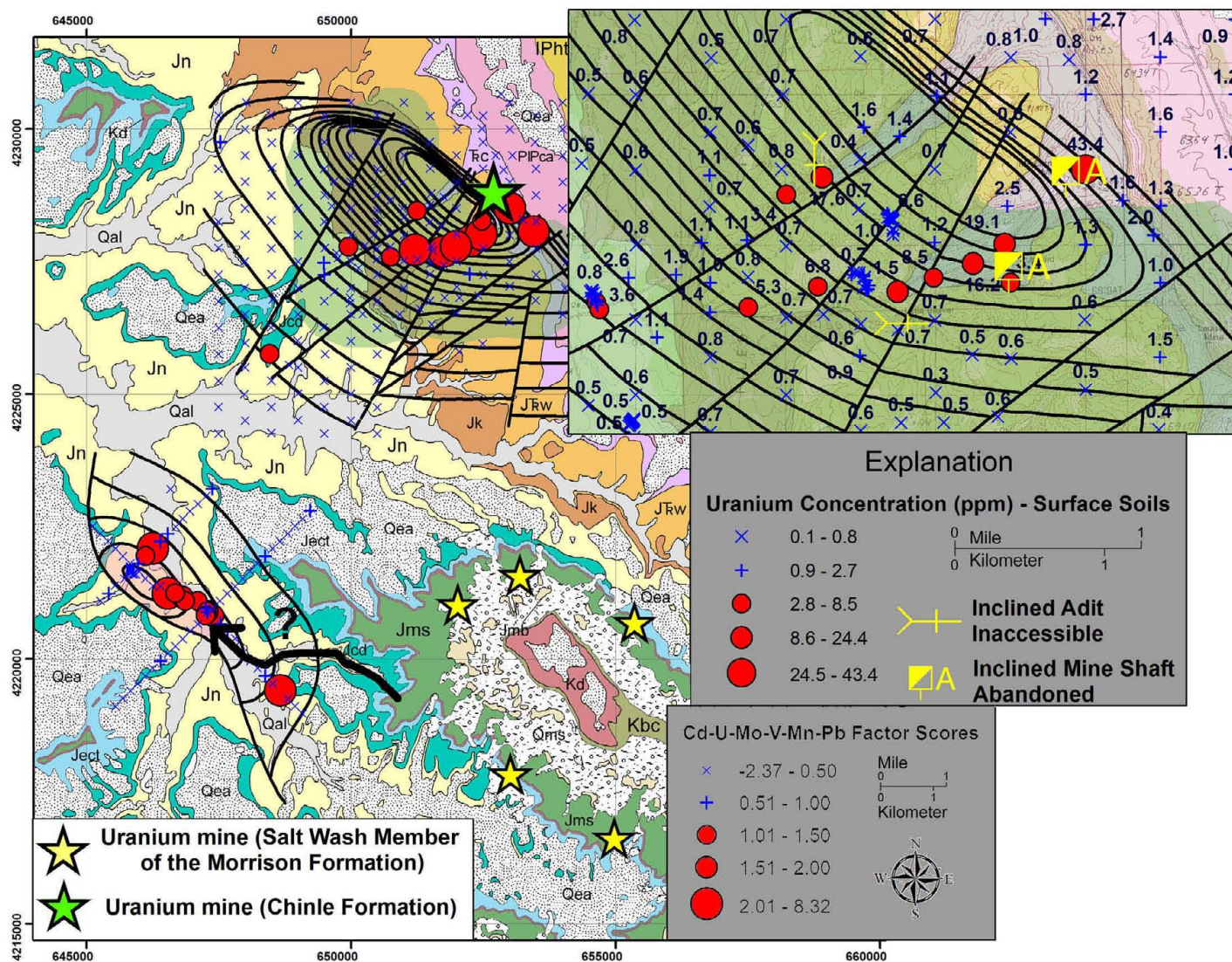


**Figure 47.** Distribution of cadmium-uranium-molybdenum-vanadium-manganese-lead factor scores in surface soils over Lisbon and Lightning Draw Southeast fields (shown in bluish green and pink, respectively) and location of uranium mines. See figure 14 for description of geologic units (geologic base modified from Doelling, 2005) and figure 7 for explanations of well symbols; form line contours based on structure contour maps of the Leadville Limestone shown on figures 7 and 8.

minimize impacts on environmentally sensitive areas while exploring for Leadville targets.

The geochemical survey consisted of collecting shallow soil samples at 1500-foot intervals (500 m) on a 16-square-mile (42 km<sup>2</sup>) rectangular grid over and around the Lisbon field to map the spatial distribution of surface hydrocarbon anomalies. The sampling grid extends beyond the proven limits of Lisbon field to establish background readings. The area chosen sufficiently covers the oil leg, gas cap, and water leg/background barren areas. In addition, samples were collected over gas, oil, and dry wells for analogue matching purposes and to refine the discriminant model for Lisbon field. Samples were collected over LDSE field along northwest-southeast and northeast-southwest grid lines and around both the producing wells and barren dry wells. Free-gas samples were also collected over LDSE field and

known non-productive areas off the structure. Finally, joints in the Jurassic Navajo and Entrada Sandstones may provide pathways for hydrocarbon microseepage to the surface. Therefore, soil, sand, bryophyte, and lichen samples were collected along joints for geochemical analyses.

The conclusion drawn from this evaluation of surface geochemical methods over the Lisbon and LDSE fields is that certain methods are effective as non-invasive, pre-screening and follow-up tools in the exploration for Leadville hydrocarbon reservoirs. More specific conclusions are as follows:

1. Light alkane (C<sub>1</sub> to C<sub>6</sub>) and heavy (C<sub>24</sub> to C<sub>36</sub>) aromatic hydrocarbons are the most important variables in surface soils and fracture-fill bryophyte, lichen, and soils for distinguishing the surface expression of

productive and non-productive areas over Mississippian Leadville reservoirs.

2. Discriminant functions developed for Lisbon and LDSE fields predict and cross-validate each other adding confidence to the models.
3. Microseepage over the Lisbon gas cap is better distinguished from the oil leg probably because of the better production from the gas cap and therefore more intense microseepage.
4. Linear combinations of thermally desorbed hydrocarbons from fracture-fill bryophyte, lichen, and soils better discriminate between the Lisbon gas cap, oil leg, and water leg.
5. Free-gas hydrocarbons, carbon dioxide, and hydrogen from Pennsylvanian Ismay and/or Mississippian Leadville Limestone reservoirs are anomalous over the LDSE field. Helium and carbon dioxide anomalies at the margin of the reservoir are probably sourced from the Leadville.
6. Heavy metals (Hg, Pb, Cd, U, Mo, V, and Mn) are indirect indicators of hydrocarbon seepage over Lisbon and LDSE fields. The mercury and lead in anomalies over the fields are probably derived from oil that ascends faults and joints. Uranium anomalies over Lisbon, however, are derived from exposed mineralization in the Chinle Formation and old mine workings. Fluoride anomalies over LDSE field could reflect the ascent of brines with oil along an alluvium-covered northwest-trending fault. The origin of the widely dispersed arsenic anomalies at LDSE, which do not spatially correlate with the oil seep over the southeast part of the field is unknown.

Recommendations for future surface geochemical surveys for Leadville exploration in the Paradox Basin are:

1. Reconnaissance exploration should include the collection of surface soils (fracture-fill bryophyte, lichen, and soils where applicable) for thermally desorbed and solvent-extractable hydrocarbons.
2. Discriminant functions and factors derived in this study should be used as a guideline for detecting microseepage related to Leadville reservoirs elsewhere in the Paradox Basin.

Anomalous areas identified in reconnaissance soil surveys should be followed up with the collection of deep free-gas samples for hydrocarbon, hydrogen, carbon dioxide, and helium analysis. Helium and carbon dioxide anomalies may be found at the margins of Leadville Limestone reservoirs.

## ACKNOWLEDGMENTS

Funding for this research was provided as part of the Advanced and Key Oilfield Technologies for Independents (Area 2—Ex-

ploration) Program of the U.S. Department of Energy, National Energy Technology Laboratory, Tulsa, Oklahoma, contract number DE-FC26-03NT15424. The Contracting Officer's Representative is Virginia Weyland. Support was also provided by the Utah Geological Survey (UGS), Salt Lake City, Utah; Direct Geochemical/Vista Geoscience Resources, Golden, Colorado; ST Oil Company, Denver, Colorado; and the Utah School and Institutional Trust Lands Administration, Salt Lake City, Utah.

Gas analyses and oil samples as well as surface access in Lisbon field were provided by EnCana Oil & Gas (USA), Inc., Denver, Colorado. We thank Dr. Larry St. Clair, Curator of Lichens and Bryophytes and Director of the Monte L. Bean Life Science Museum, Brigham Young University, Provo, Utah, for identifying bryophyte and lichen.

Cheryl Gustin, James Parker, and Sharon Wakefield of the UGS drafted figures and maps. Editorial comments by Neil Fishman (U.S. Geological Survey), Jason Blake (Titan Energy), David Tabet (UGS), and Robert Ressetar (UGS) improved the manuscript significantly.

## REFERENCES

- Bammel, B.H., Chamberlain, C.P., and Birnie, R.W., 1994, Stable isotope evidence of vertical hydrocarbon microseepage, Little Buffalo Basin oil field: Association of Petroleum Geochemical Explorationists Bulletin, v. 10, p. 1-23.
- Chenoweth, W.L., 1990, Lisbon Valley, Utah's premier uranium area, a summary of exploration and ore production: Utah Geological and Mineral Survey Open-File Report 188, 45 p.
- Chenoweth, W.L., 1996, The uranium industry in the Paradox Basin, *in* Huffman, A.C., Jr., Lund, W.R., and Godwin, L.H., editors, *Geology and resources of the Paradox Basin*: Utah Geological Association Publication 25, p. 95-108.
- Clark, C.R., 1978, Lisbon, San Juan County, Utah, *in* Fassett, J.E., editor, *Oil and gas fields of the Four Corners area*: Four Corners Geological Society, v. II, p. 662-665.
- Coleman, D.D., Meents, W.F., Liu, Chao-Li, and Keough, R.A., 1977, Isotopic identification of leakage gas from underground storage reservoirs—a progress report: Illinois State Geological Survey, Illinois Petroleum No. 111, 10 p.
- Colorado Oil and Gas Conservation Commission, 2009, Colorado oil and gas information system (COGIS)—production data inquiry: Online, < <http://cogcc.state.co.us/cogis/ProductionSearch.asp>>, accessed January 19, 2010.
- Conel, J.E., and Alley, R.E., 1985, Lisbon Valley, Utah uranium test site report, *in* Abrams, M.J., Conel, J.E., Lang, H.R., and Paley, H.N., editors, *The joint NASA Geosat test case project—final report*: American Association of Petroleum Geologists Special Publication, pt. 2, v. 1, p. 8-1-8-158.
- Doelling, H.H., 2005, Geologic map of the La Sal 30' x 60' quadrangle, San Juan, Wayne, and Garfield Counties, Utah, and



- Montrose and San Miguel Counties, Colorado: Utah Geological Survey Map M-205DM, 2 plates, scale 1:100,000.
- Duchscherer, W., 1984, Geochemical hydrocarbon prospecting, with case histories: Tulsa, Oklahoma, PennWell Publishing, 196 p.
- Duchscherer, W., 1986, Delta carbonate hydrocarbon prospecting, *in* Davidson, M.J., editor, Unconventional methods in exploration for petroleum and natural gas, symposium IV: Dallas, Southern Methodist University Press, p. 173-182.
- Harr, C.L., 1996, Paradox oil and gas potential of the Ute Mountain Ute Indian Reservation, *in* Huffman, A.C., Jr., Lund, W.R., and Godwin, L.H., editors, Geology and resources of the Paradox Basin: Utah Geological Association Publication 25, p. 13-28.
- Herbert, C.F., 1984, Geochemical prospecting for oil and gas using hydrocarbon fluorescence techniques, *in* Davidson, M.J., Gottlieb, B.M., and Price, E., editors, Unconventional methods in exploration for petroleum and natural gas, symposium III: Dallas, Southern Methodist University Press, p. 40-58.
- Hintze, L.F., and Kowallis, B.J., 2009, Geologic history of Utah: Brigham Young University Geology Studies Special Publication 9, 225 p.
- Hintze, L.F., Willis, G.C., Laes, D.Y.M., Sprinkel, D.A., and Brown, K.D., 2000, Digital geologic map of Utah: Utah Geological Survey Map 179DM, 17 p., scale 1:500,000.
- Horvitz, L., 1985, Geochemical exploration for petroleum: Science, v. 229, p. 821-827.
- Johnson, C.F., 1970, Top of structure of the Leadville Limestone, Lisbon field: unpublished map, Union Oil Company of California files.
- Kitcho, C.H., 1981, Characteristics of surface faults in the Paradox Basin, *in* Wiegand, D.L., editor, Geology of the Paradox Basin: Rocky Mountain Association of Geologists Guidebook, p. 1-21.
- Klusman, R.W., 1993, Soil gas and related methods for natural resource exploration: Chichester, John Wiley & Sons, 483 p.
- Klusman, R.W., Mahyoub, A., and Abu-Ali, M.A., 1992, The potential use of biogeochemistry in the detection of petroleum microseepage: American Association of Petroleum Geologists Bulletin, v. 76, p. 851-863.
- Lammers, D.A., 1991, Soil survey of Canyonlands area, Utah, parts of Grand and San Juan Counties: U.S. Department of Agriculture, Soil Conservation Service, 293 p., 57 sheets, general soil map, scale 1:443,520.
- Merin, I.S., and Segal, D.B., 1989, Diagenetic alteration of Wingate Formation—possible indicators of hydrocarbon microseepage, Lisbon Valley, Utah: Journal of Geology, v. 97, p. 719-734.
- Parker, J.W., and Roberts, J.W., 1963, Devonian and Mississippian stratigraphy of the central part of the Colorado Plateau, *in* Bass, R.O., and Sharps, S.L., editors, Shelf carbonates of the Paradox Basin: Four Corners Geological Society, 4th Field Conference Guidebook, p. 31-60.
- Pogorski, L.A., and Quirt, S.G., 1981, Helium emanometry in exploring for hydrocarbons—part 1, *in* Gottlieb, B.M., editor, Unconventional methods in exploration for petroleum and natural gas, symposium II: Dallas, Southern Methodist University Press, p. 124-135.
- Potter, R.W., II, Harington, P.A., Silliman, A.H., and Villenave, J.H., 1996, Significance of geochemical anomalies in hydrocarbon exploration, *in* Schumacher D., and Abrams, M.A., editors, Hydrocarbon migration and its near-surface expression: American Association of Petroleum Geologists Memoir 66, p. 431-439.
- Price, L.C., 1986, A critical review and proposed working model of surface geochemical exploration, *in* Davidson, M.J., editor, Unconventional methods in exploration for petroleum and natural gas IV: Dallas, Southern Methodist University Press, p. 245-304.
- Price, L.C., 1993, Microbial-soil surveying—preliminary results and implications for surface geochemical exploration: Association of Petroleum Geochemical Explorationists Bulletin, v. 9, p. 81-129.
- Roberts, A.A., Dalziel, M., Pogorski, L.A., and Quirt, S.G., 1976, A possible petroleum related helium anomaly in the soil gas, Boulder and Weld Counties, Colorado: U.S. Geological Survey Open-File Report No. 76-544, 7 leaves, 3 maps.
- Saunders, D.F., Burson, K.R., and Thompson, C.K., 1999, Model for hydrocarbon microseepage and related near-surface alterations: American Association of Petroleum Geologists Bulletin, v. 83, no. 1, p. 170-185.
- Schumacher, D., 1996, Hydrocarbon-induced alteration of soils and sediments, *in* Schumacher, D., and Abrams, M.A., editors, Hydrocarbon migration and its near-surface expression: American Association of Petroleum Geologists Memoir 66, p. 71-89.
- Schumacher, D., and LeSchack, L.A. (editors), 2002, Surface exploration case histories—applications of geochemistry, magnetics, and remote sensing: American Association of Petroleum Geologists Studies in Geology 48, 500 p.
- Segal, D.B., and Merin, I.S., 1989, Successful use of Landsat Thematic Mapper Data for mapping hydrocarbon microseepage induced mineralogic alteration, Lisbon Valley, Utah: Photogrammetric Engineering and Remote Sensing, v. 55, no. 8, p. 1137-1145.
- Segal, D.B., Ruth, M.D., and Merin, I.S., 1986, Remote detection of anomalous mineralogy associated with hydrocarbon production, Lisbon Valley, Utah: The Mountain Geologist, v. 23, no. 2, p. 51-62.
- Seneshen, D.M., Viellenave, J.H., and Fontana, J.V., 2006, The surface geochemical expression of carbonate-hosted hydrocarbon reservoirs and faults in New York, Ohio, Nevada, and Utah [abs.]: American Association of Petroleum Geologists Annual Convention Abstracts, v. 15, p. 98.
- Smith, K.T., and Prather, O.E., 1981, Lisbon field—lessons in exploration, *in* Wiegand, D.L., editor, Geology of the Paradox Basin: Rocky Mountain Association of Geologists Guidebook, p. 55-59.

- Smouse, D., 1993, Lisbon, *in* Hill, B.G., and Bereskin, S.R., editors, Oil and gas fields of Utah: Utah Geological Association Publication 22, non-paginated.
- Utah Division of Oil, Gas, and Mining, 2009, Oil and gas production report, October: Online, < <http://oilgas.ogm.utah.gov/Publications/Publications.htm>>, accessed January 21, 2009.
- Wood, H.B., 1968, Geology and exploration of uranium deposits in the Lisbon Valley area, Utah, *in* Ridge, J.D., editor, Ore deposits of the United States, 1933–1967: New York, American Institute of Mining, Metallurgical, and Petroleum Engineers, Inc., v. 1, p. 770-789.
- Wood, J.R., Bornhorst, T.J., Chittick, S.D., Harrison, W.B., Quinlan, W., and Taylor, E., 2001, Using recent advances in 2D seismic technology and surface geochemistry to economically redevelop a shallow shelf carbonate reservoir—Vernon field, Isabella County, MI - annual report, March 20, 2000-March 20, 2001: U.S. Department of Energy, DOE/BC/15122-1, 25 p.
- Wood, J.R., Bornhorst, T.J., Harrison, W.B., and Quinlan, W., 2002, Using recent advances in 2D seismic technology and surface geochemistry to economically redevelop a shallow shelf carbonate reservoir—Vernon field, Isabella County, MI - annual report, March 21, 2001-March 20, 2002: U.S. Department of Energy, DOE/BC/15122-2, 20 p.
- Zinger, A.S., 1962, Molecular hydrogen in gas dissolved in waters of oil-gas fields, lower Volga region: Geochemistry, no. 10, p. 1015-1023.



## **APPENDICES**

### **APPENDIX A**

#### **SURFACE SOILS – C1–C12 DATA**

### **APPENDIX B**

#### **SURFACE SOILS – SSF DATA**

### **APPENDIX C**

#### **SURFACE SOILS – ELEMENTAL DATA**

### **APPENDIX D**

#### **FRACTURE-FILL BRYOPHYTE AND LICHEN DATA**

### **APPENDIX E**

#### **FRACTURE-FILL SOIL DATA**

### **APPENDIX F**

#### **FREE-GAS SAMPLE DATA**